Identification of stem/progenitor cells in the postnatal thymus

Sviatlana Ulyanchanka

Thesis presented for the degree of Doctor of Philosophy

The University of Edinburgh

2013

Declaration

Work presented in this thesis is my own, unless stated otherwise

Sviatlana Ulyanchanka

Acknowledgements

First and foremost I would like to thank Clare Blackburn for giving me an opportunity to undertake a PhD in her laboratory. I would also like to thank her for being an enthusiastic and supportive supervisor and allowing me great freedom in my experimental work, as well as providing much needed stress relief by kindly allowing me to ride her wonderful horses.

I would also like to thank all the members of the Blackburn group for being a huge help in day to day experimental work, as well as great fun on a night out. In particular I would like to thank Nick and Alison for their tireless support, helpful discussions, and Harsh for help with dissections.

I would also like to thank Carolyn Manson, Kevin Stewart, Laura Walker and Stephanie Logan for their excellent animal care and willingness to go the extra mile.

I am also grateful to the Darwin Trust of Edinburgh for their financial support.

Thanks also goes to Simon Monard and Olivia Rodriguez for help with sorting. A special thank you to Sabrina Gordon Keylock for taking the time to teach me in utero mouse surgery.

And last but not least big thank you to my parents and my sister, for their endless love and support.

Abstract

The thymus is the principal site of T-cell development and maturation. Failure to develop a functional thymus leads to severe immunodeficiency, while partially incorrect function of the organ can lead to a variety of autoimmune diseases as well as higher risk for infections and cancer. The thymus is organized into cortical and medullary regions, which are functionally distinct. The diverse array of thymic epithelial cells (TEC) are the key components of the thymic stroma, both the cortical and medullary TEC subsets are responsible for the establishment of a self-tolerant and self-restricted T-cell repertoire.

The thymus is most active in young individuals, and undergoes a progressive naturally occurring involution from birth, which accelerates after puberty. Thymic involution is characterized by loss of thymus organization and function, including an overall reduction in the amount of functional thymic tissue. This results in decreased production of new naïve T-cells, and contributes to the diminished capacity of the aged immune system to adequately respond to new antigenic challenge. Involution of the thymus, both natural and in response to different therapies such as chemotherapy, raises interest in developing cell based treatment methods that will allow the restoration of the thymic architecture and so elevate immune reconstitution in vivo.

The cellular mechanisms by which the postnatal thymus is maintained during homeostasis and involution are currently unknown. The earliest thymic progenitors in the thymus express Plet1; it has been established that from E12.5 to E15.5 these cells when purified are able to generate all thymic epithelial cell types and initiate thymus organogenesis. However, at least the latter capacity is reported to be lost from E18.5. A number of papers published provide evidence for the existence of both bipotent and unipotent TEC progenitors in the adult thymus. However the identity of these cells remains unknown, nor has the relationship between the mature and immature postnatal TEC compartments been established.

The aim of my research was to investigate the cellular mechanism(s) that maintain the postnatal thymus. Specifically, I aimed to determine whether the thymus is

maintained by a stem cell mechanism or by division of terminally differentiated thymic epithelial cells, and whether or not postnatal thymic epithelial stem/progenitor cells express functionally relevant levels of the transcription factor Foxn1.

To address these aims, I used two approaches: in vivo genetically heritable lineage tracing and a novel grafting assay to assess the contribution of different lineages of TEC.

This thesis describes the characterization of a novel mouse strain, the Foxn1^{CreERt2} line, which was predicted to allow conditional inducible manipulation of gene expression in TEC. I show that this deletor strain, while thymic epithelial cell-specific, could induce cre-mediated recombination in only in a low proportion of TEC and thus could not be used to address the initial aim of this work as described above. However, lineage tracing experiments using this line have provided evidence for a persistent cortical thymic epithelial progenitor/stem cell type, that was capable of rapid expansion within the cortical compartment over time. In parallel with characterisation of the *Foxn1*^{CreERt2} strain, I investigated the potential of various defined epithelial populations to contribute to the thymic environment in an assay of TEC potency. Using this technique I have established the potential of defined TEC subpopulations isolated from postnatal mice to generate cortical and medullary TEC. Among the populations analysed I have identified a minor TEC subset that can robustly contribute to both cortical and medullary TEC that coexpress Ly51 and Plet1. I have further shown, using a limiting dilution approach, that this population contains a postnatal common thymic epithelial stem/progenitor cells, present at a frequency of between 87.5 and 92.5 within this population. I have also produced evidence of a unipotent cortical progenitor population that is capable of long term expansion in vivo.

Table of contents

Declaration..... I
Acknowledgements..... II
Abstract..... III
Abbreviations.....VIII
Chapter 1: Introduction..... 1
1.1 The thymus.....1
1.2 Cellular composition of the thymus.....1
1.2.1 Non epithelial components of the thymic stroma..... 1
1.2.2 Thymic epithelium..... 4
1.2.2.1 The cortical thymic epithelium..... 4
1.2.2.2 The medullary thymic epithelium..... 5
1.3T cell development in the thymus..... 6
1.4Thymus organogenesis.....8
1.4.1 Origin of thymic epithelium..... 9
1.5 Identification of thymic epithelial progenitor cells.....9
1.6 Foxn1 and its role in thymic development.....12
1.7 Thymic involution.....17
1.8 Mechanisms of thymic involution.....21
1.9 Role of Foxn1 in thymic involution.....24
1.10 Identifying stem/progenitor cell activity.....27
Aims:..... 30
Chapter 2: Materials and Methods..... 31
2.1 Mice.....31
2.1.1 Mouse lines used in experiments.....31
2.2 Tamoxifen treatment of mice.....34
2.3 Embryo collection.....34
2.4 Immumohystochemistry..... .34
2.4.1 Staining procedure..... 35
2.4.2 Imaging..... 35
2.5 Cell preparation for cell sorting and FACS analyses.....35
2.5.1 Preparation of embryo thymic tissue for cell sorting and Facs analyses 35
2.5.3 Postnatal enrichment of TEC.....36

2.6 Cell Staining....37
2.6.1 Antibodies used for IHC....37
2.6.2 Antibodies for flowcytometric analyses....37
2.7.3 Flow cytometry instruments....38
2.8 Tissue culture....39
2.8.1 Preparation and maintenance of MEFs....39
2.8.2 Thymic reaggragation....39
2.9 Kidney Grafting....40
2.10 Inutero injections....40
2.11 Isolation of nucleic acids....41
2.12 Genotyping PCR....42
2.13 Southern blott analyses....43
Chapter 3: Characterization of the Foxn1CreERt2 mouse line....44
Introduction:....44
3.1 Analysis of recombination in the Foxn1CreErt2 mouse line....47
3.1.1 Analysis of recombination during fetal development....48
3.1.2 Analysis of recombination frequency in fetal TEC....50
3.1.3 Phenotypic analysis of recombined cells....53
3.1.4 In utero injection of tamoxifen....56
3.1.5 Recombination rate in the Foxn1CreERT2 E15,5 thymus....58
3.2 Postnatal analyses of the Foxn1CreErt2 mouse line....60
3.2.1 Identification of the optimal reporter strain for postnatal lineage analyses....60
3.2.2 Analyses of recombination in postnatal mice....61
3.3 Discussion....64
Chapter 4: In vivo cell tracking of Foxn1+ cells in a model of thymus regeneration after injury....67
Introduction....67
4.1 Preliminary analysis of the effect of tamoxifen on the adult thymus....68
4.1.1 Effect of tamoxifen on thymocytes....68
4.1.2 Effect of tamoxifen on TEC....74
4.2 Effect of tamoxifen on adult TEC....76
4.3 Lineage tracing....83
4.4 Discussion....91
Chapter 5: Identification of a multipotent epithelial progenitor in the postnatal thymus....93

Introduction:..... 93
5.1 Characterization of postnatal TEC populations..... 96
5.2 TEC potency assay: experimental strategy..... 99
5.2 Differentiative potential of UEA1+ mTEC.....103
5.3 Differentiative potential of Ly51+ cTEC.....104
5.3.1 Potency of the Ly51+ Plet1- population..... 104
5.3.2 Potency of Ly51+Plet1+ TEC..... 106
5.4 Frequency of TEPC within the Ly51+Plet1+ TEC.....108
5.4.2 Analyses of contribution of 500 inputLy51+Plet1+GFP+test cells.....108
5.4.2 Analyses of contribution of 250 input Ly51+Plet1+GFP+ test cells. .109
5.4.3 Analyses of contribution of 125 input Ly51+Plet1+GFP+ test cells. .109
5.4.4 Analyses of contribution of 60 Ly51+Plet1+GFP+ test cells..... 114
5.5 Localization of Ly51+Plet1+ cells in the postnatal thymus.....115
5.6 Capacity of Ly51+Plet1+ TEC to initiate de novo thymus formation.....117
5.7 Summary.....120
Chapter 6: Summary and concluding remarks..... 124
Bibliography:..... 128

Abbreviations

4OHT	4-hydroxy-tamoxifen
BM	Bone marrow
BSA	Bovine serum albumin
CMJ	Contico-medullary junction
cTEC	Cortical thymic epithelial cell
$cTEC^{hi}$	MHC II^{hi} cortical epithelial cell
$cTEC^{lo}$	MHC II^{lo} cortical epithelial cell
DC	Dendritic cell
DN	Double negative
DP	Double positive
EpCAM	Epithelial cell adhesion molecule
Fgf	Fibroblast growth factor
HC	Haematopoietic cell
HPC	Haematopoietic progenitor cell
HSCT	Haematopoietic stem cell transplant
IC	Isotype control
IL	Interleukin
IP	Intraperitoneal
K	Keratin
KGF	Keratinocyte growth factor
MHC	Major histocompatibility complex
MHC II	Major histocompatibility complex II
mTEC	Medullary thymic epithelial cells
$mTEC^{hi}$	MHCIIhi medullary thymic epithelial cell
$mTEC^{lo}$	MHCIIlo medullary thymic epithelial cell
NC	Neural crest

PBS	Phosphate buffered saline
SP	Single positive
Tam	Tamoxifen
TEC	Thymic epithelial cell
TN	Triple negative
U	Unit
UEA	Ulex europaeus agglutinin

Chapter 1: Introduction

1.1 The thymus

The thymus is a bilobed organ situated at the midline above the heart, and is a primary organ of the adaptive immune system in vertebrates (Bajoghli et al. 2009; Bajoghli et al. 2011). The fully formed thymus is encapsulated and lobulated, with three histologically defined regions: the subcapsule, cortex and the medulla. The subcapsule is a layer of simple epithelium that divides the cortex from the connective tissue that comprises the capsule and trabeculae (Figure 1A). Blood vessels run along the trabeculae and contribute to the extensive vascular network of the thymus (Boyd et al. 1993).

1.2 Cellular composition of the thymus

1.2.1 Non epithelial components of the thymic stroma

The cellularity of the mature thymus is extremely heterogeneous. The majority of the cells that populate the thymus are developing T-cells, that comprise >95% of its total cellularity. Bone-marrow (BM) derived cells, mesenchymal cells, vasculature and the thymic epithelial cells (TEC) make up the remaining 1-2% of total cellularity. BM-derived cells are spread throughout the organ, however macrophages are more concentrated in the cortex, while the dendritic cells are localized predominantly at the cortico-medullary junction and in the medulla (Figure 1B) (Ardavín 1997; Boyd et al. 1993; Gray et al. 2002).

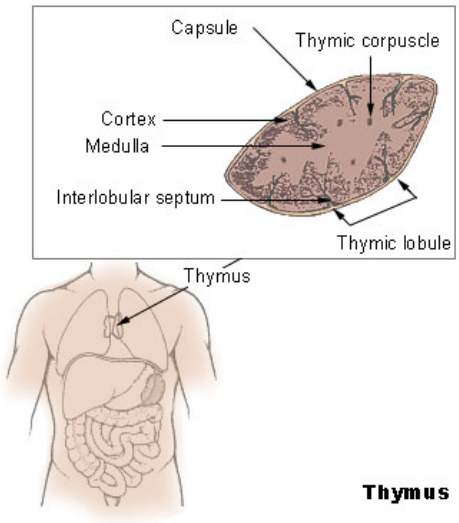
Both cell types carry out important tasks, with the dendritic cells having the ability to present antigens and being intricately involved in the negative selection process of T-cell in the thymus (Ardavin 1997), and the macrophages being primarily responsible for the removal of T-cells that have undergone apoptosis (Duijvestijn & Hoefsmit 1981).

The thymus also contains fibroblasts, these cells are responsible for secreting extracellular matrix (ECM). The secreted substances that comprise the ECM, such as glycoproteins and collagen, are important for thymocyte differentiation and migration (Boyd et al. 1993; Savino et al. 1993). Another important component of

the thymic stroma is the thymic vasculature. In order to facilitate thymus function, a vast vascular network allows for the entry of haematopoietic progenitor cells, and the exit of naïve T-cells into the blood stream when the maturation process is complete (Boyd et al. 1993; Kato & Schoefl 1989).

In addition to the cell types described above the thymus also contains mesenchymal cells that are Neural Crest derived (NCC), these cells form the capsule, as well as the trabeculae (the invaginations into the body of the thymus that surround blood vessels) and pericytes (Jiang et al. 2000; Foster et al. 2008) These cells play an important role in the establishment of the thymus by secreting mitogenic soluble factors that are required for TEC, and by providing a source of pericyte precursors (Revest et al. 2001; Foster et al. 2008).

A



B

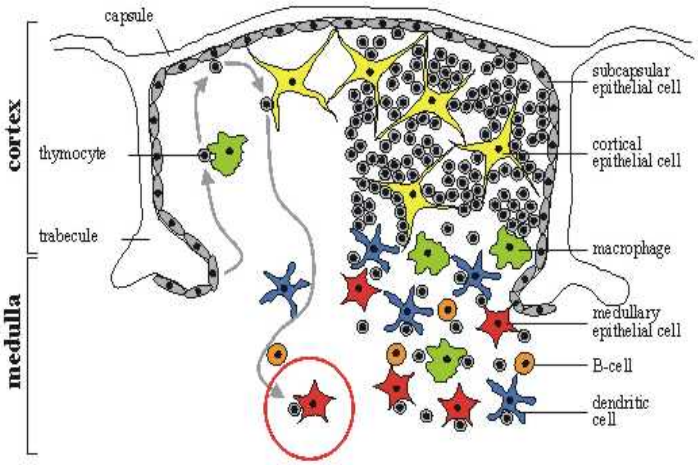


Figure 1 Schematic representation of thymus structure showing location and broad architecture (A) and cellular composition (B)

1.2.2 Thymic epithelium

The cortical and the medullary regions of the thymus each contain an extensive network of epithelial cells that is tightly packed with thymocytes. There are several different types of thymic epithelial cell (TEC) populations classified in different subsets due to both morphological and phenotypical differences (Boyd et al. 1993). The thymic stroma constitutes around 1-2% of total thymus cellularity, with the TEC making up a fraction of these cells (Gray et al. 2006). One of the unique aspects of thymus epithelium is its openly configured three dimensional network, which contrasts with other epithelial organs that tend to be organized as layers on a basal membrane (van Ewijk et al. 1999). The TEC are the primary cell type responsible for guiding the T-cells through multiple stages of expansion and differentiation and selection. The TEC can be subdivided into two main groups: cortical and medullary TEC, which, through direct interaction with T-cells, are responsible for mediating specific stages of T cell development (Boyd et al.. 1993).

1.2.2.1 The cortical thymic epithelium

Cortical TEC are commonly divided into two subpopulations, identified by their expression of a specific set of cytokeratins (K).The phenotype of the predominant population is $K5^{-}K14^{-}K8^{+}K18^{+}$,while the phenotype of the minor subset of cTEC defined in this way is $K5^{+}K14^{-}K8^{+}K18^{+}$ (Klug et al. 1998). Ultrastructural and immunohistochemical analyses have also revealed six different subsets of cortical thymic epithelial cells. These subsets have been assigned the term clusters of epithelial staining or CTES, namely type I, II, III, IIIB, IIIC, IV, based on different mAb staining, with each type of cell occupying a distinct area within the cortex. The outermost cortical population are type II epithelial cells, characterized by their pale appearance in electronmicrographs. Deeper into the cortical tissue are the type III epithelia that have intermediate electron lucency, the innermost cTECs are characterized as type IV epithelial cells that have high electron lucency and characteristic oval or spindle shaped nuclei. (Wijngaert et al. 1984). Ultrastructural analysis revealed that large complexes of epithelial cells and developing thymocytes were comprised of type II and III epithelial cells. These subsets of cells show strong expression of MHC class II (Wijngaert et al. 1984).

1.2.2.2 The medullary thymic epithelium

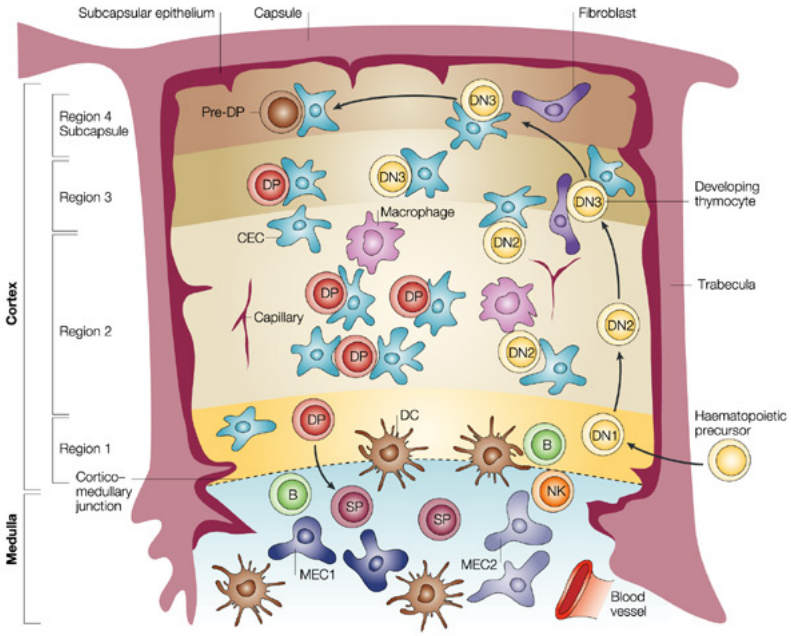
Unlike the cTEC most medullary TEC (mTEC) display a $K5^{+}K14^{+}K8^{-}K18^{-}$ phenotype and also express mAb MTS10 (Godfrey et al. 1990). A minor subset of mTEC are $K5^{-}K14^{-}K8^{+}K18^{+}$ (Klug et al. 1998). The lectin Ulexeuropaeus agglutinin 1 (Uea1) strongly stains a subpopulation of mTEC as determined by immunohistochemical analysis, but by flow cytometry binds all mTEC -providing a way to reliably distinguish these cells from cortical cells without depending on the cytokeratin expression (Klug et al. 2002).

Ultrastructural analysis revealed several subsets of mTEC. Similar to the cortex, a type III subset of cells was identified. In addition ultrastructural analysis also revealed type V epithelial cells. These cells seem to exist in small isolated clusters at the CMJ, and are classified as undifferentiated cells. (Wijngaert et al. 1984). In addition type VI epithelial cells were identified in the medulla and are believed to be precursors of differentiated cells.

All mTEC are highly MHC class I positive, whereas MHC class II expression varies. A subset of mTEC expresses the transcriptional factor Autoimmune Regulator (Aire) which plays an essential role in establishing self-tolerance. (Anderson et al. 2002).

1.3 T cell development in the thymus

The thymus is the central organ for T-cell development. T-cell precursors enter the thymus at the cortical medullary junction (CMJ) and are then guided through their differentiation process by the thymic epithelial cells. At different stages in development the T-cells are directed to different zones within the thymus where the appropriate TEC compartment is responsible for guiding them through their developmental check point (Figure 2). Since T-cell development is not essential to understanding the work presented in this thesis and T cell development, and the role of thymic epithelium in this process, has been reviewed extensively in recent reports (Lind et al. 2001; Petrie 2002; Rothenberg & Dionne 2002; Hinterberger et al. 2010; Takahama 2006; Blackburn & Manley 2004) it will not be discussed further.



2

Figure 2. Migration of thymocytes through the thymus at different stages of development. (Blackburn & Manley 2004)

1.4 Thymus organogenesis

The precise embryological origin of the thymus, as well as the number of thymus organs per animal, and the final anatomical positions of the thymus lobes vary significantly depending on the species in question. The common theme is that the thymus originates from the pharyngeal pouches. Mammals usually have one thymus composed of bilateral lobes, which are formed from the third and/or fourth pharyngeal pouchs (Rodewald 2008).

In the mouse the thymus arises from the third pharyngeal pouches (3PP) and shares a common primordium with the parathyroid gland. At E9.0 each of the 3PP consists of a single layer of epithelium, which is surrounded by neural crest cells (NCC) (Gordon et al. 2004). The NCC later form the thymic capsule. Thymus organogenesis is evident at day 10 of embryonic development in mouse (E10) (Gordon et al. 2004). At E12.5 the common primordia separate from the pharynx and begin forming the thymus and parathyroid organs, with the thymus forming in the ventral part. The patterning of these organs begins early on, with the future parathyroid expressing Gcm2, which is restricted to the dorsal and anterior part of the common primordia, while the ventral part of the primordia that later forms the thymus can be distinguished by high levels of Foxn1 expression (Gordon et al. 2001).This is then followed by complete separation of the thymus and parathyroid glands, with each organ undergoing migration to their final position within the organism (Blackburn & Manley 2004).

The NCC surrounding the thymus are derived mainly from the migratory neural crest. The NCC migrate into the pharyngeal arches from approximately day 9.0 in embryonic development and are the source of mesenchymal cells which form the capsule of the thymus (Jiang et al. 2000; Foster et al. 2008). The mesenchymal cells provide a wide range of soluble factors that are essential for TEC proliferation, including fibroblast growth factor 10 (Revest et al. 2001).

The TEC show the first indication of cortical and medullary subtypes at E12.5. Development of the two compartments then proceeds in a lymphocyte-independent manner until E15.5 (Klug et al. 2002). At E12.5, expression of MHC class II can be

detected (Nowell et al. 2011). Newborns posses a functional thymus, however its full organization is not achieved until several weeks after birth (Manley et al. 2011).

1.4.1 Origin of thymic epithelium

The endodermal vs ectodermal origin of the TEC had been a cause of debate for some time, with some research groups proposing a dual ectodermal/endodermal origin of the TEC (Cordier & Haumont 1980), while others proposed a single endodermal origin of the TEC (Blackburn and Manley, 2004, Gordon et al. 2004). A single endodermal origin was confirmed by two studies, with the earlier study utilizing chick/quail chimeras (Nantes 1975) and the latter confirming and extending the findings in mice (Gordon et al. 2004). In these experiments, transplantation of pharyngeal endoderm was performed. This tissue was isolated from embryos at E8.5-E9. When the 3PP are just beginning to form, but thymus formation itself is not evident. These experiments showed that the grafted endoderm was sufficient to give rise to a properly formed thymus with both cortical and medullary TEC. In a separate experiment, lineage tracing analyses in which the ectoderm was labeled using a cell tracker dye CMFDA found no contribution of ectoderm to the 3PP. Taken together, these studies definitively proved that the TEC have a single origin and forms from the endoderm, which indicated the possibility of a common endodermal progenitor for the cTEC and mTEC.

1.5 Identification of thymic epithelial progenitor cells.

Early evidence supported the possible existence of a common thymic epithelial progenitor cell was acquired from analyses of human thymic epithelial tumours, where cells co-expressing markers normally associated with either cTEC or mTEC were discovered in tumours that contained both compartments (Schluep et al. 1988). Immunohistochemical analyses of fetal TEC then showed that these cells co-express markers that in the adult TEC are restricted to the cTEC or mTEC compartments (Haynes et al. 1984; Schluep et al. 1988, Lampert et al. 1988). These data were taken to suggest that a common thymic epithelial progenitor cell (TEPC) existed that co-expressed markers that later segregated to the cTEC and mTEC sub-lineages.

Further information on the phenotype of the TEPC was provided by the analysis of the T cell differentiation mutant mice. CD3e26tg mice display a block in T-cell differentiation, which is unable to progress further that the DN1 stage (Klug et al. 1998). These mutant mice lack defined cortical and medullary regions, with the majority of cells displaying a $K5^{+}K8^{+}$ phenotype, which is usually observed only in fetal TEC (Klug et al. 1998). Interestingly if CD3e26tg thymi were transplanted into mutant mice that displayed a later block in T-cell development this lead to the emergence of a large number of $K5^{-}K8^{+}$ cells, suggesting that further differentiation had taken place, and thus that the newly acquired cells were derived from the $K5^{+}K8^{+}$ cells, making these cells potential progenitors (Klug et al. 1998). This study also emphasized the importance of lympho-epithelial crosstalk for proper TEC development to take place.

Further information on the phenotype of TEPCs was provided by the study of *nude* mice (Blackburn et al. 1996), which are congenitally athymic and hairless. In these studies, aggregation chimaeras were generated using MHC mismatched *nu/nu-wt/wt* embryos. These chimaeras were analysed in order to determine the contribution of the cells derived from the *nude* donor embryo to mature TEC networks. *Nude*-derived cells were unable to contribute to the major TEC subsets, and were present either as single cells or linear aggregates in the medulla. Wildtype TEC or wild type haematopoietic cells are unable to restore function to these cells, indicating that the *nude* defect is cell autonomous. These *nude*-derived cells were also shown to bind mAbs MTS20 and MTS24 (the determinant for which was later identified as Plet1; Depreter et al. 2008), which are bound by most epithelial cells in the nude thymic rudiment but whose binding becomes restricted to a subset of mTEC in the postnatal thymus (Bennett et al. 2002). These cells also did not express any markers associated with stages of terminal TEC differentiation, which led to the conclusion that the product of the *nude* gene (Foxn1) is required for the development of all mature TECs. In the absence of the *nude* gene, the TEC do not progress in development to mature TEC, suggesting that these cell undergo maturation arrest and persist in a progenitor like cell state, characterized by the expression of $MTS20^{+}24^{+}$ (Blackburn et al. 1996)

In a more recent study, the functional capacity of the MTS20^{+}24^{+} population of cells was determined. When isolated from fetal thymic TEC at E12.5 and tested in a reaggregation assay with subsequent grafting under the kidney capsule of *nude* mice, these cells were able to give rise to both cortical and medullary populations as well as support T-cell development (Bennett et al. 2002). A similar study, where MTS24^{+}MHC Class II^{-} TEC were isolated at E15.5, showed that these cells were able to give rise to a thymic organoid upon ectopic transplantation (Gill et al. 2002). MTS24^{-} cells were later reported to have the same capacity to form a functional thymus when grafted in large cell numbers (Rossi, Chidgey, et al. 2007). Since the MTS24^{-} cells are a heterogenous compartment containing TEC at various stages of differentiation and lineage commitment this result, their ability to be able to form a thymic organoid when large cell numbers are used is not surprising. Strikingly Plet1+ cells when isolated from E18.5 embryonic thymi, were unable to initiate organogenesis (Rossi, Chidgey, et al. 2007). Data discussed above suggests that the Plet1+ population of cells contains multipotent progenitors that are able to initiate thymic organogenesis upon transplantation, however this potential is lost further on in development.

The existence of a common TEPC was confirmed by two studies which analysed the potency of TEC at the single cell level. A single Plet1^{+}Epcam^{+} cell isolated from a E12.5 thymic lobe was able to give rise to both mTEC and cTEC when transplanted into an E12.5 thymic lobe and grafted under the kidney capsule (Rossi et al. 2006). Furthermore, an elegant study performed in a mouse model in which a conditionally revertible Foxn1 null allele was reactivated with Cre recombinase. In these experiments, a tamoxifen-inducible Cre (CreER) was used, and a low level of recombination was observed in perinatal mice in the absence of tamoxifen induction. This was demonstrated to occur at a low enough frequency to permit clonal analysis, and established that reactivation of Foxn1 in a single cell resulted in formation of small thymic lobes with both mTEC and cTEC regions. This proved the existence of a common progenitor, as well as indicating that Foxn1 is not required for the formation or maintenance of the progenitor cells (Bleul et al. 2006). A K14CreERT2;eYFP mouse model that exhibited a low level of recombination even in the absence of tamoxifen allowed for clonal labeling of these cells in the perinatal

thymus. Cells labeled with YFP were detected in small clusters, suggesting their clonal origin. Some clusters were cTEC only and others mTEC only, while others formed clustes containing both cTEC and mTEC, suggesting that in the peinatal thymus there are common, and lineage restricted progenitor TEC (Bleul et al. 2006).

However studies using chimaeric mice appear to show no evidence to support the clonal origin of individual medullary islets and the immediately adjacent cTEC (Rodewald et al. 2001). This could suggest that unlike in the fetal thymus where a bipotent progenitor is clearly present, the adult thymus might utilize separate populations of cells to maintain the mTEC and cTEC compartments, although the persistence of a multipotent progenitor in the adult thymus cannot be excluded.

In other studies, grafting experiments were used to identify medullary restricted progenitors. In these studies Claudin $3,4^{hi}Uea1^{+}$ cells isolated at E13.5 were able to give rise to $Aire^{+}$ cells upon transplantation (Hamazaki et al. 2007).

Thus, there is evidence to support the existence of multipotent and lineage restricted progenitors in thymus in embryonic development, and in perinatal mice. However the identity of the multipotent progenitor in adult thymi remains unknown, as well as the relationship between different TEC subsets.

1.6 Foxn1 and its role in thymic development.

Foxn1 is a member of the forkhead family of transcription factors and contains a DNA binding domain and a C-terminal transactivation domain (Schlake et al. 1997). There are over 40 members of Forkhead family of transcription factors.
Mutations of the *Foxn1* gene leads to the nude phenotype in mice, a condition that is characterised by hairlessness as well as athymia, which leads to severe immunodeficiency (Flanagan 1966; Nehls et al. 1994). A similar phenotype is observed in humans with mutations in the *Foxn1* gene (Frank et al. 1999). *Foxn1* is expressed in the thymic primordium from E11.25 by *insitu* hybridization (Gordon et al. 2001), while *Foxn1* transcripts can be detected as early as E9-E10.5 by RT-PCR (Balciunaite et al. 2002; Nehls et al. 1994). *Foxn1* is also expressed in the epidermal layer of the skin and hair follicles, where it can be detected from E15.5 (Lee et al. 1999). *Foxn1* is expressed in all TEC in the embryo, and is required cell

autonomously for normal function and development in these cells. Studies have shown that in the nude mutants, normal initiation and sequence of organogenesis displayed until E11.5-12.0 (Cordier, 1974).After this time point, the nude mutants display an arrest in thymus organogenesis with the hallmark signs being: failure of lymphocyte precursor migration into the thymic primordium; failure to undergo vascularization, and the epithelial cells show a halt in proliferation after E12.5 (Itoi et al. 2001; Blackburn et al. 1996; Gordon et al. 2007; Flanagan 1966; Nehls et al. 1994). This suggests that *Foxn1* is not required for the initial establishment of the thymus, but is required after E12.5 for normal development to take place. In the Foxn1 null thymi, the TEC express Plet-1, a known marker of fetal TEPC, and do not display signs of differentiation, appearing to be trapped in a progenitor-like state (Blackburn et al. 1996; Depreter et al. 2008). As discussed above, in a model of clonal *Foxn1* reactivation, formation of cortical and medullary areas can be observed (Bleul et al. 2006), confirming the idea of TECs being arrested in a progenitor-like state in *Foxn1* null mice.

A series of experiments performed on mice displaying defined levels of *Foxn1* mRNA expression, from 7 to 50% of WT levels, showed that *Foxn1* is required in a dose dependant manner to facilitate the differentiation of the TEPC, with progressively higher levels being required to mediate differentiation into mature TEC types for both the mTEC and cTEC lineages (Nowell et al. 2011) (Figure 3). Interestingly *Foxn1* was not required for the emergence of a putative mTEC progenitor, as cells co-expressing Keratin 5 and Claudin 4 (a cell type previously identified as the mTEC precursor) are readily identified in the *Foxn1* null mice (Hamazaki et al. 2007; Nowell et al. 2011).

There have been several reports characterizing *Foxn1* expression in the postnatal TEC, which showed strikingly different proportions of TEC that are positive for *Foxn1*. A study performed by Itoi and colleagues in 2007, which utilized an α-Foxn1 antibody, demonstrated *Foxn1* expression in only 24% of TEC in mice 2-4 weeks of age; while studies utilizing a Foxn1:eGFP reporter detected *Foxn1* expression in up to 90% of TEC in a 10 day old thymus (Corbeaux et al. 2010).

These differences might be due to the sensitivity of the methods allowing for *Foxn1* detection. It is important to emphasize that the Foxn1:eGFP line was made using random integration, and as such could be subject to chromosomal positional effects, resulting in transgene silencing which could lead to underestimation of the number of *Foxn1* positive cells. Data from our laboratory using a *Foxn1*GFP reporter mouse suggests that most, or possibly all TECs express Foxn1 in the postnatal thymus, with different subsets of TEC displaying high, intermediate or low expression of *Foxn1* (Bredenkamp, unpublished).

Interestingly the expression of Foxn1 decreases with age, with studies done on sorted total TEC showing that compared to 1 month old mice there was a three fold decrease in *Foxn1* mRNA expression at 7 months of age. Expression levels of *Foxn1* declined further over time, with mRNA levels of Foxn1 decreasing sixteen fold in 12 month old mice (Ortman et al. 2002).

A more detailed analyses performed in our laboratory confirmed these data and provided information on Foxn1 expression in different TEC subsets and the changes that occur in aging mice. This study showed that *Foxn1* levels drop up to ten fold in mice twelve months of age, when compared to two month old controls, and showed a decrease in *Foxn1*^{hi} expressing cells, which comprise the majority of the TEC population at 3 months of age, with mice 6 to 12 month of age showing an increase in Foxn1^{lo} and intermediate population of TEC (Bredenkamp, unpublished). This study also demonstrated heterogenous levels of *Foxn1* expression in different TEC subsets, with highest levels of *Foxn1* expression detected in the cTEC (Bredenkamp, unpublished), however the reasons for the different levels of expression are unclear. Interestingly, there is a decrease in *Foxn1* levels concomitant with thymic involution, suggesting that *Foxn1* plays a role in this process.

Studies performed on a series of hypomorphic mice, expressing various defined levels of *Foxn1* showed that both cTEC and mTEC differentiation is blocked in mice that express 15% of wild type Foxn1 mRNA levels, with the cTEC showing a more pronounced effect-consistent with data discussed above showing higher levels of

Foxn1 expression in cTEC versus mTEC. Mature markers of cTEC (such as Ly51) and mTEC (such as Aire) were restored within two days after restoration if WT levels of *Foxn1*, strongly suggesting that Foxn1 is required for terminal differentiation of these cells (Nowell et al. 2011; Bredenkamp, unpublished).

Data discussed above suggests that at least in embryo development the specification to TEC lineage, and even the emergence of lineage restricted mTEC precursor takes place early on, and *Foxn1* is not required for this process to take place. This raises the question of the molecular requirements of progenitor cells in the adult thymus, and whether *Foxn1* expression is present, and if so at what levels, in these cells.

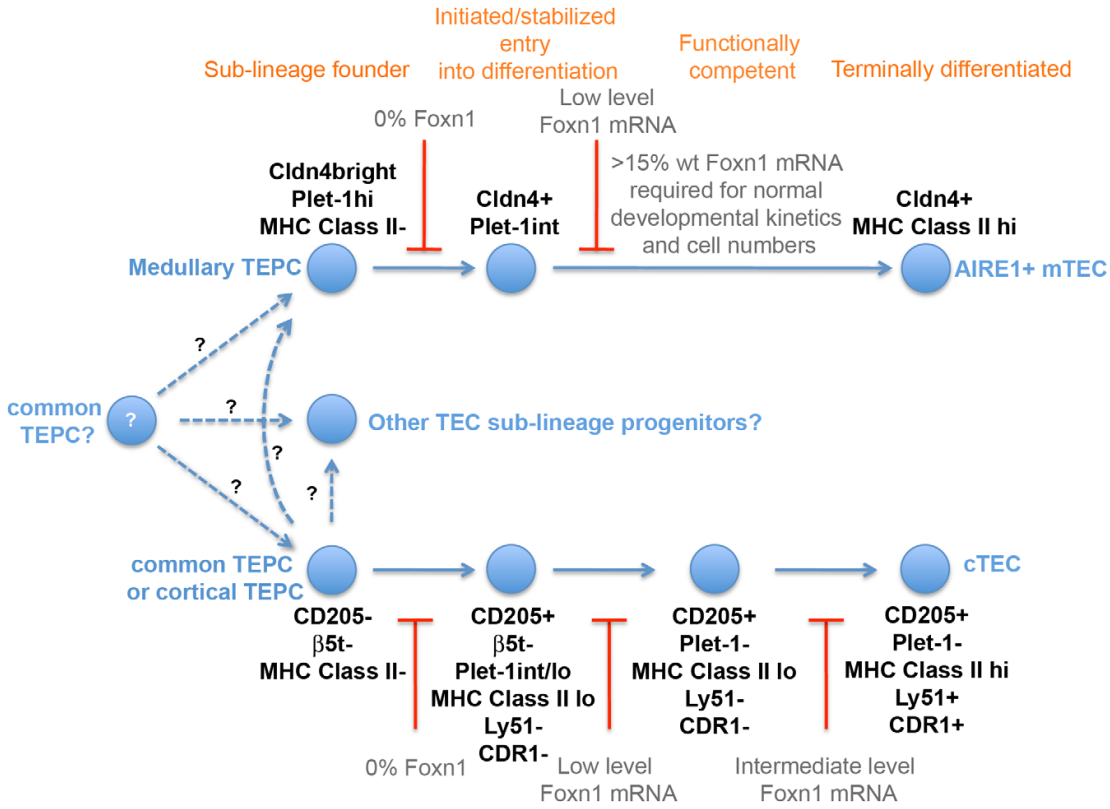


Figure 3: Role of Foxn1 in thymic epithelial development. (Nowell et al. 2011).

1.7 Thymic involution

The thymus displays high levels of activity in early life. In humans it reaches its maximum size (25 cm^3 on average) at 12 months postnatally (George & Ritter 1996). However it starts to degenerate, a process referred to as involution, early in life. The decline of the adaptive immune system with age - or immunosenescence, is a complex process, and is achieved by several mechanisms. It has been demonstrated that the thymus starts to undergo involution from the first year of life in humans, displaying a 3% decrease in thymic epithelial space (TES) from the early years of life to 35-45 years of age, and a steady rate of 1% TES decrease in subsequent years (Steinmann et al. 1985; Min et al. 2004). As well as the TES decrease, a steady expansion of the perivascular space (PVS), which shifts the ratio of TES/PVS content of the thymus, is evident in the aging thymus with the TES comprising less than 10% of the total thymus tissue by 70 years of age (Hale 2004). These changes are illustrated in figure 4a, which shows the differences between thymus structure of healthy young donors 3 days (left), and 60 years (right) of age. In mice, the thymus begins reaches its maximum size at 4 weeks and after a relatively short period of homeostasis starts to show the first morphological indications of involution at 3 months postnatally. Disorganization of the cortico medullary junction (CMJ), decrease in overall thymic size, decrease in T-cell output and cortical thinning are the main indications of thymic involution (Sempowski et al. 2002; Chen et al. 2009; Gray et al. 2006; Manley et al. 2011). (Figure 5).

Though the reason for thymic involution is unclear there are two main theories proposed to explain the necessity of this process. One states that the thymus is an organ that requires a lot of resources from the body to keep it working at full capacity and that in later life this energy is redirected towards reproduction instead, while a second theory suggests that involution allows for the expansion and selection of optimal T-cell clones in the peripheral blood system (Dowling & Hodgkin 2009; George & Ritter 1996).

Changes in thymic structure are accompanied by severe decrease in mature T-cell output in the aged thymus as illustrated in figure 5b. (Lynch et al. 2009). This is accompanied by a shift of frequency of naïve and memory T-cell, in favour of the

memory T-cells (Schwab et al. 1997), and a decrease in TCR diversity in both populations (Arstila et al. 1999; Gorozy and Weyand, 2005)

The results of these changes are increased vulnerability to infection, higher incidence of cancer and autoimmune disease, decrease of vaccination efficiency. It is also important to point out that a number of medical treatments including radiation and chemotherapy can cause acute transient thymic involution. Recovery of the peripheral T-cell pool after BM transplant in elderly patients is severely delayed, or in some cases abscent (Hakim 2005). These patients, as well as patients suffering from severe infections, including HIV, that impede the correct function of the immune system would greatly benefit if their immune system could be boosted or stimulated in order for rapid restoration to take place.

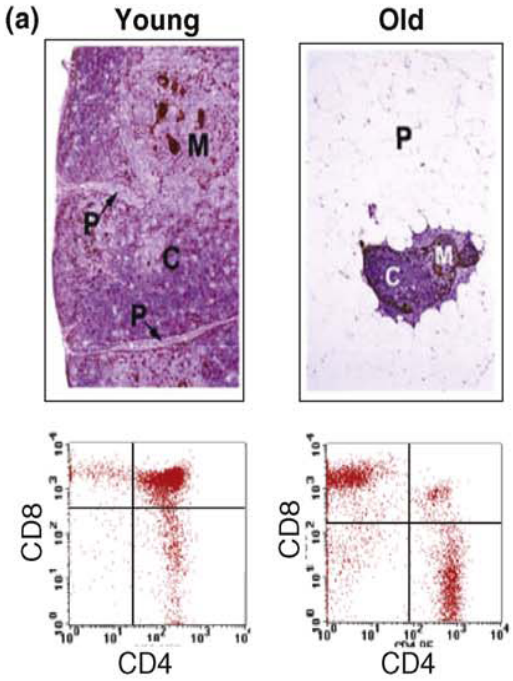


Figure 4 Thymic function decreases with age. (a) Top panel shows cytokeratin-immunostained and hematoxylin& eosin (H&E)-counterstained thymus sections from healthy young and aged human donors. Aged thyme show an expansion of the perivascular combpartment (P), and constriction of cortex (C) and medulla (M).
There is also a clear reduction in double positive (DP) CD4+CD8+ T in aged individuals. (Sempowski et al. 2009)

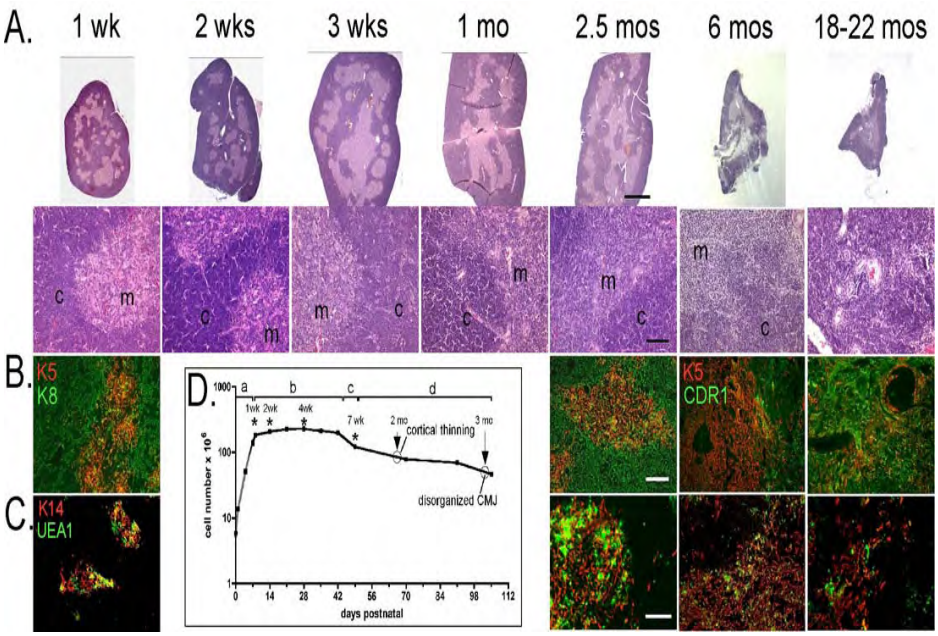


Figure 5. A.Lifespan analysis of thymus structure (Manley lab). A. H&E stained sections of mouse thymus from 1 week postnatal through 18-22 months of age, show age induced changes (A). Reduction in size and cortico-medullary disorganization with age(A,B,C), reduction in T-cell numbers (D)**.** .

1.8 Mechanisms of thymic involution

Thymic involution becomes well defined at around the same time as the onset of puberty in humans. This, along with the fact that surgical or chemical castration leads to active thymic rebound (Henderson 1904) has implicated sex steroids in thymic involution. Exogenous introduction of sex steroids in the adult leads to almost a complete collapse of thymocyte development due to apoptosis mainly of the immature cells located in the cortical region of the thymus, whereas castration or chemical blockade of sex steroid production leads to rapid regeneration of the thymus (figure 6). Interestingly the thymus also undergoes a reversible transient involution during pregnancy (Tibbetts et al. 1999).

A contributing factor in age-related thymic involution may also be the accumulation of defects in the T-cell progenitor cells, which leads to reduced proliferation and survival rates of T-cells compared to young mice (Min et al. 2004; Bennett et al. 2002). This could lead to effects on the thymic stroma, and interfere with the ability of the stroma to support T-cell development, leading to a reduction in output of T-cells (Min, Montecino-Rodriguez et al. 2004; Linton & Dorshkind 2004).

Interestingly it has been demonstrated that transplantation of BM derived from young mice into mice that have an aged thymus does not lead to increase in thymopoises, whereas the transplantation of BM derived from old mice into young mice with a non involuted thymus did not diminish thymopoisis, suggesting that defects in stroma compartments are primarily responsible for the decrease in T-cell output observed with age (Mackall et al. 1998)



Figure 6. Comparison of mice thymus at different age and after SSA.

Models of thymic regeneration after involution.

When aged mice displaying all signs of thymic involution underwent castration their thymi were able to regenerate and reached the same size observed in young mice before the onset of involution (Gray et al. 2006; Heng et al. 2005; Sutherland et al. 2005).

Within 3 days of castration, there is a significant increase in all the TN subsets, by day 5 these levels are identical to levels in the young individuals. An increase in number of these populations is also accompanied by elevation of IL-7 levels (which has been shown to influence T-cell survival) and increased proliferation in all subsets of thymocytes. Increase in number of mature DP cells are achieved by day 10 and total thymocyte numbers reach levels of young controls by day 7 and further increase for 2-4 weeks (Lynch et al. 2009).

It has been demonstrated that aged thymi can be regenerated when transplanted into young mice, which could indicate a role of cytokines in the regeneration process (Nobori et al. 2006). Keratinocyte growth factor (KGF) has been shown to induce TEC proliferation after administration, with T-cell output numbers increasing, and restoration of thymic architecture observed (Nobori et al. 2006; Min et al. 2007; Rossi, Jeker, et al. 2007). Administration of KGF to young mice increased thymus cellularity, with increase is cell number reported in all T-cell compartments, while administration of KGF in old mice lead to increase in cellularity to levels observed at 1 month postnatally (Min et al. 2007) KGF is produced by mesenchymal cells in the thymus and acts through a IIIb isoform of FgfR2 (FgfR2IIIb), which is expressed on TECs of all lineages. KGF is required for correct organogenesis to proceed during development, however KGF null mice do not display any adverse phenotype in homeostatic condions, but.show poor recovery rates after injury (Alpdogan et al. 2006). KGF is currently administrated to patients before myeloablative therapy (Radtke & Kolesar 2005) Another factor that stimulated thymus regeneration is IL-7, however this regeneration is not complete. Administration of IL-7 in order to stimulate recovery of an involuted thymus have produced varying results, with some studies reporting no effect of IL-7 on thymic rebound , while some reported an increase in TN T-cells

(Andrew & Aspinall 2001; Pido-Lopez et al. 2002; Sempowski et al. 2002). However IL-7 treatment in models of henatopoetic stem cell transfer has proven extremely beneficial and has been shown to boost T-cell reconstitution (Abdul-Hai et al. 1996; Alpdogan et al. 2003; Bolotin et al. 1996; Mackall et al. 2001).
Drugs based on IL-7 are currently undergoing clinical trials for use in humans.

1.9 Role of *Foxn1* in thymic involution

Foxn1 has been implicated to play an important role in thymus involution. A recent report that demonstrated that mice that display an early decrease in *Foxn1* levels, with levels at 5 weeks of age comprising only 20-30% of wild-type expression levels, have a phenotype that strongly resembles early onset involution (Chen et al. 2009). The premature reduction of *Foxn1* expression levels causes decreased thymocyte output, as well as a decrease in TEC numbers and proliferation rate, and loss of functional TEC – in particular mature mTEC (Chen et al. 2009) Figure 7.

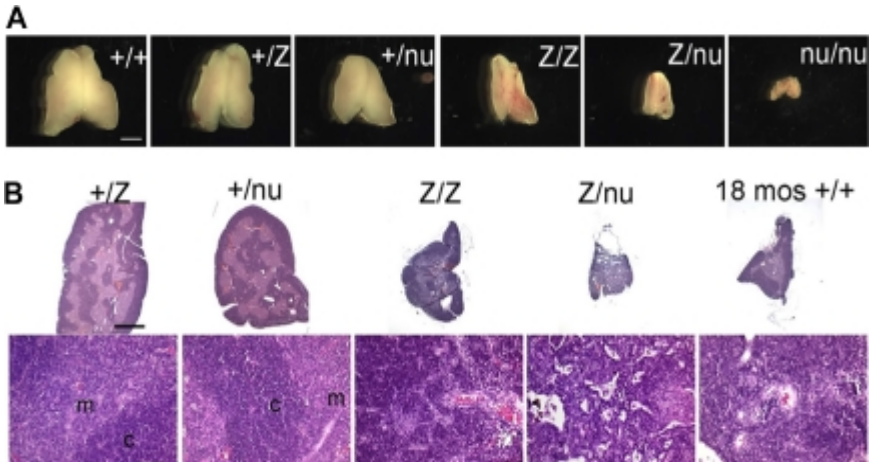


Figure 7 Reduction of Foxn1 levels induce thymic involution in postnatal mice.

Another study utilized a transgenic mouse model where loxP sites were introduced in order to achieve Cre mediated excision that lead to the disruption of the *Foxn1* locus. Postnatal disruption of *Foxn1* expression resulted in thymic atrophy and degeneration of TEC architecture (Cheng et al. 2010). All though the results of this study are in line with previous findings, a caveat if this study is that it utilized a ubiquitously expressed CreER^{tm}. It has been demonstrated that activation of Cre in all cells has been shown to result in a multitude of defects in hematopoietic cell types, such as high apoptosis rate, proliferation defects (Higashi et al., 2009). Without the use of appropriate controls allowing to determine effect of ubiquitous Cre activation, which were absent in this study, the specific affects of *Foxn1* disruption cannot be determined.

In a further mouse model mice expressing the human defteria toxin receptor under the control of *Foxn1* were developed. Diphteria toxin was then injected into pregnatnt females at E10.5-E12.5, this strategy ensured acute ablation of *Foxn1*+ cells, and showed an inability of restoration of the thymus. Taking this data into account the authors conclude that TEC progenitors are *Foxn1* positive and so are lost during the administration of the DT treatment. The same study also provided data on the results of chronic sub-acute ablation of *Foxn1*+ cells in the thymus. In this mouse model, a transgene coding for a Foxn1 fusion protein engineered to contain an extension of 82 glutamine residues to the N-terminus of the protein was expressed in *Foxn1*+ cells. This fusion protein is cytotoxic, making it possible to ablate *Foxn1*$^{+}$ cells. Ablation of the *Foxn1*$^{+}$ cells resulted in decreased T-cell output and degeneration of the TEC network. This analyses reveals that loss of *Foxn1*$^{+}$ cells results in severe effects to thymic architecture and T-cell differentiation (Corbeaux et al. 2010). The authors of this study conclude that progenitor cells are *Foxn1*+ since both models of cytoablation display an inability to regenerate a functional thymus.
However this conclusion may be premature, since it is unclear how such harsh disruption of the thymic environment can affect other cells. Another explanation could be that all though progenitor cells in the thymus are *Foxn1*- or low, they are intimately linked with the *Foxn1*+ compartment, and are unable to recover after their loss.

In a recent study performed in our lab it was demonstrated using a Foxn1ER mouse model, where high levels of *Foxn1* could be artificially induced in TEC, that maintaining high levels of *Foxn1* expression delayed the onset of involution (Bredenkamp unpublished) while inducing high levels of *Foxn1* expression in involuted thymi restored thymic architecture and T-cell output to levels observed in young mice (Bredenkamp unpublished).
A similar study where *Foxn1* was continuously driven from a human Keratin14 promoter, showed that continuous expression of *Foxn1* lead to higher T-cell numbers, showed less of a decline in recruitment of early T-cell progenitors, and displayed less morphological disorganization than age matched controls. These mice also displayed an increase in the number of MHC II^{hi} cells compared to age matched controls (Zook et al. 2011).

Collectively, the studies described above show that *Foxn1* is indispensable for thymic maintenance in the postnatal thymus.

1.10 Identifying stem/progenitor cell activity

The ability to mark single cells in a way that is capable of being passed on to the progeny of these cells is the major component of any lineage trace. These studies are becoming increasingly popular, as it provides information on the exact location of the labeled cells in vivo, number of generated progeny and their ability to give rise to different cell types.

There are several ways in which lineage tracing can be carried out, all these methods as well as their advantages and disadvantages have been discussed in detail in a recent review (Kretzschmar & Watt 2012).

Transplantation of tissues of cells is yet another way to assess the capability of cells to contribute to other cell lineages. This method can be used to generate interspecies chimeras or same species chimeras with a possibility to discern between the cell (for example this can be accomplished by MHC II mismatching or fluorescent labeling of cells) (Blackburn et al. 1996).

The primary goal of work described in this thesis was to establish the relationship between different subsets of TEC and to identify stem/progenitor cells that are capable of maintaining the thymus. In order to achieve this goal two separate methods of lineage tracing were used and are described below.

One of the methods used - direct transplantation of cells isolated using fluorescent cell tagging and flow cytometry. This method provides the ability to purify the cell type of interest and assess its potency by transplantation into an ectopic site of an immunocompatible mouse, was used in a variety of studies in different tissues (Oshima et al. 2001; Rochat et al. 1994; Bennett et al. 2002). Although this assay is capable of providing information on the plasticity and differentiation capacity of the input test cells it is important to keep in mind that this method has a potential flaw. In order to transplant the test cells they need to be isolated from the tissue, which leads to a disruption in the structure of the tissue, and cell to cell interactions. This can significantly alter cells behavior. Indeed several studies have shown that transplantation assays can give a different result from in vivo cell labelling that does not disrupt tissue homeostasis, and often recapitulate in vivo regeneration mechanisms that occur after injury or infection, and not in a stable state. Lineage tracing of adult bulge cells has shown that in a homeostatic environment they exhibit a more restricted lineage potential (Levy et al. 2007; Tumbar et al. 2004; Ito et al. 2005), however the same cells are able to give rise to all epidermal cell types when tested using transplantation assays (Morris et al. 2004; Jaks et al. 2008). This was further demonstrated in a recent study which showed that Lrig1+ cells upon transplantation can give rise to all lineages of the epidermis in transplantation assays, showed a more restricted contribution in an undisrupted steady state in vivo environment (Jensen et al. 2009).

Another method used for assessing potency and differentiation capaciry of cell is -labeling cells with a genetically heritable marker. This has become one of the most popular choices for lineage tracing. In mice the Cre-loxP system is one of the most common methods used. It requires Cre, or CreERT2 recombinase to be expressed from a promoter specific to the cell type of interest (Zhang et al. 1996). Mice expressing Cre or CreERT2 can then be crossed with mice of a reporter mouse strain,

where loxP-stop-loxP or “floxed” sequence. When animals expressing both construct are generated in allows for the Cre or CreERT2 to excise the “floxed” stop sequence and permanently label the cells of interest, and ensure that the label is passed onto any progeny this cell may produce. This method allows to determine the differentiation capacity of a specific cell type in a homeostatic in vivo environment.

Used in combination these methods become powerful tools in identifying stem/progenitor cells and their ability to contribute to other cell lineages.

Aims:

The initial aim of the work presented in this thesis was to investigate possible mechanisms of thymus maintenance and regeneration. This work was designed to help determine whether the thymus is maintained by a stem cell mechanism, or if its structure is maintained by division of terminally differentiated TEC. The additional aim of this work was to establish the molecular requirements of the TEC progenitor/stem cell compartment, specifically the experiments designed were aimed to test whether *Foxn1* is required in these cells, or if these cells are in fact negative or low for *Foxn1*. Furthermore the establishing the lineage relationship between the different subsets of TEC was one of the primary goals of this work.

Chapter 2: Materials and Methods

2.1 Mice

All experiment were performed in accordance with the UK Animal (Scientific Procedures) Act 1986. Animals were house in the University of Edinburgh Roger Land Animal Facility until 2011, and then moved to the new animal Unit in the SCRM building. Mice were kept on a 12-hour light/dark cycle and had no restrictions in food and water supply.

2.1.1 Mouse lines used in experiments

Foxn1^{CreERT2} a novel mouse line developed in our laboratory by Terry Gaskell a former post doc. The Cre recombinase expression in these mice is driven by the *Foxn1* promoter, and targeting the IRES-CreERt2-frt-neo-frt insert into the 3' UTR allows for unimpeded Foxn1 expression. When crossed to a silent reporter strain and injected with tamoxifen the Cre can undergo nuclear translocation and act on specific excision points, allowing the expression of the reporter fluorescent protein.

Rosa26^{CreERT2} mouse line expressing Cre under the ubiquitous Rosa26 promoter. When crossed to a silent reporter strain and injected with tamoxifen the Cre can undergo nuclear translocation and act on specific excision points, allowing the expression of the reporter fluorescent protein (Hameyer et al. 2007).

sGFP-7 is a silent reporter strain that harbours a randomly integrated transgene (PGK-loxP-Puro-STOP-loxP-EGFP-pA) which upon excision of the STOP cassette constitutively expresses cytoplasmic GFP (Gilchrist et al. 2003) (Figure 2 A)

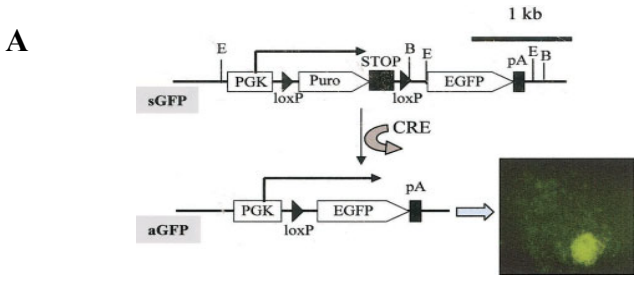
Rosa26-td-RFP is a silent reporter strain that harbours a td-RFP transgene in reverse orientation floxed by heterotypic lox sites, loxp and loxp2272, knocked in at the Rosa26 locus by homologous recombination. RFP is activated by Recombinase mediated gene expression (RAGE) following an inversion of td-RFP and excision of STOP cassette by Cre mediated recombination. (Luche et al. 2007) (Figure 2 B)

Rosa26-CN2-YFP silent reporter strain expressing nuclear bound YFP protein upon excision of STOP cassette (Srinivas et al. 2001). The transgene SA-loxP-PGK-neo-

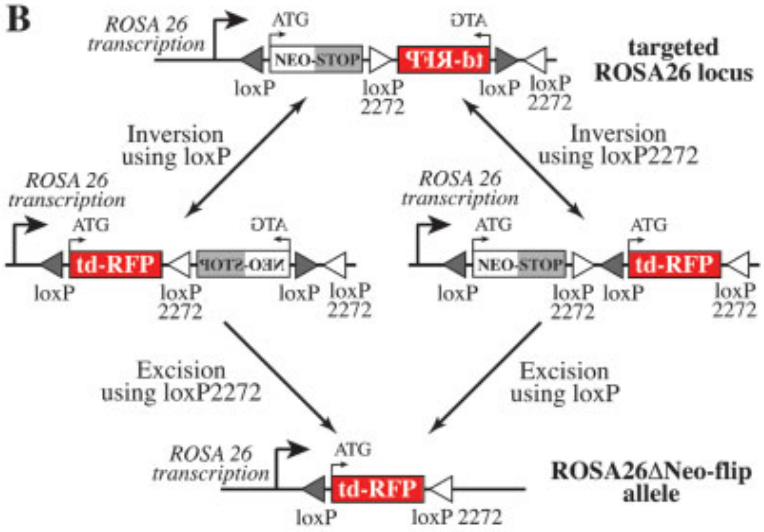
tpA-loxP-EYFP-bpA was targeted to the mouse Rosa26 locus via homologous recombination. EYFP expression is driven by the endogenous Rosa26 promoter following Cre mediated excision of the Neo selection cassette (Figure 2 C)

Gt(ROSA)26Sortm4(ACTB-tdTomato,-EGFP)Luo/J, hereafter referred to as the RED/GREEN reporter strain (R/G), - double-fluorescent Cre reporter mouse that expresses membrane-targeted tandem dimer Tomato (mT) prior to Cre-mediated excision and membrane-targeted green fluorescent protein (mG) after excision. (Figure 2.1) (Muzumdar et al. 2007)

Foxn1Cre mouse line was generated by homologous recombination with an IRES-Cre cassette insertion targeted to the 3' UTR of *Foxn1*. (Gordon et al. 2007)



Gilchrist et al, 2003



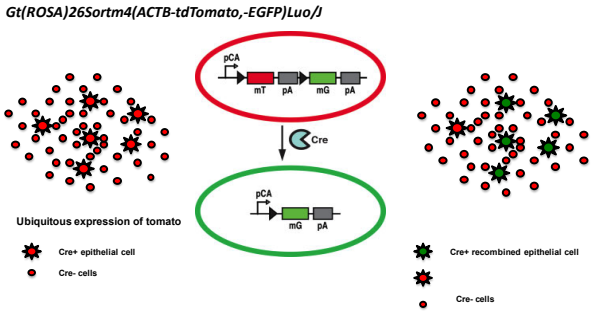
C

Luche et al, 2007



Srinivas et al, 2001

D



Muzumbar et al. 2007

Figure 2.1 Schematic representation of the sGFP-7, Rosa26-td-RFP, Rosa26-CN2-YFP and Red/Green reporter line function.

2.2 Tamoxifen treatment of mice

Tamoxifen and 4OH-tamoxifen were dissolved in 100% ethanol and further diluted with a cremaphore/PBS solution.

For embryo analyses pregnant mothers received either one or several intraperitoneal (IP) injection of either 4OH-tamoxifen (4OHT) (Sigma-Aldrich) or tamoxifen (Sigma-Aldrich) at the developmental stage of interest. Females were sacrificed 24 hours after the last injection and their uteri were removed. Pups were removed from uterus, and only viable embryos were included in the analyses.

For adult analyses animals received a single or multiple injections spread out over a maximum of 4 days. Depending on the analyses mice received IP injections from 1,5 to 5mg of tamoxifen per injection in a 0.5ml injection volume.

2.3 Embryo collection

When required mating were set up between *Foxn1*^{CreERT2} males with various reporter strain females, or C57BL/6 females and CBA males. Mice were set up in the same cage in the late afternoon and kept together overnight. The following day females were examined for the presence of a vaginal plug. The day when the vaginal plug is noted is taken as embryonic day 0.5 (E0.5). On the day of the necessary developmental stage used for analyses pregnant females were sacrificed using an approved schedule 1 method (cervical dislocation). The uterus was dissected out and kept in PBS on ice. The embryos were removed from the uterus and all extraembryonic tissue removed. Embryos were decapitated and E12,5-17,5 thymi removed from the chest cavity and collected in tubes containing PBS and 10% FCS.

2.4 Immumohystochemistry

Tissue dissected from mice was embedded in OCT compound (Tissue Tek, Mie Inc., USA) and placed on dry ice for an hour to set. After this the blocks were transferred to a -80^{o}C freezer for long term storage. For further analyses frozen block were sectioned using a cryostat (Leica CM1900). 8μm sections of tissue were collected onto poly-L-lysine coated glass slides (VWR International). Sections were either used for staining immediately or stored at -80^{o}C until required for analyses.

2.4.1 Staining procedure

Tissue sections collected on poly-L-lysine coated glass slides were recovered from -80C storage and allowed to air dry for 15-20min. Sections were then fixed for 2 minutes in ice cold acetone and allowed to dry again. A wax pen was used to surround each sectioned. Tissue was then blocked using a blocking solution consisting of PBS and 5% serum native to the animal of the secondary antibody species. Primary antibodies were added in the relevant dilution in PBS and 1% serum solution and allowed to incubate for an hour or overnight when necessary. The primary antibody solution was washed off by submerging the slides in PBS for 5min 2-3 times. Secondary fluorochrome-conjugated antibodies were added in PBS/1% serum solution in 1:1000 dilution and incubated in the dark for 45 minutes. Fluorochrome-cojugated antibodies used were Alexa with an emmision spectrum of 488, 568, 647. After the incubation time was finished the same washing steps as described for the primaries were applied. Sections were then allowed to air dry and mounted using the Vectashield hardening mountant (Vector labs) or glycerol/PBS mix.

2.4.2 Imaging

Fluorescent images were acquired using the Leica AOBS confocal microscope or Olympus BX61 widefield microscope using the appropriate excitation conditions. Images were processed using the Image J free software or Adobe Illustrator.

2.5 Cell preparation for cell sorting and FACS analyses

2.5.1 Preparation of embryo thymic tissue for cell sorting and Facs analyses

Thymi dissected out of embryos were resuspended in PBS containing Ca and Mg with hyalorudinase, 0,7mg/ml (Sigma), and collagenase, 0,36mg/ml, enzymatic mix also containing 0.05mg/ml deoxyribonuclease I. Thymi were incubated for 15 min at 37^{o}C. Every 4 minutes the samples were gently pippetted to aid the dissociation. Dissociated cells were then spun down at 1200rpm at 4^{o}C for 5 min and collected into FACS wash (PBS with 5% fetal calf serum). Cells were then stained with primary antibodies on ice for 20min. They were then washed in Facs wash and where necessary secondary antibodies were applied and washed off in 15 min.

2.5.2 Preparation of adult thymic tissue for cell sorting and flowcytometry analyses

Thymi were dissected out into a PBS filled Petri dish and further cleaned of any non-thymic tissue. The thymic capsule was ripped and the lobes were gently agitated to release T-cells. The thymic lobes are then transferred into a tube and disrupted using scissors. They are then resuspended in a dissociation media (RPMI-1840 HEPES media (Invitrogen) with collagenase D 1.25mg/ml (Roche) and Dnase I 0.05mg/ml) for 15 minutes at 37^{0}C. To aid the dissociation process every 5 minutes the solution with the thymic fragments was disrupted by pippeting using a 1ml blue tip. After the incubation was complete the supernatant was taken off and filtered through a 70μm cell strainer. The remaining thymic fragments were resuspended in fresh dissociation media and the process described above was repeated a further 2 times. Any remaining fragments of tissue are resuspended in RPMI-1840 HEPES media with collagenase/dispase 1.25mg/ml for a further 30min.

2.5.3 Postnatal enrichment of TEC

In order to maximize the efficiency of cell sorting, a depletion of CD45 positive T-cells was performed using α-CD45 magnetically labelled antibodies (Miltenyi Biotech). The procedure was executed according to the guidelines of the manufacturer (5μl of magnetic microbeads per 10^7 cells). The cell suspension was then incubated at +4^{0}C in the dark. After a wash step the cell suspension was then either run on a AutoMacs (Miltenyi Biotech) using the Depletes programme available on the instrument, or in other instances LS columns (Miltenyi Biotech) were used with the QuadroMacs (Miltenyi Biotech). The CD45- fraction was collected by centrifugation and then resuspended in the necessary antibody cocktails for staining.

2.6 Cell Staining

Below is a list of antibodies used for IHC and Flowcytometric analyses.

2.6.1 Antibodies used for IHC

Name	Clone	Source	Species and isotype	Specificity	Dilution
α-K5	AF 138	Covalence Research Products	Rabbit IgG	Subset of mTEC	1/800
α-K8	Troma 1	DSHB	Rat IgG2a	Subset of cTEC	1/5
α-K14	AF 64	Covalence Research Products	Rabbit IgG	mTEC	1/800
CD205		AbD Serotec	Rat IgG	cortex	1/10
UEA1	Biotinilated	Vector Labs	biotinilated	medulla	1/400
B5t	Rabbit pAb	MBL PD021	Rabbit IgG	cortex	1/250
CD45	30-F11	eBiosciences	Rat IgG2b	T-cells	1/50
Pancyto keratin	pAb	DAKO	Rabbit IgG	All TEC	1/200
MTS24	mAb	Gift of R. Boyd	Rat IgG	Subset of mTEC	1/3
Ly51	6C3	Biolegend	Rat IgG2a	cortex	1/50
Aire1	pAb	Santa Cruz Biotechnology	rabbit	medulla	1/250
α-GFP	Chicken pAb	Abcam	IgY	GFP	1/1000

2.6.2 Antibodies for flowcytometric analyses

Name	Clone	Source	Fluorochrome	Species
NK1.1	PK136	Biolegend	FITC	Rat IgG2a
CD45	30-F11	eBiosciences	APC, FITC, PerCP/Cy55	Rat IgG2b
CD8	53-6.7,	eBiosciences	Fitc, APC, PerCP/Cy5.5	Rat IgG2a
CD4	RM4-5	eBiosciences	Fitc, APC, PerCP/Cy5.5	Rat IgG2a
CD3e	145-2C11	eBiosciences	Fitc, APC, PerCP/Cy5.5	Hamster IgG
TCR B	H57-597	Biolegend	Fitc, APC, PerCP/Cy5.5	Hamster IgG
CD31	390	Biolegend	Fitc, APC, PerCP/Cy5.5	Rat IgG2a
Epcam	G8.8	Biolegend	Fitc, PE, APC, PerCP/Cy5.5, APC Cy7	Rat IgG2a
Ly51	6C3	eBiosciences	Fitc, PE	Rat IgG2a
MHC II	M5/114.15.2	eBiosciences	PE Cy7, PE	Rat IgG2b
CD11c	HL3	eBiosciences	APC, FITC, PerCP/Cy5.5	Hamster IgG1
Ter119	Ter-119	eBiosciences	Fitc, APC, PerCP/Cy5.5	Rat IgG2b
CD19	1D3	Biolegend	Fitc, APC, PerCP/Cy5.5	Rat IgG2a
GR-1	RB6-8C5	Biolegend	Fitc	Rat IgG2b
UEA1	Biotinilated lectin	Vector Labs	Biotinilated	

2.7.3 Flow cytometry instruments

All flow cytometric analyses was performed on the BD LSRFortessa cell analyzer. This cell analyser made it possible to include up to 8 fluorocromes in any given analyses simultaneously with minimum compensation problems.

All cell sorting was performed by Simon Monard and Olivia Rodrigues using the BD FACSAria II at the Institute of Stem Cell Research.

Data collected was analysed using the Flowjo analyses software.

2.8 Tissue culture

All procedures were performed in a sterile environment using a Laminar flow sterile hood and employing the necessary sterile techniques. The appropriate solutions were warmed to 37^0C before use. Were necessary cells were examined using an inverted microscope (Olympus CK2). Cell counts were performed using a haemocytometer.

2.8.1 Preparation and maintenance of MEFs

E13,5 mouse embryos were extracted from the uterus and cleaned of all extraembryonic tissue. Embryos were then decapitated and all the internal organs were removed. The remaining tissue was washed with sterile PBS several times and then resuspended in 5ml trypsin for 10 minutes at 37^0C. After the addition of 10 ml of Fibroblast media, they were gently pulled through a 10ml pipette and centrifuged at 1200rpm for 5 minutes at room temperature. The cell pellet was then resuspended in 5 ml of fresh Fibroblast media. Any remaining fragments were allowed to settle before aliquots were distributed into T25 or T75 tissue culture flasks in 5 or 10ml of media respectfully. Media was replaced the next day to remove any non-adherent cells. Generally MEFs were used within a week before they required passaging, however in some cases up to two passages were allowed.

<u>Contents of the Fibroblast media</u>

1xDulbeco modified Eagle medium (DMEM)

10% FCS

2mM sodium pyruvate

50ug/ml penicillin

50ug/ml Streptomycin

2.8.2 Thymic reaggragation

Cells isolated from an adult aGFP mouse 4-8weeks old were isolated using the appropriate antibodies by flow cytometry (using the Facs Aria). Approximately 10 thousand sorted cells of interest were mixed with 200 thousand MEFs and E12,5-E13,5 wild type thymic lobes and spun down in a plugged pipette tip and placing on a 0.8mm filter overnight according to the method developed previously in our laboratory (Sheridan et al. 2009). The next day the formed reaggregates were grafted under the kidney capsule of an immunologically compatible mouse.

Reaggregate medium

1x DMEM with HEPES and glutamax

2% non essential amino acids

10% faetal calf serum

2mM sodium pyruvate

50ug/ml penicillin

50ug/ml Streptomycin

2.9 Kidney Grafting

The surgery was performed in a specially designated procedure room in aseptic conditions. F1 male mice were anaesthetized using isofluorane. For pain relief a subcutaneous injection of 0.1ml Rimadyl was administered to the animals prior to the beginning of the surgery. Under general anaesthesia an incision was made on the side of the mouse between the ribcage and hind leg, and the corresponding kidney was exposed. A tear was made in the kidney capsule using fine forceps and the reaggregate inserted under the kidney capsule. The kidney was returned to its original location and the peritoneal cavity closed by suturing, the skin was clipped to close the wound resulting from the incision.

2.10 Inutero injections

Surgery was performed using aseptic techniques in a specially designated lab space. The pregnant females were anaesthetized using either isufluorane or an injectable anaesthetic. Mice were then injected subcutaneously with 0.3ml PBS, and 0.1ml of Rimadyl to provide pain relief. Hair was then removed from the abdominal area. The first incision was made in the midline of the lower abdomen, care was taken to avoid major blood vessels. One of the horns of the uterus was then carefully pulled through the incision site using blunt forceps. Once exposed injections were administered either into the amnion or placenta using a mouth pipette. The horns of the uterus were then carefully restored to their original position. Dissolvable sutures were then used to close the incision made in the muscle tissue, while the skin was sutured with non dissolvable sutures or sealed using a surgical clip.

2.11 Isolation of nucleic acids

Genomic DNA isolation

Mouse ear punch DNA: lysis buffer cointaining proteinase K was added to the sample and was incubated over night at 55ºC. In order to denature the proteinase K the sample were incubated for 10 minutes at 95ºC, after which the samples were spun down for 10 minutes at 13 thousand rpm. The cell lysate was used for PCR analyses.

Mouse tail DNA: lyses buffer was added and incubated at 55ºC overnight. DNA was acquired using standard phenol extraction, and then precipitated using equal volume of isopropanol, washed with 70% ethanol and dissolved in TE buffer.

RNA isolation: all RNA isolation was performed using the RNAse easy kit (Qiagen). DNase treatment was performed on the colume using RNase-free DNase (Qiagen).

2.12 Genotyping PCR

Genotyping PCR was performed using DNA isolated from ear punches of relevant mice. For genotyping of the Foxn1CreErt2 mice CRE145F and CRE817R primers were used with an expected product size of 403bp for transgenic mice. For the Red/Green mouse line the oIMR7318, oIMR7319, oIMR7320 primers were used that allowed to distinguish between homozygous, heterozygous or WT mice, with a single product of 250bs expected for the homozygous mutant mice, two products of 250 and 330bs expected for the heterozygous mutants, and a single 330bs product indicating a WT mouse.

For Foxn1^{CreERT2} a PCR strategy was developed that allowed for distinction between homozygous and heterozygous animals. For this PCR three primers were used (Foxn1^{CreERT2} F; Foxn1^{CreERT2} WT, Foxn1^{CreERT2} R). Foxn1$^{CreERT2/CreERT2}$ mice and WT mice displayed a single 1200bp or 863bp product respectively, while the heterozygous mice displayed both products mentioned above.

PCR primer	Sequence (5'-3')
Cre145F	GACCAGGTTCGTTCACTCATGG
CRE817R	CCTTAGCGCCGTAAATCAATCG
GFP F	ACATGGTCCTGCTGGAGTTC
GFP R	TCAAGGTTCAGGGGGAGGT
oIMR7318	CTCTGCTGCCTCCTGGCTTCT
oIMR7319	CGAGGCGGATCACAAGCAATA
oIMR7320	TCAATGGGCGGGGGTCGTT
Foxn1^{CreERT2} F	TAGTGAAACAGGGGCAATGGTG
Foxn1^{CreERT2} WT	CCGCATCACCAGACTCCTGTTC
Foxn1^{CreERT2} R	GGGATGAGGTTTGGAGGGGTGAT

2.13 Southern blot analyses

All work with radioactivity was performed in accordance with the regulation on radioactive work in a specifically designated area. Hybridizations were carried put using the Amersham Rapid-hyb buffer (GE Healthcare) in Techne hybridization bottles, which were placed in a Techne HB-1 rotation oven overnight at 65ºC. Rapid-hyb buffer was used for pre-hybridization of Southern blots. 20 ng of labelled probe was added to the buffer and allowed to hybridize overnight. Blots were then washed for 2x15 minutes in pre-warmed to 65ºC 2xSSC with 0.1% SDS. If radioactivity levels remained high the blots received additional 2x15 minute washes in 1xSSC with 0.1% SDS. In some instances another wash using 0.5xSSC with 0.1% SDS was required. Blots were then wrapped in Saran wrap and placed in a lightproof cassette with autoradiographic film at -80ºC for 2days and up to 2 weeks. The film was developed using the film developer.

Chapter 3: Characterization of the Foxn1^{CreERt2} mouse line

Introduction:

In Foxn1 null mice development of the thymus is arrested between day 11.5 of embryonic development (E11.5) and E12.5 (Cordier, 1975, Flanagan, 1966; Nehls et al., 1994). In these mice the thymic primordium fails to undergo vascularisation and seeding with lymphocytes. Foxn1 null TEC also showed reduced proliferation at E12.5. Furthermore, Foxn1 null TEC could not contribute to TEC networks in allophenic chimeric mice (Itoi et al., 2001, Blackburn et al., 1996; Gordon et al., 2007; Flanagan, 1966; Nehls et al., 1996). Perinatal reactivation of *Foxn1* in a conditional revertible null transgenic model resulted in development of properly formed medullary and cortical areas (Bleul et al. 2006), establishing that in the absence of *Foxn1,* TEC development is arrested at an early progenitor stage. This pool of arrested progenitor cells remains stable and can be reactivated up to 4 months postnatally (Nowell et al. 2011). It has also been shown, using an array of mutants generated from hypomorphic, wild type and null alleles of *Foxn1,* that *Foxn1* is required in a dose dependant manner to mediate the cortical and medullary TEC differentiation programmes, from exit from the earliest progenitor state to terminal differentiation (Nowell et al., 2011). *Foxn1* is expressed in all TECs throughout development, displaying a heterogeneous expression pattern depending on TEC sub-type, with the highest levels of *Foxn1*in adult mice being detected in mature cortical thymic epithelial cells (TEC) (Bredenkamp unpublished). Taken together, these data indicate that *Foxn1* is not required for lineage specification or commitment, but is required as a critical regulator of TEC differentiation. It is now clear that in addition to its role in fetal TEC, Foxn1 is also required for thymic maintenance and homeostasis in postnatal mice (Chen et al 2009, Cheng et al 2010, Sun et al 2010).

Based on these data I set out to determine whether *Foxn1* negative thymic epithelial progenitor or stem cells might be responsible for maintenance of the TEC compartment of the adult thymus. For this purpose, I proposed to use a *Foxn1*^{CreErt2}

transgenic mouse model that was generated in this laboratory, in which CreERt2 was knocked in to the 3'UTR of *Foxn1* by homologous recombination in ES cells, using the homology arms previously used to generate the well characterized Foxn1Cre delete line (Gordon et al. 2007). At the time of starting this work, the *Foxn1*^{CreERt2} mouse strain had been generated but not characterized (Figure 3.1 A,B).

In order to establish whether the thymus is maintained by Foxn1^{+} or Foxn1^{-} cells, I proposed to utilize the *Foxn1*^{CreERt2} mouse, in combination with a conditional reporter mouse line, to determine whether or not cortical and medullary TEC are replenished by *Foxn1*$^{+}$ TEC. For this, I proposed to use a pulse-chase approach, to heritably genetically label TEC that expressed *Foxn1* at a given time-point, and then determine the fate of the labelled cells (Dor et al. 2004). If the postnatal thymus is maintained by Foxn1^{+} cells, then after tamoxifen induction the chase group of mice would exhibit a steady number of GFP labelled cells. However if the thymus is maintained by a Foxn1^{-} thymic epithelial stem cell or progenitor cell, the number of GFP labelled cells would decline over time (Figure 3.1 C).

In this Chapter, I describe detailed characterization of this novel deleter strain, including optimization of conditions for attaining maximum Cre-mediated deletion in fetal and adult TEC.

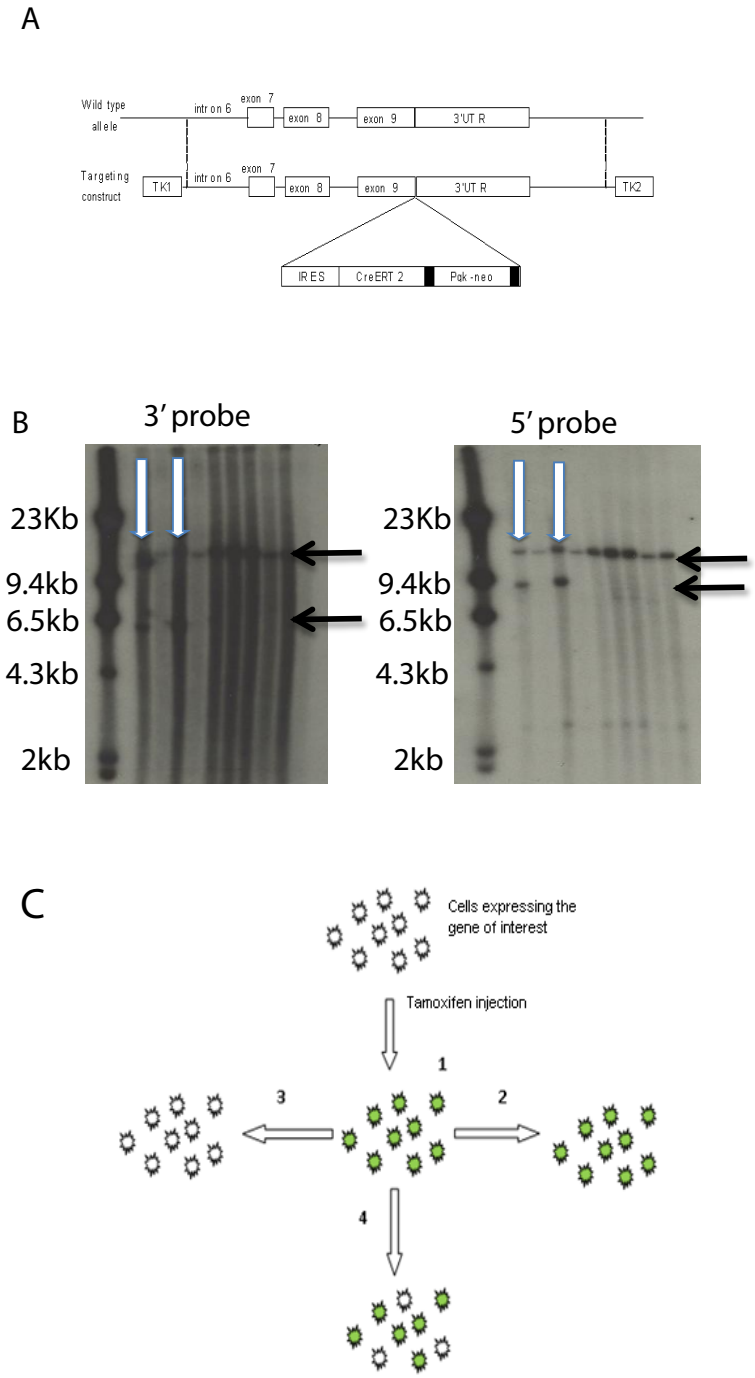


Figure 3.1 Novel Foxn1CreERT2 mouse line.
Schematic representation of the targeting vector used for homologous recombination (A),
Verification of correctly targeted mutants by Southern blott analyses (B). Possible outcomes of lineage tracing experiments performed on these mice (C).

3.1 Analysis of recombination in the Foxn1^{CreErt2} mouse line

In order to determine whether CreERt2 activity faithfully reported *Foxn1* expression, rigorous analysis to establish the specificity of recombination, and to test for any tamoxifen-independent Cre-mediated recombination (called 'spontaneous recombination' hereafter) events, was carried out. Tamoxifen titration was thus carried out at different stages of fetal and postnatal development, in order to establish the optimal dose of tamoxifen for cell labeling *in vivo*, as well as specificity of labeling and possibility of spontaneous recombination.

3.1.1 Analysis of recombination during fetal development.

Foxn1 can initially be detected by RT-PCR as early as E9 in whole embryos, E10.5 in the thymus (Balciunaite et al. 2002), with peak levels of expression in the thymus detected at E12.5 in TEC (unpublished data, Blackburn laboratory). In accordance with these data I initially tested the outcome of inducing Cre activity by tamoxifen injection at E12.5 and E15.5, in order to test the fidelity of recombination in thymus at different stages in fetal development.

Thus, *Foxn1*$^{CreERt2/+}$ males were crossed with females of different reporter lines. The pregnant females were injected at E12.5 or E15.5 with different doses of 4-hydroxy tamoxifen (4OHT). For controls, pregnant females were injected with carrier solution, to identify any spontaneous recombination that had occurred. These experiments also utilized CreERt2-negative littermates to control for effects of 4OHT on the system.

The female mice were given either a single injection of 4OHT, or one injection on each of two consecutive days, and the embryos analysed 24 hours after the last injection. Thymi were dissected, dissociated and then stained with a panel of antibodies before analyses using flow cytometry, or were processed for IHC.

In this analysis, the *Foxn1*^{CreERt2} mouse line was crossed with four independent reporter strains. These were the Red/Green reporter line (Muzumdar et al, 2007), and the Rosa26-CN2-YFP (Srinivas et al, 2001), sGFP-7 (Gilchrist et al, 2003), and Rosa-td-RFP (Luche et al, 2007) lines, that express cytoplasmic YFP, GFP and RFP

fluorescent proteins respectively after Cre mediated recombination (see Materials and Methods for further details).

I first analysed embryos produced from crosses of *Foxn1*^{CreERt2} males with either sGFP-7 or Red/Green reporter females by IHC, to determine the specificity of recombination. The pregnant females were injected at E12.5 and E13.5 with 2mg of 4OHT and the embryos were analysed at E14.5. Microdissected thymic lobes, or whole embryos, were snap frozen in OCT, sectioned, and every 5thsection was analysed for GFP expression by antibody staining, as described in Materials and Methods.

Analysis of the carrier-injected *Foxn1*$^{CreERt2/+}$*;sGFP-7* mice revealed no evidence of spontaneous recombination; no GFP expression was observed in the thymus or in any other organ of these embryos (Fig 3.2 A,B,C). In contrast, in the embryos that had been exposed to 4OHT, GFP expression was evident and was specific to the thymic lobes (Fig 3.2 D,E,F). Analyses of frozen thymic sections of *Foxn1*$^{CreERt2/+}$*;Red/Green* (referred to in the figures as *Foxn1*$^{CreERt2/+}$*;R/G)* mice revealed that GFP expression was restricted to the TEC compartment, in which *Foxn1* is expressed, as GFP expression was observed exclusively in pan-cytokeratin^{+} cells (Fig 3.2 G,I). GFP expression was seen in both medullary TEC (identified by K5 antibody staining) and cortical TEC (K5 negative GFP^{+} areas) (Fig 3.2 H). No GFP expression was detected in the carrier-injected mice (Fig 3.2 J).

These data established that Cre-recombinase activity in the *Foxn1*^{CreERt2} line is specific to *Foxn1* positive cells, and that the *Foxn1*^{CreERt2} line does not display any spontaneous recombination activity in the fetal thymus.

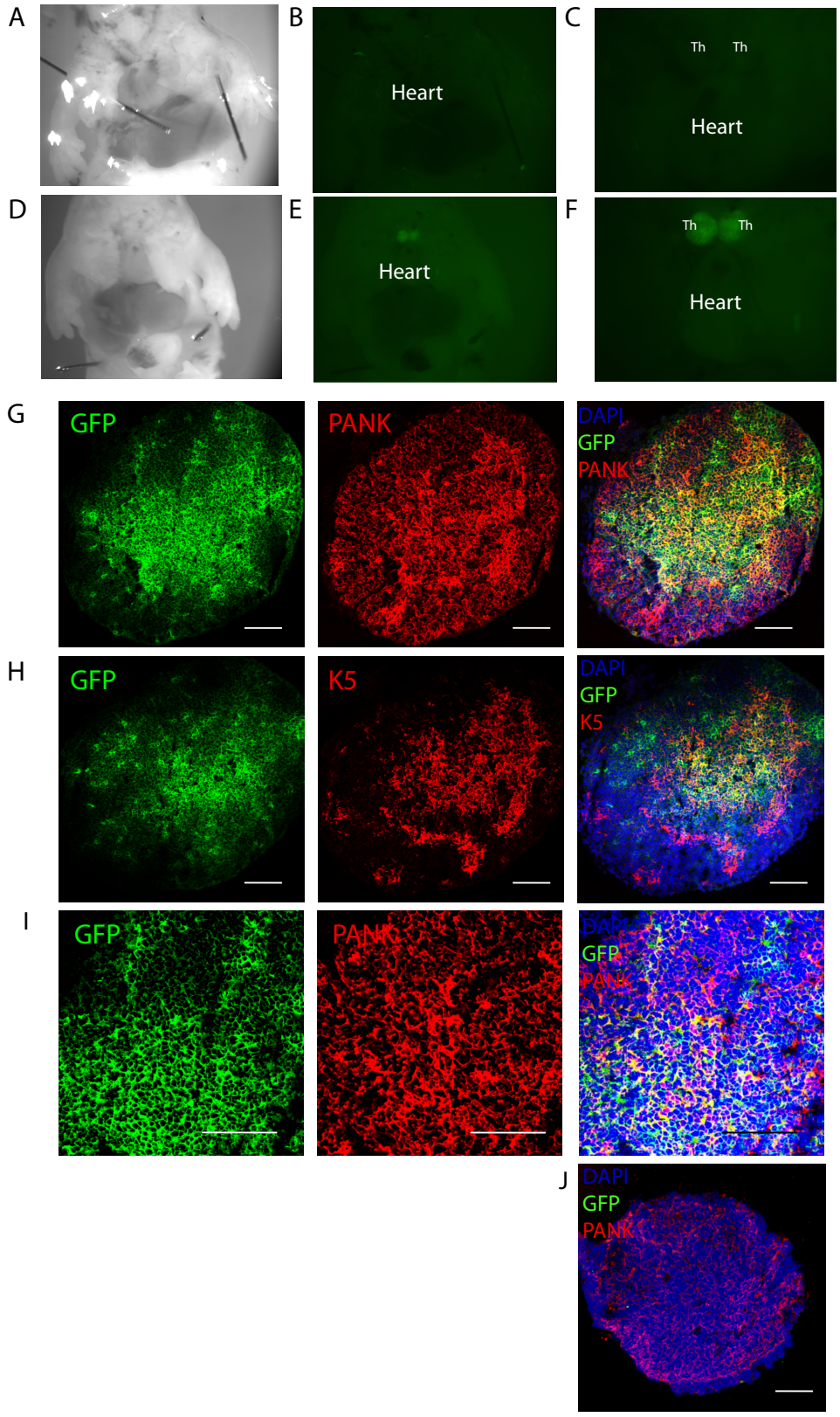


Figure 3.2 IHC analyses of Foxn1CreERt2 mice. Females were given two injection of 2mg 4OH tamoxifen on day E12.5 and E13.5, all analyses was performed at E14.5. Experimental Foxn1CreERT2/CreERT2;sGFP-7 showed no GFP+ cells in the carrier only controls (A,B,C), while mice injected with 4OH tamoxifen showed thymus specific GFP expression when injected with 4OH (D,E,F) Under the same conditions Foxn1CreERT2/CreERT2;R/G mice showed GFP positive cells only in the TEC compartment as illustrated here by Pank staining (G). Recombination occured in both medullary (as shown here in K5 positive stain) and cortical compartment (K5 negative, GFP positive areas) (H). Carrier only injected mice showed no GFP expression (I). Secondary antibodies used (anti-chiicken alexa 488, anti-rabbit alexa 647)

3.1.2 Analysis of recombination frequency in fetal TEC

To establish the percentage of TEC in which Cre-mediated recombination had occurred using the above protocol, and to determine the optimal dose of 4OHT required to effect recombination in the maximum proportion of TEC, I next performed a series of experiments where pregnant females were injected with doses of 4OHT ranging from a single 1.5mg injection to 2 injections of 2.5mg. These experiments were performed using the sGFP-7 reporter strain unless otherwise specified. Pregnant female mice were injected at E12.5, and the embryos were analysed at E13.5 if a single injection of 4OHT was administered or at E14.5 if two injections of 4OHT were administered. Thymi were microdissected and dissociated to single cell suspensions and processed for flow cytometric analysis with a panel of markers, as described in Materials and Methods. Figure 3.3 A shows the staining and analysis strategy for these experiments.

As before, mice injected with carrier-only showed no evidence of spontaneous recombination. Mice that received 4OHT injections exhibited no non-specific recombination in either intrathymic $CD45^{+}$cells or in $CD45^{-}EpCam^{-}$ non epithelial thymic stromal cells. GFP was detected specifically in the $EpCam^{+}$ TEC (Figure 3.3B, C).

In mice that received 4OHT injections, I observed a specific dose dependent rate of recombination (Fig 3.3D). This ranged from 9.67%-12% (10.75±1.44%; standard deviation used; n=4) following a single 1.5mg dose to 23%-40% with 2x2mg injections, for *Foxn1*$^{CreERt2/+}$;sGFP-7 mice. Successive injections over 2 days with 1.5mg 4OHTresulted in an activation rate of 19.65±4.6% (range 16-23%; n=4), while 2 injections of 2mg 4OHT produced a recombination rate of29.68±7.8% (n=5) for heterozygous mice. Embryos from females injected with a single dose of 2.5mg 4OHT displayed a recombination rate of 25.2±3.5% (range 23-28%; n=3), but had a high mortality rate. Mice injected with 2.5mg of 4OHT for 2 days aborted most of the litters; any embryos that were recovered were dead and some displayed different physical abnormalities.

Since increasing the dosage of 4OHT led to embryo lethality, the dose for use in these experiments that led to the highest levels of recombination and still yielded viable embryos was determined as 2 injections of 2mg, at a 24 hour interval.

I next tested whether homozygosity for *Foxn1*^{CreERt2}might increase the recombination rate at this dose. *Foxn1*$^{CreERt2/+}$*;sGFP-7*males were therefore set up with *Foxn1*$^{CreERT2/+}$*;Rosa-td-RFP* females, to produce pups homozygous for CreERt2. Since two reporter alleles were present in this cross, this strategy also allowed in the recombination rate in different reporter strains to be determined.

At E12.5 and E13.5 the pregnant females received consecutive injections of 2mg 4OHT. Analyses of the embryos was performed 24 hours after the last injection, at day E14.5. This regime resulted in up to 40% recombination in embryos which were heterozygous for *Foxn1*^{CreERT2} and sGFP-7, while in Foxn1$^{CreERT2/CreERT2}$;sGFP^{+} embryos from the same experiments, 60% of TEC were GFP positive (Figure 3.3B). Thus, embryos that were homozygous for *Foxn1*^{CreERt2} showed higher recombination frequency than those that were heterozygous at this locus, indicating that at this dose of 4OHT, the level of CreERt2 expression was limiting in the heterozygous embryos (Figure 3.3 D).

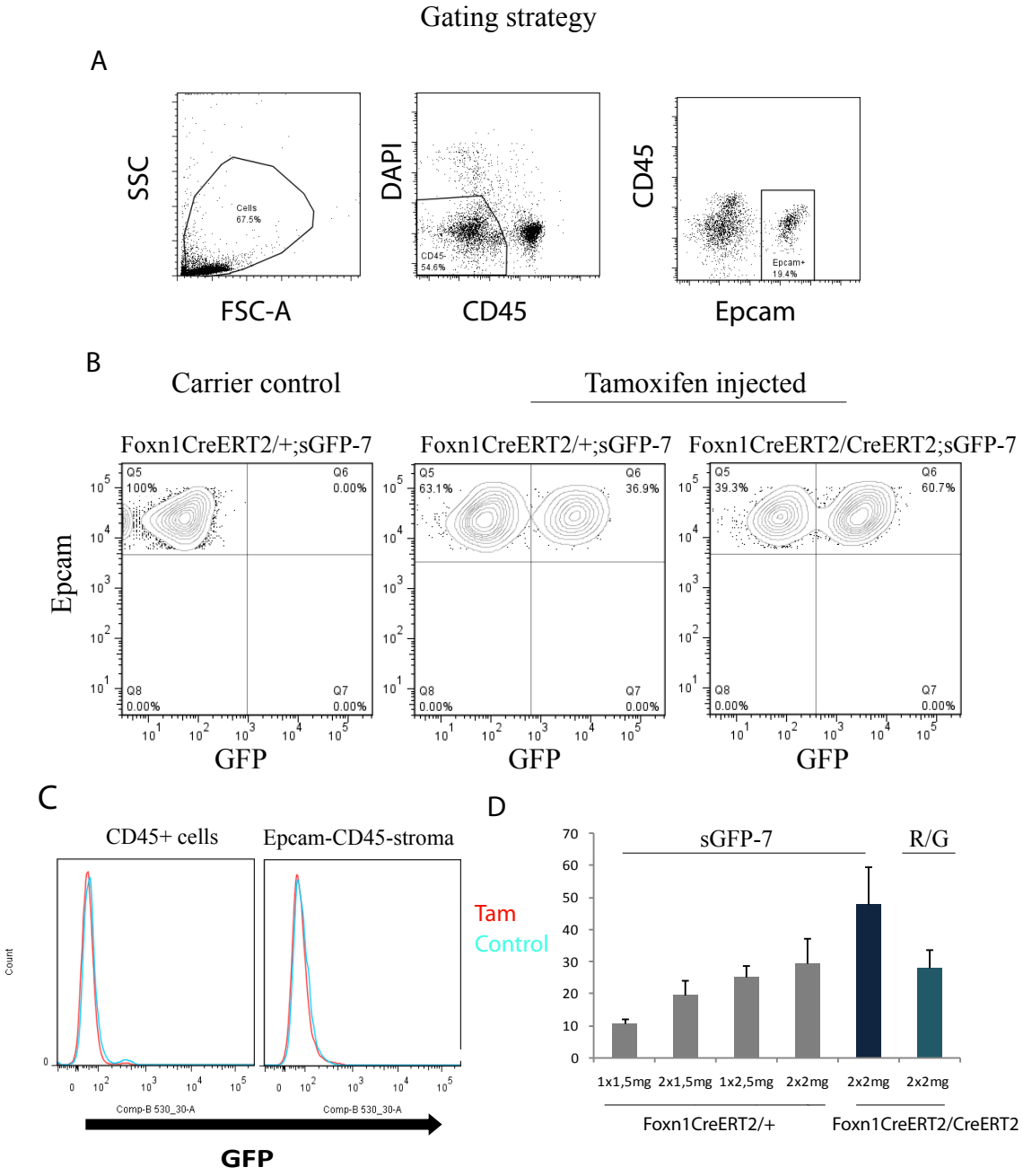


Figure 3.3 Flow cytometric analyses of recombination rate in Foxn1CreERT2 mice. Pregnant females were given one or two tamoxifen injections starting at E12.5, embryos were taken for analyses 24 hours after the last injection. Gating strategy for flow cytometry analyses is displayed in A. Carrier only injected Foxn1CreERT2/+; sGFP-7 mice showed no spontaneous recombination, while Foxn1CreERT2/+;sGFP-7 and Foxn1CreERT2/CreERT2;sGFP-7 mice showed TEC specific recombination, with homozygous mice showing a higher rate of recombination (B). There was no GFP expression detected in CD45+ T-cells or Epcam- stromal cells (C). Recombination rates increased when using higher tamoxifen doses, and increased when using homozygous mice (D).

I also compared the efficiency of recombination at different reporter loci, using a standardized dose of 4OHT. In embryos generated in the cross described above, that carried RFP in addition to GFP reporter alleles, only 0.7% of TEC were RFP-positive in Foxn1$^{CreERT2/+}$;Rosa-td-RFP embryos, and only 2% of TEC were positive for RFP in Foxn1$^{CreERT2/CreERt2}$;Rosa-td-RFP embryos (Figure 3.4A). In a separate experiment, in *Foxn1*$^{CreERT2/+}$;Rosa26-CN2-YFP embryos subject to the same treatment conditions (i.e. two injections of 2mg 40HT at 24 hour intervals at E12.5 and E13.5), only 4% YFP positive TEC were detected in *Foxn1*^{CreERT2} heterozygous embryos (Figure 3.4 C). These recombination rates contrasted with a maximum of 40% and 60% for *Foxn1*$^{CreERT2/+}$;sGFP-7 and *Foxn1*$^{CreERT2/CreERT2}$;sGFP-7 mice respectively, as described above.

Interestingly, the Foxn1$^{CreERt2/CreERt2}$;Red/Green mice when analysed under similar conditions were the only other reporter strain to produce results comparable with the levels of recombination observed when using the sGFP-7 reporter strain, with recombination levels reaching 40% in homozygous embryos (Figure 3.4 D).

These analyses thus revealed a massive difference in recombination rates driven by Cre expressed from the *Foxn1*^{CreERt2} allele in different reporter strains. In fact, of the 4 reporter strains used, it was established that only the sGFP-7 and Red/Green reporter strains gave consistent, high-level, recombination after 4OHT injections in fetal TEC.

Taken together, the experiments above established both the optimum dose of 4OHT and the best reporter strains for use in future lineage analysis.

3.1.3 Phenotypic analysis of recombined cells

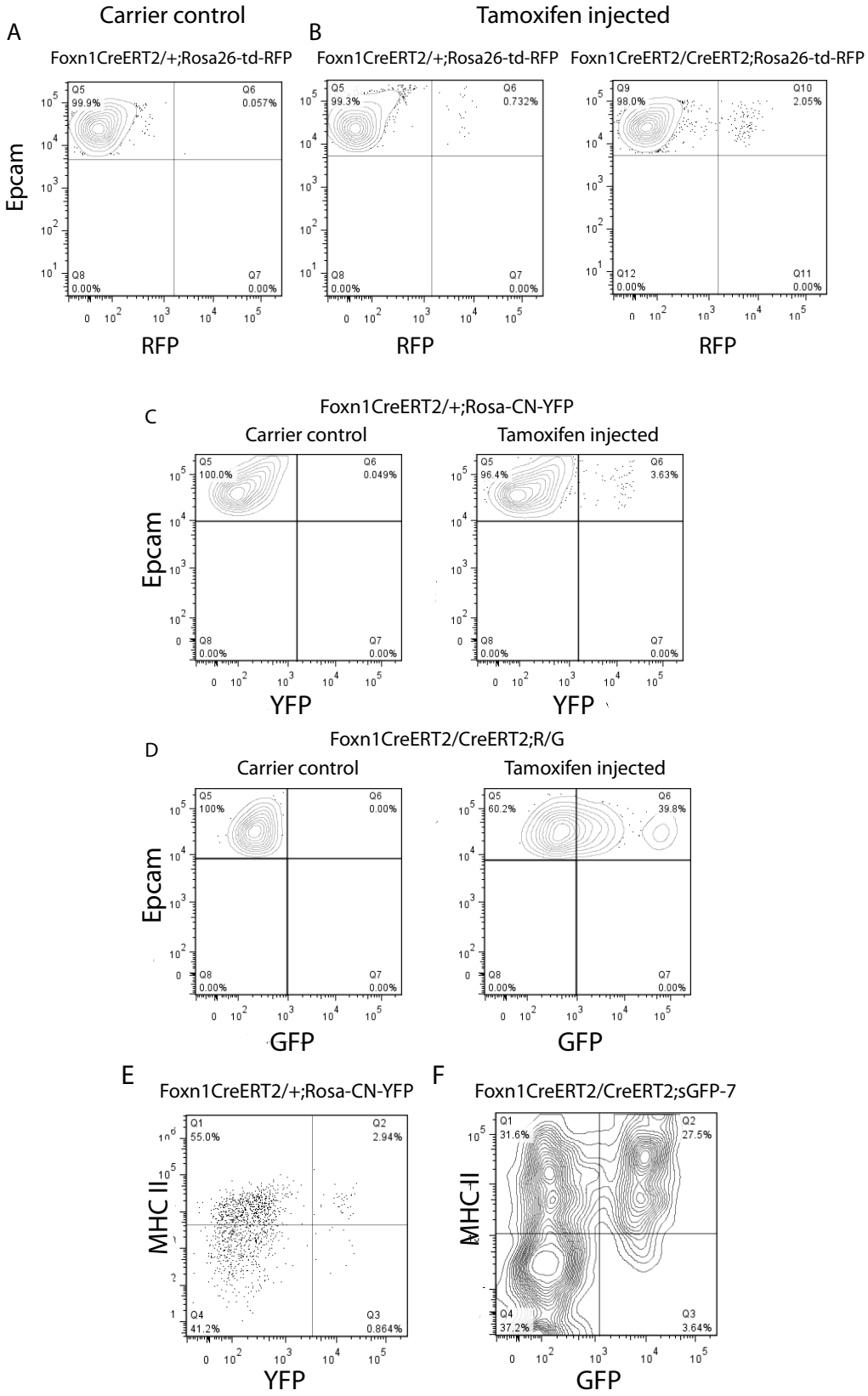
I next set out to determine whether Cre-mediated recombination in fetal *Foxn1*^{CreERt2} mice occurred preferentially in TEC of a particular phenotype, by flow cytometric analysis of TEC 24 hours after 4OHT-injection.

At E12.5, TEC are relatively homogeneous, with over 80% of TEC expressing Plet1 (Nowell et al, 2011). However later in development Plet1 expression is progressively lost and phenotypically and functionally heterogeneous TEC populations, expressing a variety of distinct markers, are established. Notably, expression of MHC Class II

can be observed as early as E12.5. MHC Class II is considered a marker associated with TEC maturity, with the highest levels of MHC Class II observed in mature cells (Nowell et al, 2011). Thus, TEC can be divided into MHC II^{hi}, MHC II^{int} and MHC II^{lo} in the fetal thymus (Nowell et al, 2011), these can in turn be further subdivided into cTEC and mTEC, using UEA1 or Ly51 respectively in the later fetal and adult thymus (Gray et al, 2006)

I thus determined whether GFP^{+} TEC were found preferentially in MHC II^{hi}, MHC II^{int} and MHC II^{lo} compartments. These analyses showed that most YFP positive cells in the *Foxn1*$^{CreERt2/+}$*;Rosa26-CN2-YFP* heterozygous mice were MHC $ClassII^{hi}$ (Figure 3.4 E), consistent with literature reports indicating that among adult TEC, the MHC $ClassII^{hi}$ population expresses higher levels of *Foxn1* than the MHC $ClassII^{lo}$ compartment (Nowell at al., 2011). In the *Foxn1*$^{CreERt2/CreERT2}$*;sGFP-7* homozygous mice the rate of recombination in the MHC $ClassII^{hi}$ and MHC $ClassII^{int}$ populations was comparable, and a low level of recombination was also observed in the MHC $ClassII^{lo/-}$ cells (Figure 3.4F). Collectively, these data suggested that in *Foxn1*$^{CreERt2/+}$mice, *CreERt2* expression reached the threshold level required for efficient recombination at the sGFP-7 and Red/Green reporter alleles only in TEC that express high levels of *Foxn1* mRNA. In *Foxn1*$^{CreERt2/CreERt2}$mice, the higher level of CreERt2 expression was sufficient to permit recombination in MHC $ClassII^{int}$ cells.

Figure 3.4 Representative flow cytometrix analyses of recombination efficiency in Foxn1CreERt2/+ and Foxn1CreERt2/CreERT2 mice when crossed with the Rosa26-td-RFP, Rosa26-CN2-YFP, Red/Green reporter strains, all plots gated on Epcam+ cells. Pregnant females were injected at E12.5 and E13.5 with a 2mg 4OH-tamoxifen dose and analysed at E14.5. Foxn1CreERt2/+;Rosa26-td-RFP showed no recombination in carrier only controls (A), and a 0,7% and 2% recombination rate in heterozygoes and homozygoes embryos respectively (B).
Under the same conditions Foxn1CreERt2/+;Rosa26-CN2-YFP mice showed a 3% recombination rate (C), while Foxn1CreERT2/CreERT2;RedGreen showed up to 40% (D). Heterozygous Foxn1CreERT2 mice showed preferential recombination in the MHC IIhi compartment (E), while the hozygous Foxn1CreERT2 mice showed recombination in MHC IIhi, MHC IIint and MHCIIlo TEC (F).


A
Carrier control
Foxn1CreERT2/+;Rosa26-td-RFP
Epcam
RFP
Q5 99.9%
Q6 0.057%
Q8 0.00%
Q7 0.00%
B
Tamoxifen injected
Foxn1CreERT2/+;Rosa26-td-RFP
Q5 99.3%
Q6 0.732%
Q8 0.00%
Q7 0.00%
Foxn1CreERT2/CreERT2;Rosa26-td-RFP
Q9 98.0%
Q10 2.05%
Q12 0.00%
Q11 0.00%
C
Foxn1CreERT2/+;Rosa-CN-YFP
Carrier control
Q5 100.0%
Q6 0.049%
Q8 0.00%
Q7 0.00%
YFP
Tamoxifen injected
Q5 96.4%
Q6 3.63%
Q8 0.00%
Q7 0.00%
YFP
D
Foxn1CreERT2/CreERT2;R/G
Carrier control
Epcam
Q5 100%
Q6 0.00%
Q8 0.00%
Q7 0.00%
GFP
Tamoxifen injected
Q5 60.2%
Q6 39.8%
Q8 0.00%
Q7 0.00%
GFP
E
Foxn1CreERT2/+;Rosa-CN-YFP
MHC II
Q1 55.0%
Q2 2.94%
Q4 41.2%
Q3 0.864%
YFP
F
Foxn1CreERT2/CreERT2;sGFP-7
MHC II
Q1 31.6%
Q2 27.5%
Q4 37.2%
Q3 3.64%
GFP

3.1.4 *In utero* injection of tamoxifen

In order to proceed with lineage tracing experiments and track the *Foxn1* positive cells and their fate in postnatal mice, I wished to try to increase the recombination frequency to closer to 100%. Therefore, the issue of embryo lethality had to be addressed. I therefore decided to use a novel surgical method -*in utero* injection. Using this procedure, small volumes of tamoxifen that are not toxic can be delivered straight to the developing fetus through injections into the amnion or placenta (Figure 3.5 A,B). This technique is used in our institute and has yielded excellent results. However it had only been used in embryos that were substantially younger (mostly E8.5, with the latest stage not exceeding E11.5), I therefore performed a series of pilot experiments to determine optimal conditions for older embryos. *Foxn1*$^{CreERT2/CreERT2}$;RG embryos were injected at E12.5 and collected for analyses the next day.

In younger embryos it had been established that injections through the amnion produced robust, high levels of recombination (V. Wilson and Sabrina Gordon-Keylock, personal communication). However when performing surgery on older embryos, injections through the amnion lead to an excessive loss of amniotic fluid and as a result high levels of embryo death. When injections were made into the placenta the mortality rate decreased and I was able to recover viable pups. However preliminary results suggest that a dose of 800 μM tamoxifen in 5μl of total volume is enough to facilitate recombination (up to 38%) and yield embryos that are viable for at least a day after the procedure (Figure 3.5 C,D,E,F).These experiments are currently ongoing and it remains to be seen if higher levels of recombination can be obtained with a non-toxic concentration of tamoxifen, that will allow the pups to be born, and be analyzed at later stages in adulthood.

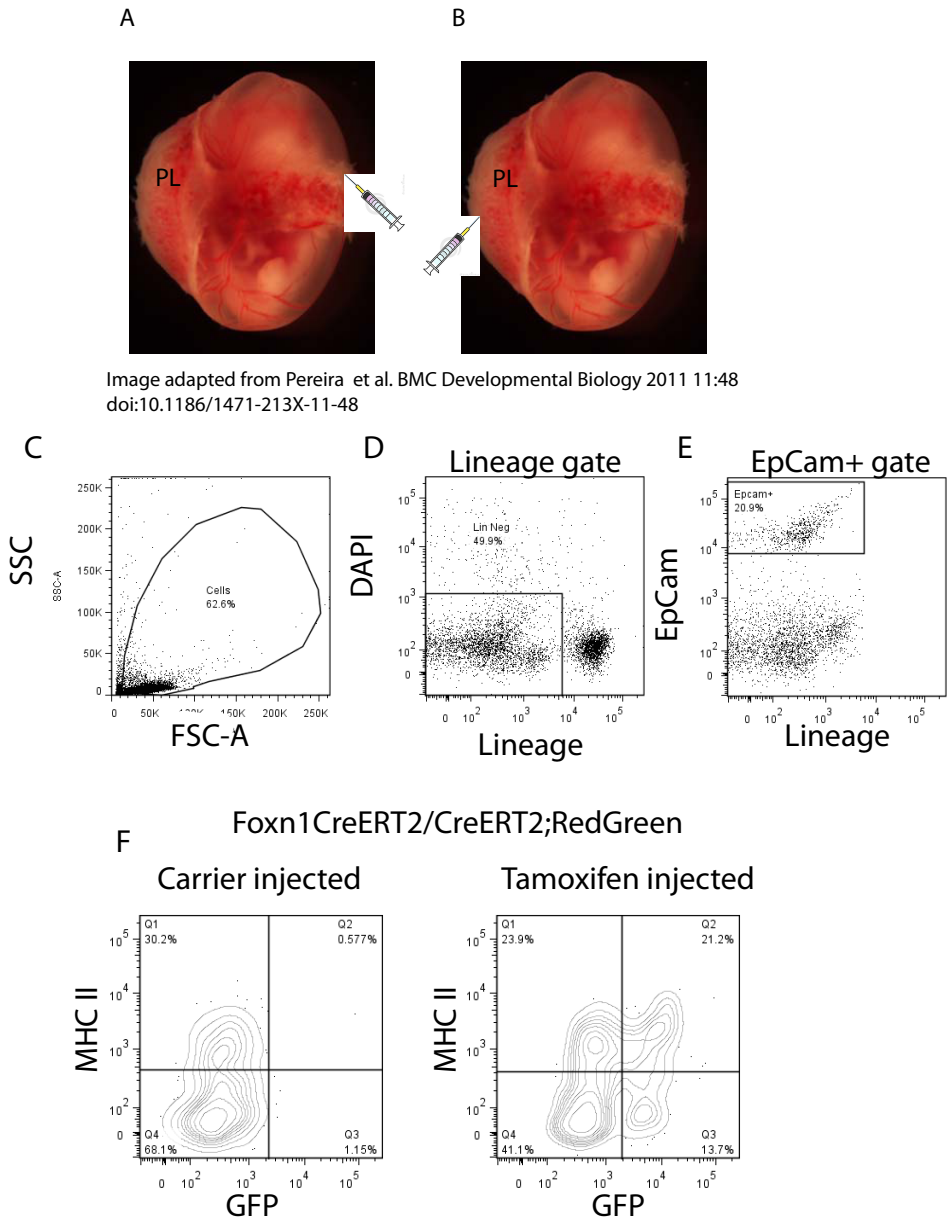


Figure 3.5 Analyses of recombination rates in the Foxn1CreERT2/CreERT2;R/G mice following inutero injections of tamoxifen. Injections were administered through the amnion or placenta at E12,5 and embryos were collected for analyses 24 hours after surgery (A). Gating strategy for Flow cytometric analyses is illustrated C-E. Carrier injected mice showed no spontaneous recombination, while embryos that recieved tamoxifen injections showed specific recombination in the TEC compartment in the MHC IIhi and MHCIIlo compartment.

3.1.5 Recombination rate in the Foxn1CreERT2 E15,5 thymus

In order to establish the recombination efficiency in TEC at a later stage in development, pregnant female *Foxn1*$^{CreERt2/CreERt2}$;sGFP-7 mice crossed with males of identical genotype mice were injected at E15.5 with different doses of 4OHT, and embryos were recovered 48 hours later (at E17.5) for analyses.

Strikingly, even at higher doses of 4OHT (5mg dose) the recombination rate in the TEC was extremely low, reaching a maximum of 4%.

Foxn1 mRNA levels at E15.5 show a three-fold reduction compared to E12.5 TEC (unpublished data, Blackburn laboratory), suggesting that this lower CreERT2 level was insufficient to facilitate efficient recombination (Figure 3.6 A,B)

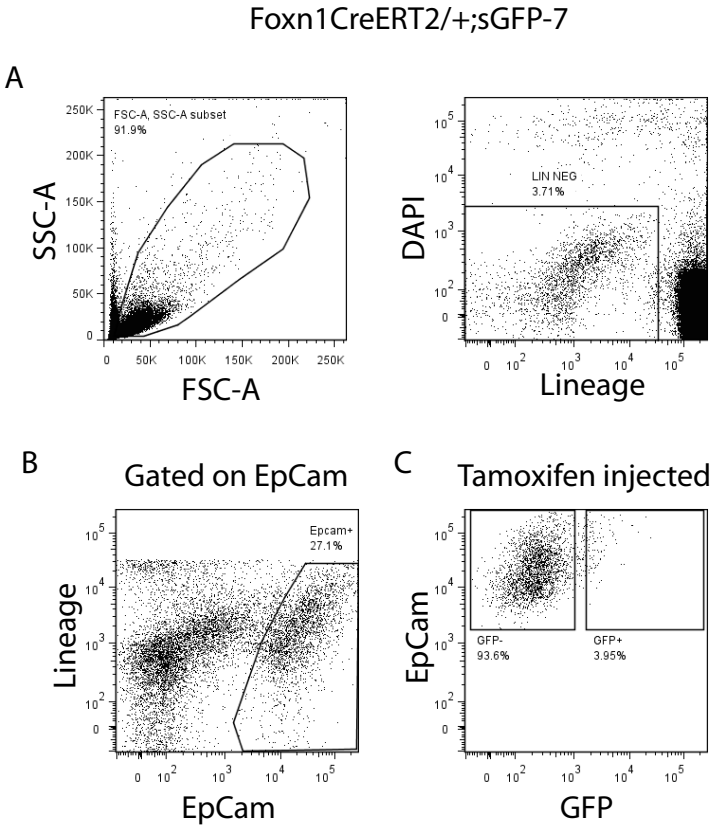


Figure 3.6 Flow cytometric analyses of E.17.5 Foxn1CreERT2/+;sGFP-7 thymic lobes.
Females were injected at E15.5 and E.16.5 and analysed
24 hours later. Gating strategy for analyses is displayed in A,B.
Low level of recombination was observed in the TEC of tamoxifen injected mice (C).

3.2 Postnatal analyses of the Foxn1^{CreErt2} mouse line.

Having validated the *Foxn1*^{CreERt2} strain for manipulation of the fetal thymus, I next set out to test its utility for manipulation of postnatal TEC. In order to establish optimal tamoxifen dosages for Cre-mediated deletion in TEC in adult mice using this strain, I performed a series of pilot experiments. *Foxn1*^{CreErt2} mice were crossed with different reporter strains (Rosa-td-RFP, Rosa-CNF-YFP, sGFP-7, Red/Green), to produce mice carrying the *Foxn1*^{CreERt2} allele and a given reporter allele. These mice were injected at four or eight weeks of age with different doses of tamoxifen or 4OHT, ranging from1.5mg to5mg. Some received a single injection while others were injected once a day for up to 4 days. Mice were sacrificed for analyses at 2.5 or 14 days post injection, and analysed using flow cytometry (Figure 3.7 A).

3.2.1 Identification of the optimal reporter strain for postnatal lineage analyses

In these experiments it was established that, in accordance with the experiments described above, not all reporter strains underwent recombination at the reporter allele following tamoxifen injection. Thus, the *Foxn1*$^{CreERt2/+}$;Rosa-td-RFP and *Foxn1*$^{CreERt2/+}$;Rosa-CNF-YFP reporter strains did not produce any significant level of recombination with the *Foxn1*^{CreERt2} mouse line (data not shown). Similarly, the *Foxn1*$^{CreERt2/+}$;sGFP-7 line, that showed high-level recombination in the fetal analyses, failed to undergo any detectable recombination in adult TEC in mice that received single injections of tamoxifen ranging from 1.5 mg to 5mg (Fig 3.7 B). Multiple injection of high doses of tamoxifen failed to produce any detectible level of recombination.

To control for expression from the reporter locus in TEC in adult mice, *Foxn1*^{Cre};sGFP-F mice, in which Cre recombinase is expressed in TEC from E11.25 through ontogeny, were therefore used as a positive control. Most if not all postnatal TEC were GFP^{+} in these mice (Fig 3.7C), indicating that the reporter gene was expressed in postnatal TEC.

To test if the Red/Green reporter line was suitable for use in postnatal TEC Rosa26$^{CreERT2/+}$;Red/Green mice were injected with 3mg of tamoxifen for 4 days.

When analysed 48 hours after the last injection these mice showed a high proportion of TEC were GFP positive (62.4%±19.4%, n=3) Figure 3.7 (D).

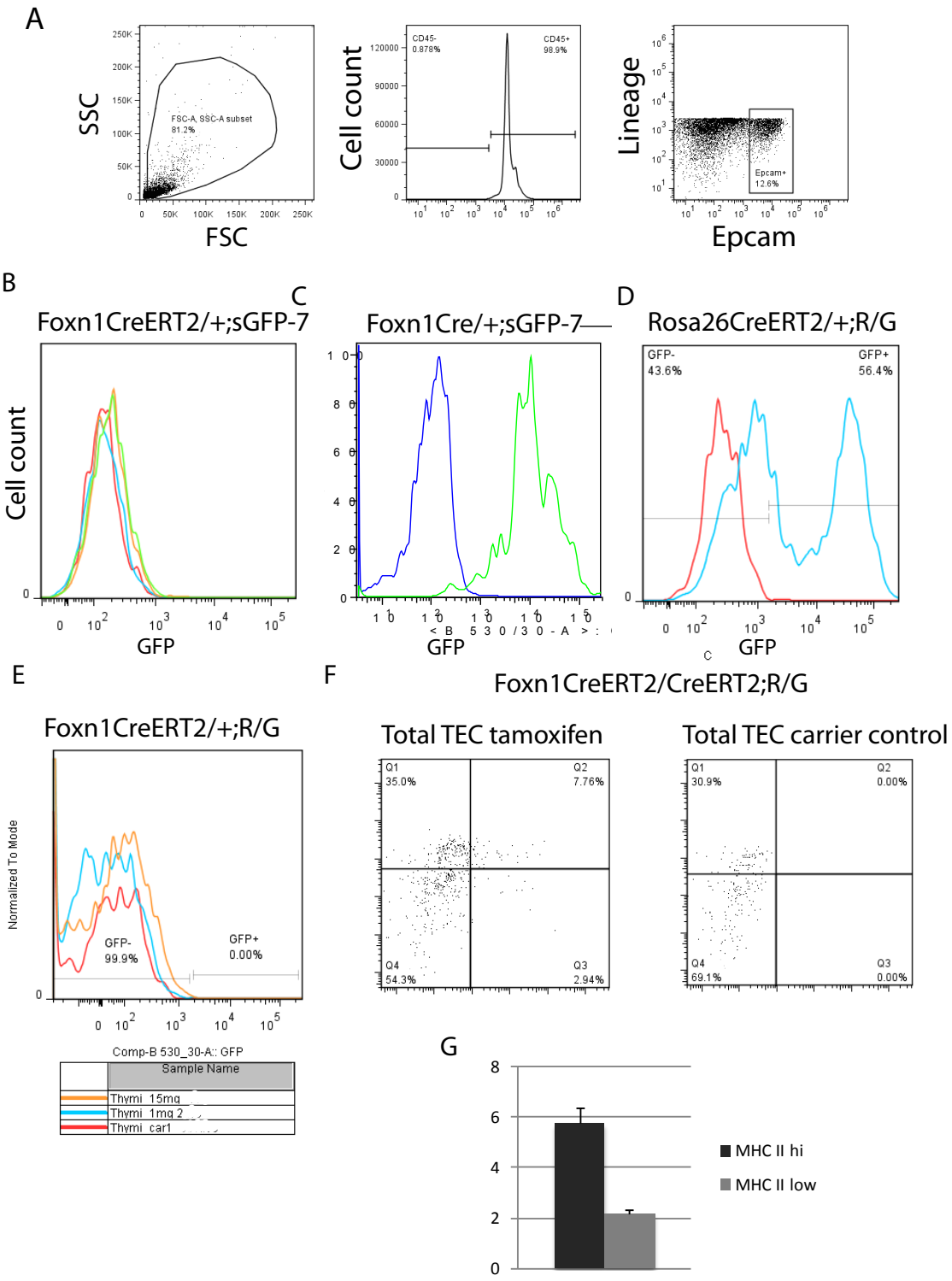
When *Foxn1*$^{CreERt2/+}$;RG mice were injected with 1 or1.5mg of 4OHT and analysed 2 days later, no GFP^{+} cells were detected (Figure 3.7 E). However injections with 3mg of tamoxifen every 24 hours for 4 days resulted in Cre-mediated recombination in a low percentage of TEC, as evidenced by the presence of GFP^{+} TEC (Figure 3.7 F)

3.2.2 Analyses of recombination in postnatal mice

In initial experiments, *Foxn1*$^{CreERt2/+}$;Red/Green$^{+/-}$ mice were injected at 5-6 months of age. At this age, single doses of 4OHT ranging from 0.5 to 2mg (Figure 3.7 E) produced little if any recombination in Foxn1-positive TEC. Injections with Tamoxifen at 3mg per single injection to a total dose of 12 mg over 4 days consistently resulted in recombination in a fraction of total TEC (Figure 3.7 F). In addition there were 2-3 fold more GFP+ cells in the MHC II^{hi} TEC than the MHC II^{lo} (Figure 3.7 G).

The *Foxn1*$^{CreERt2/+}$*;Red/Green*$^{+/-}$tamoxifen-injected mice typically showed small islets of GFP^{+} cells in bright clusters, often accompanied by GFP^{lo} cells (Figure 3.8 A-E). These clusters were present both in the cortex, as shown by co-staining with β5t (cortical TEC) and Ly51 (mature cortical TEC) (Figure 3.8 B,D) and the medulla, as shown by co-staining with K5 (large subset of medullary TEC) and UEA1 (medullary TEC), and were also found at the cortico-medullary junction (Figure 3.8 A,C,E). Foxn1$^{CreERt2/+}$Red/Green$^{+/-}$ carrier-only injected mice did not show any GFP positive cells, revealing no spontaneous recombination (Figure 3.8F).

3.7 Flow cytometric analyses of recombination rates in the Foxn1CreERT2 mice in the postnatal thymus. Analyses was performed by gating on EpCam+ cells (A), and then analysing them for the presence of GFP labelled cells. Foxn1CreERT2/+;sGFP-7 mice failed to produce any significant levels of recombination when injected with tamoxifen : single injection of 1.5mg tamoxifen - blue line, 3mg tamoxifen- green line, 5mg tamoxifen- orange line, carrier-only injected- red line (B). Foxn1Cre;sGFP-F mice (Green) displayed recombination in most if not all TEC in the postnatal thymus (WT control in blue) (C). While Rosa26CreERT2;R/G mice showed a high level of recombination in TEC after 4 consecutive injections of 3mg tamoxifen (blue) and no spontaneous recombination was observed in the carrier only injected mice (Red) (D). When injected with 1 (Blue) to 1.5mg (Orange) 4OHT Foxn1CreERT2/+;R/G mice showed no detectectable levels of recombination, and no spontaneous recombination was observed in the carrier only controls (Red) (E). When Foxn1CreERT2/CreERT2;R/G mice were given 4 injection of 3mg tamoxifen low levels of recombination were detected in the TEC compartment (F), and no recombination was observed in the carrier only controls. More GFP+ cells were detected in the MHC IIhi compartment (G) $n=3$; $p<0.05$.


A
SSC
FSC
FSC-A, SSC-A subset
81.2%
Cell count
CD45-
0.878%
CD45+
98.9%
Lineage
Epcam
Epcam+
12.6%
B
Foxn1CreERT2/+;sGFP-7
Cell count
GFP
C
Foxn1Cre/+;sGFP-7
GFP
D
Rosa26CreERT2/+;R/G
GFP-
43.6%
GFP+
56.4%
GFP
E
Foxn1CreERT2/+;R/G
Normalized To Mode
GFP-
99.9%
GFP+
0.00%
Comp-B 530_30-A:: GFP
Sample Name
Thymi 15mg
Thymi 1mg 2
Thymi car1
F
Foxn1CreERT2/CreERT2;R/G
Total TEC tamoxifen
Q1
35.0%
Q2
7.76%
Q4
54.3%
Q3
2.94%
Total TEC carrier control
Q1
30.9%
Q2
0.00%
Q4
69.1%
Q3
0.00%
G
MHC II hi
MHC II low

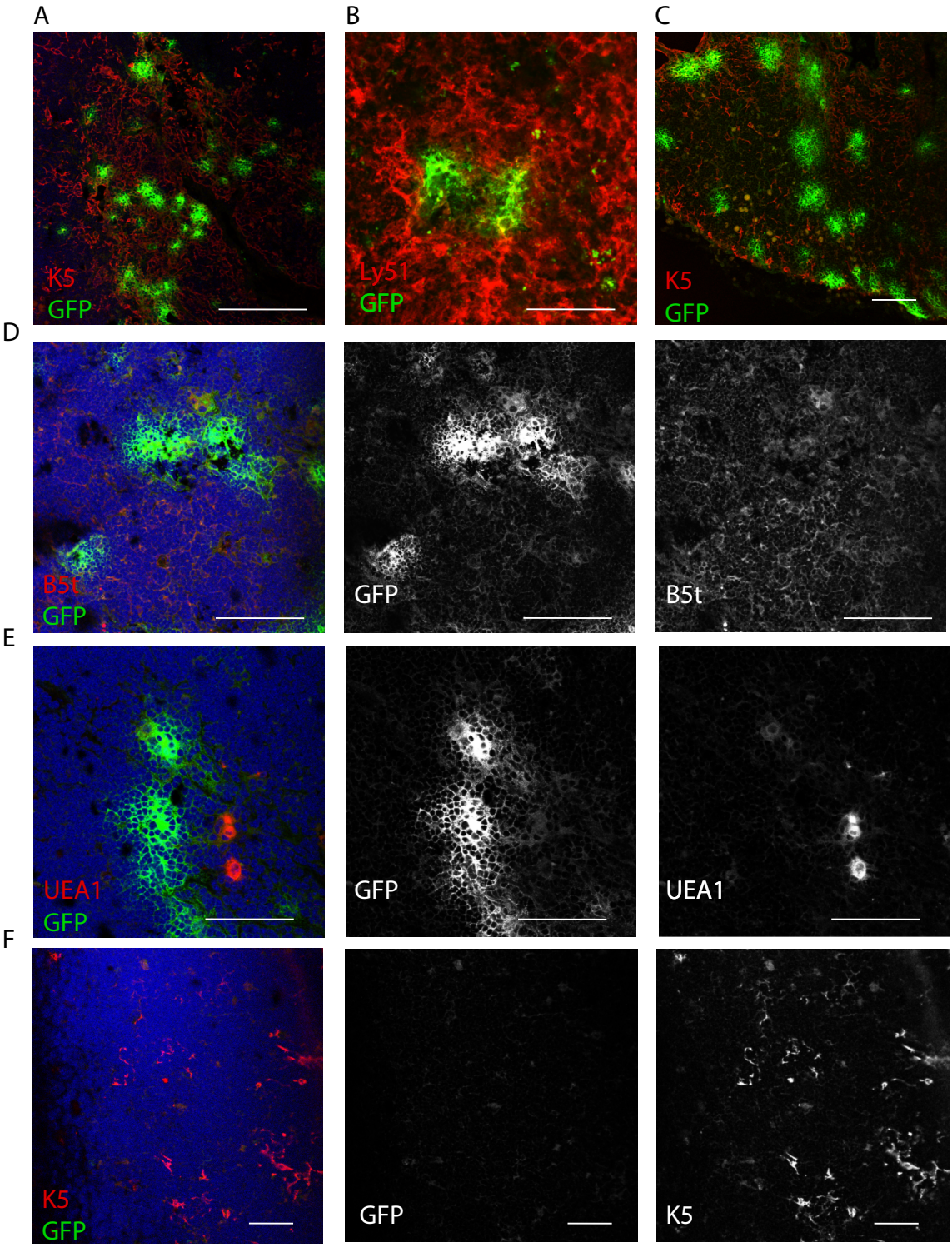


Figure 3.8 Immunohystochemical analyses of Foxn1CreERT2/CreERT2;R/G mouse line. Mice were injected with 3mg of tamoxifen on four consecutive days at six months of age. This injection regime produced a steady low level recombination in the TEC, with GFP+ clusters of cells present in both the mTEC (K5+ or UEA1+) and cTEC (Ly51+ or B5t+) compartments A-E. No recombination was detected in the carrier only injected controls (F). Scale bar 150μm.

3.3 Discussion

The data in this Chapter describe the characterization of a novel mouse line – the *Foxn1*^{CreERt2} strain. The data presented establish that, in the E12.5 fetal thymus, the *Foxn1*^{CreERt2} mouse line drives recombination specifically in *Foxn1*-positive cells, with no non-specific labeling detected in any other tissues, and no spontaneous recombination detected in carrier-only controls.

These experiments also revealed a marked difference in recombination efficiency in different reporter strains, with the Rosa-td-RFP and Rosa26-CN2-YFP showing very low levels of recombination, while the sGFP-7 and Red/Green reporters showing a high level of recombination - reaching a maximum of 60% and 40% respectively in *Foxn1*$^{CreERt2/CreERt2}$fetal mice. However none of the conditions tried yielded a 100% recombination rate, this could be due to tamoxifen dosage, however as stated before increase in dosage of the drug increased the risk of embryo mortality, with doses of 2x2.5mg proving lethal to the embryos.

In order to proceed with the lineage analyses, and track the *Foxn1* positive cells and their fate in postnatal mice, I wished to try to increase the recombination frequency to closer to 100%. Therefore, the issue of embryo lethality had to be addressed. I there for tested the utility of a novel surgical method – *in utero* injection – for delivering high local doses of 4OHT to the fetal thymus. Using this procedure, small volumes of tamoxifen that are not toxic can be delivered straight to the developing fetus through injections into the placenta or amnion. Using a 800 μM dose of tamoxifen I was able to achieve 38% recombination in the TEC compartment.

These experiments are currently ongoing and it remains to be seen if sufficient levels of recombination for our experiments can be obtained with a non-toxic concentration of tamoxifen, that will allow the pups to be born, and analyzed at latter stages in adulthood.

My initial aim was to use this mouse model to track *Foxn1*$^{+}$TEC in the postnatal thymus and determine whether these cells are responsible for replenishing the TEC in the postnatal thymus, or if a *Foxn1* negative cell is responsible for thymus maintenance.

still be used if the doses of tamoxifen can be attenuated in order to label only the MHC II^{hi}, and might be utilized to determine the role of these cells in postnatal thymus development. Furthermore, the strain can be used for forward lineage tracing analysis of the cells that are labeled as described above.

However the data obtained from the pilot experiments in postnatal mice have shown that the recombination level is low, never exceeding 10% -with the MHC ClassII^{hi} cells showing 3 fold more GFP+ cells, than the MHC Class II^{lo} compartment which is hypothesized to contain TEC progenitors (Rossi, Kim, et al. 2007; Gray et al. 2007). It is unclear at this point if this can be explained by preferential activation in the MHC II^{hi} compartment, which expresses higher levels of *Foxn1* mRNA, or whether this is the result of the MHC II^{lo} GFP^{+} TEC differentiating into the MHC II^{hi} cells, and so increasing the number of labeled cells in that compartment. However, the former possibility is supported by data obtained from *Foxn1*$^{CreERT2/+}$ and *Foxn1*$^{CreERT2/CreERT2}$ embryos injected with tamoxifen, which showed that after 48 hours the *Foxn1*$^{CreERT2/+}$ mice showed GFP+ cells only in the MHC II^{hi} compartment, while the *Foxn1*$^{CreERT2/CreERT2}$ showed an equal amount of GFP+ cell in the MHC II^{hi} and MHC II^{int} compartment

These results are further compounded by the fact that *Foxn1* levels progressively decrease with age, making it difficult to obtain a reasonable recombination efficiency in aged TEC (Bredenkamp unpublished).

The reason for low levels of recombination observed for Foxn1CreERT2 line are currently unclear. Injections of the Rosa26CreERT2 mice showed that there was no issue with tamoxifen delivery when labeling TEC with the Red/Green reporter strain in the adult thymus, and controls performed using the *Foxn1*^{Cre} mice showed that the reporter gene was expressed in postnatal TEC. This One possibility is that levels of *Foxn1* mRNA expression might not be constant. All data on expression of *Foxn1* in postnatal and fetal TEC has been acquired by sorting populations of cells for analyses, however a single cell analysis has not been performed to date, it might be that *Foxn1* is not continuously expressed in TEC, but rather switched on and off during development, or that expression is heterogeneous within this population.

From these data I concluded that this mouse model was not suitable for addressing my initial goal of determining whether the *Foxn1*$^{+}$ or negative cells are responsible for thymus maintenance, as most *Foxn1* positive cells are not labeled using this delete strain. However the model might still be of use if it can be determined that there is preferential recombination in the MHC II^{hi} TEC, in which case the model can

Chapter 4: *In vivo* cell tracking of Foxn1+ cells in a model of thymus regeneration after injury.

Introduction

This chapter details the outcome of a preliminary lineage tracing experiment performed using the Foxn1$^{CreERT2/CreERT2}$;Red/Green transgenic mouse strain. The work described was performed in an effort to gain more insight into the lineage relationships between different TEC compartments in the postnatal organ, which remain largely unclear, and into the mechanisms resulting in cellular regeneration in the thymus. Work from other labs has provided some evidence to suggest that MHC Class II^{lo} mTEC (mTEC^{lo}) are able to give rise to MHC Class II^{hi} mTEC (mTEC^{hi}). This was demonstrated by injection of mTEC^{lo} into fetal thymic lobes, or reaggregation of these cells with embryonic TEC, upon which the mTEC^{lo} could give rise to mTEC^{hi} including terminally differentiated Aire^{+} cells (Rossi, Kim, et al. 2007; Gray et al. 2007). However, except for these data, little is known about the relationships between the postnatal TEC subsets.

During the course of the work described in Chapter 3 and other work performed during the course of my PhD, I noticed a severe decrease in size and thymus total cellularity following tamoxifen injections. Interestingly there are conflicting reports in literature concerning the effect of tamoxifen administration on the thymus, with some studies reporting that this treatment is beneficial (Sfikakis et al, 1998), while others reporting a negative effect (Kalu et al. 1991).This effect appeared transient, with thymus cellularity showing signs of recovery from 7 days to 14 days post injection. Furthermore, several recent reports have documented effects of cytotoxic agents on thymocytes (Fletcher et al. 2009). I therefore set out to determine how tamoxifen treatment affected TEC subsets, as this might influence the interpretation of any tamoxifen-dependent lineage tracing or genetic manipulation experiments. Chapter 4 thus details the results of this investigation, and further describes the outcome of a preliminary lineage analysis performed using the *Foxn1*^{CreERt2} deleter strain described in chapter 3.

4.1 Preliminary analysis of the effect of tamoxifen on the adult thymus.

4.1.1 Effect of tamoxifen on thymocytes

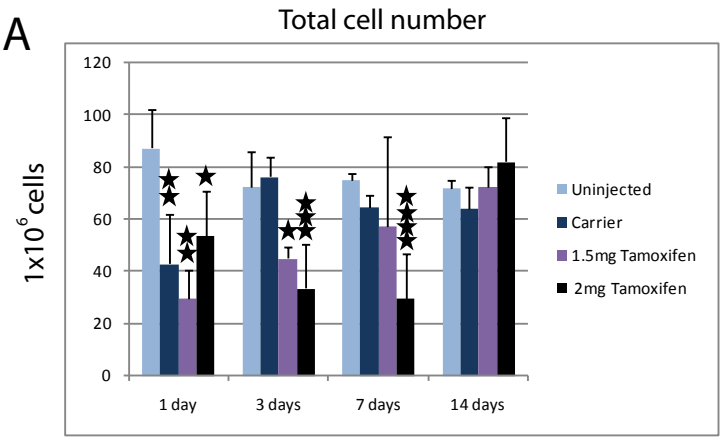
To investigate the effect of tamoxifen on the adult thymus, I performed a series of experiments using 5-7 week old C57BL/6 mice. Littermates with approximately the same body weight were injected with a single 1.5 or 2mg dose of Tamoxifen, to determine the effect of the drug on thymus cellularity. As a control, littermate mice were injected with carrier solution alone, to control for effects not specific to tamoxifen. These experiments also utilized untreated littermate controls, referred to further in the text as uninjected controls (UI). The mice were analyzed 1, 3, 7, 14 days post injection, to determine the timeframe of thymus recovery. Thus, mice were sacrificed at the stated time-points and their thyme were removed by dissection, with one lobe kept for IHC analyses and the other processed for flow cytometric analysis.

The results of these analyses, shown in Fig 4.1A, revealed a dramatic decrease in total thymic cell numbers in both the carrier-only and tamoxifen-injected mice by 24 hours post injection (mean±SD - 2mg injections, $53.54x10^6$±$18.9x10^6$ cells per lobe, n=5; 1.5mg injections, 29.8±$10.88x10^6$ cells per lobe, n=2; carrier-injected $43x10^6$±$14.9x10^6$ cells per lobe, n=4; untreated, $74x10^6$±$17.9x10^6$ cells per lobe, n=13). These data indicated that both carrier and tamoxifen-injected thymi initially responded similarly, suggesting a negative effect of the carrier solution on thymus cellularity.

By day 3 post injection, the carrier-only injected mice showed a complete recovery, with total cell numbers matching those of the untreated controls (carrier-only injected, $76.375x10^6$±$13.6x10^6$ cells per lobe,n=4). In contrast, both groups of tamoxifen-injected mice showed a continued decrease in thymic cellularity, with total cell numbers well below those in untreated controls ($45x10^6$±$4.24x10^6$ cells per lobe, n=2, and $33.6x10^6$±$7.3x10^6$ cells per lobe, n=5, respectively). These data indicated that even though the initial response appeared similar in the carrier and tamoxifen-injected mice, the tamoxifen-injection had a prolonged negative effect on thymus cellularity, while the carrier-only injected mice showed a rapid restoration of cell numbers.

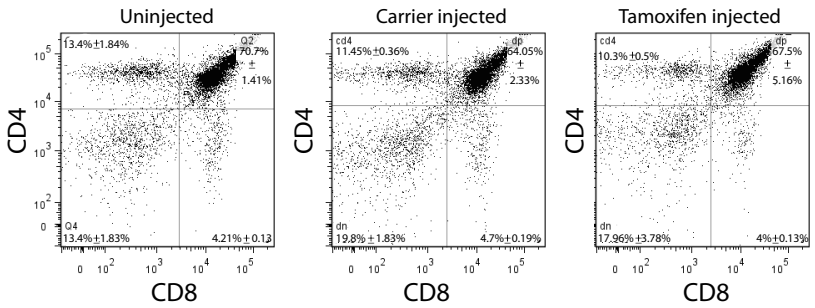
Figure 4.1 Tamoxifen injection have a negative effect on the thymus. 5-6 week old C57/BL6 were given a single injection of 1.5 or 2mg tamoxifen and taken for analyses 1,3,7,14 days later. Analyses revealed a decrease in total cell numbers as early as 24 hours after injection in both tamoxifen and carrier injected controls, however carrier injected mice showed a full recovery by day 3, but the tamoxifen injected mice showed a prolonged dose dependent negative effect on total cell numbers (A). There was no difference in T-cell proportion between uninjected, carrier and tamoxifen injected mice (B-E). The only difference in T-cell proportions was detected 3 days post injection, showing a statistically significant increase in the DN compartment (C).

A



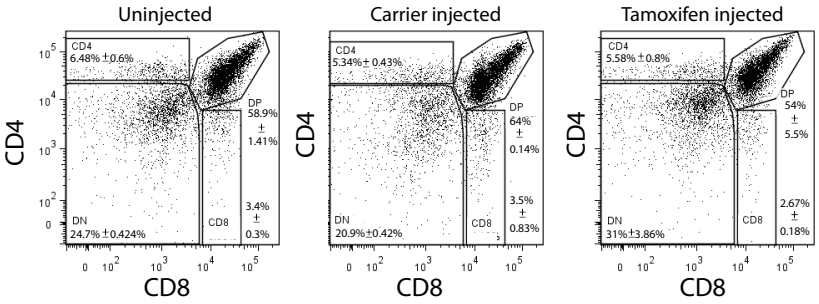
1 day post injection

B



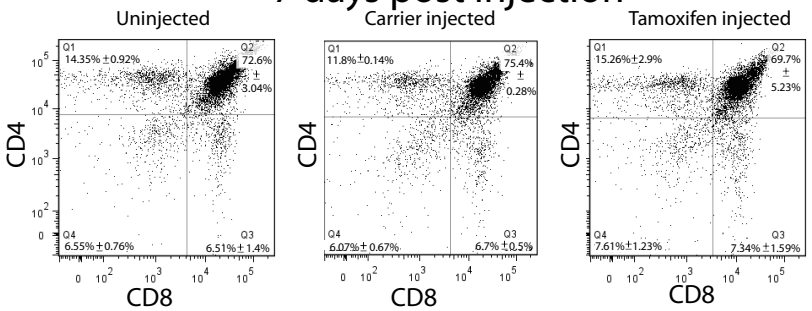
3 days post injection

C



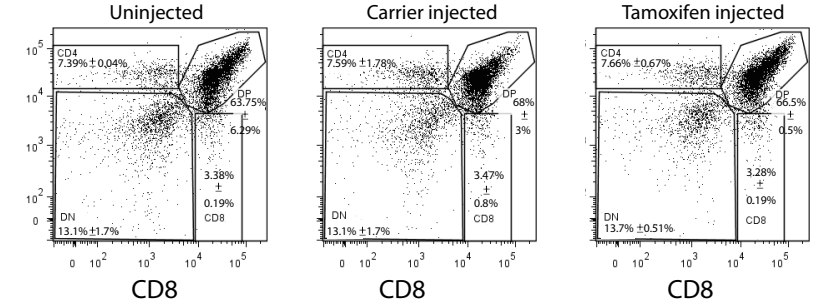
7 days post injection

D



14 days post injection

E



When analyzed 7 days post injection, mice that had received 1.5mg tamoxifen showed the first indication of restoration of total thymic cell numbers ($57.25x10^6 \pm 34.64x10^6$ cells per lobe) while the 2mg tamoxifen injected group had not recovered at this time ($29.6x10^6 \pm 4.46x10^6$ cells per lobe). By 14 days, all groups displayed normal cell numbers, indicating a full recovery. Collectively, these data therefore indicate a dose-dependent response to tamoxifen, with higher doses requiring a longer recovery time.

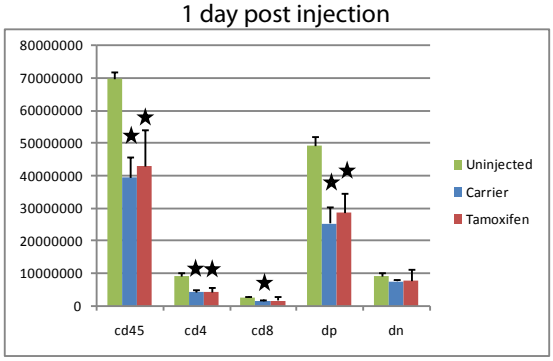
Mice injected with 2mg of tamoxifen were used for further analyses to establish the effect of tamoxifen on the main T-cell compartments.

When analysed 1 day post injection there was no difference in the proportion of different subsets in between the uninjected, carrier and tamoxifen injected groups, suggesting that there was an equal negative effect on all subsets rather than any specific effect on any given subset (Figure 4.1 B). When analysed at the later time-points, no difference was observed in the proportion of the T-cell subsets (Figure 4.1 B-E). In fact the only difference was observed at day 3, when the tamoxifen injected mice displayed an increase in the double negative compartment, and no difference was detected between the carrier only injected or uninjected mice (Figure 4.1 C) with the uninjected mice displaying 24.7%±0.424% (n=2); carrier injected mice displayed 20.9%±0.42% (n=2), while tamoxifen injected displayed 31%±3.86% DN cells. p=0.03, n=3).

When cell number of T-cell compartments was analysed there was a marked decrease in total $CD45^+$ cell numbers in both carrier and tamoxifen injected mice one day post injection (uninjected $6.9x10^7 \pm 0.2x10^7$, carrier $3.9x10^7 \pm 0.6x10^7$; tamoxifen $4.3x10^7 \pm 1.1x10^7$ $p \leq 0.05$) and a decrease in both of the SP compartments ($CD4^+$SP – uninjected $0.93x10^7 \pm 0.09$ $x10^7$; carrier $0.4x10^7 \pm 0.05x10^7$; tamoxifen $0.4x10^7 \pm 0.1x10^7$ and $CD8^+$ SP - uninjected $0.29x10^7 \pm 0.0000103x10^7$; carrier $0.187x10^7 \pm 0.02x10^7$; tamoxifen $0.184x10^7 \pm 0.1x10^7$) as well as DP cells (uninjected $4.9x10^7 \pm 0.25x10^7$; carrier $2.5x10^7 \pm 0.49x10^7$; tamoxifen $2.87x10^7 \pm 0.61x10^7$). Interestingly, at day 1, the DN cells displayed no significant difference between uninjected, carrier and tamoxifen injected, suggesting no initial negative effect on this compartment.

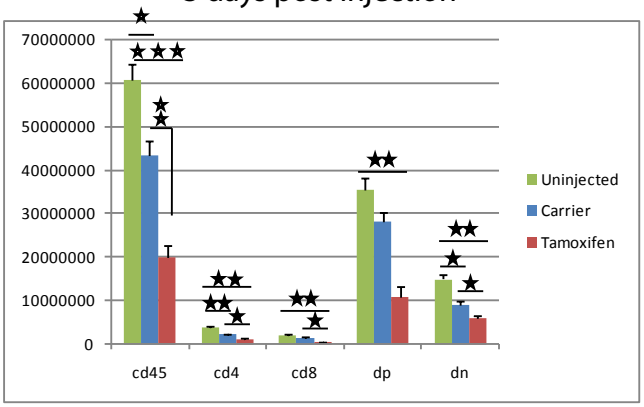
Figure 4.2 Decrease in T-cell numbers following tamoxifen injections. C57/BL6 mice were given a single injection of 2mg tamoxifen. Mice were analysed 1,3,7,14 days post injection. A significant decrease in T-cell numbers was observed as early as 1 day post injection, with a significant decrease observed in both SP and the DP T-cell compartments (A). Carrier only injected controls showed the first signs of recovery by day 3, however the tamoxifen injected mice displayed a prolonged negative effect (B). By day seven there was no difference between uninjected and carrier only injected mice, with an increase in CD4+ and CD8+ T-cells observed in the carrier when compared to uninjected controls, however the tamoxifen injected mice still displayed a severe decrease in T-cell numbers (C). At day 14 there is no difference in T-cell numbers between the uninjected, carrier and tamoxifen injected mice (D). ★ - $p<0.05$, ★★- $p<0.005$,★★★- $p<0.0005$

1 day post injection

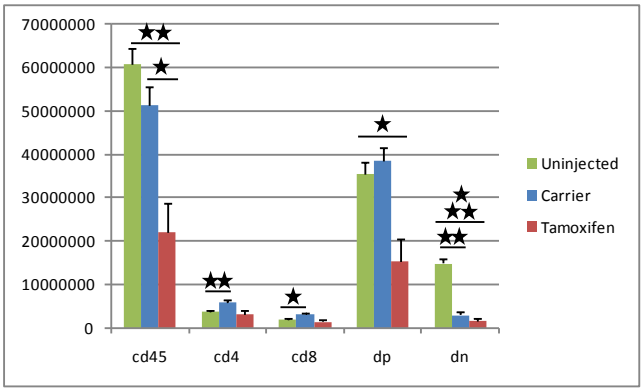


Uninjected n=2
Tamoxifen n=3
Carrier n=2

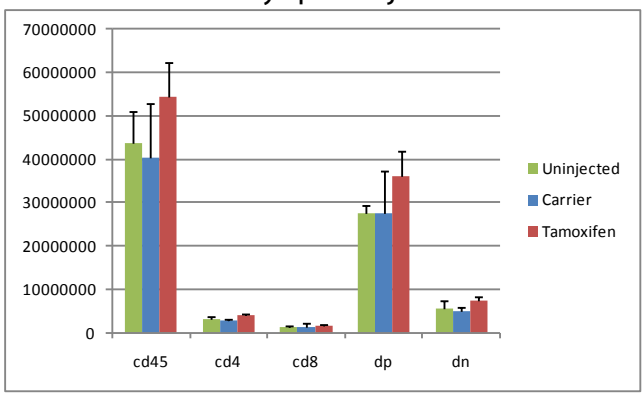
3 days post injection



7 days post injection



14 days post injection



When analysed 3 days later, both carrier and tamoxifen-injected mice still displayed a significant decrease in number in total $CD45^+$ T-cells (uninjected $6.1x10^7 \pm 0.3x10^7$; carrier $4.3x10^7 \pm 0.3x10^7$ $p \leq 0.05$; tamoxifen $1.99x10^7 \pm 0.3x10^7$ $p \leq 0.0005$). There was a significant decrease in $CD4^+$between the tamoxifen and uninjected groups (uninjected $0.39x10^7 \pm 0.02x10^7$; carrier $0.11x10^7 \pm 0.03x10^7$ $p \leq 0.005$; tamoxifen $0.1x10^7 \pm 0.03x10^7$ $p \leq 0.005$) and $CD8^+$ SP compartments (uninjected $0.2x10^7 \pm 0.03x10^7$; carrier $0.15x10^7 \pm 0.002x10^7$ $p > 0.05$; tamoxifen $0.05x10^7 \pm 0.007x10^7$ $p \leq 0.005$) and as well as in the DP compartment (uninjected $3.6x10^7 \pm 0.3x10^7$; carrier $2.8x10^7 \pm 0.3x10^7$; tamoxifen $1.08x10^7 \pm 0.4x10^7$). At this time point, there was also a reduction in number in DN cells (uninjected $1.5x10^7 \pm 0.1x10^7$; carrier $0.9x10^7 \pm 0.08x10^7$ $p \leq 0.05$; tamoxifen $0.6x10^7 \pm 0.05x10^7$ $p \leq 0.005$). This is probably due to the differentiation of these cells into DP cells in order to replenish cell numbers. At this time point there was also a difference in number between the carrier and tamoxifen injected groups, with the carrier-injected mice showing signs of recovery, while the tamoxifen-injected mice displayed prolonged negative effect on all compartments analysed (Figure 4.2 B).

When analysed 7 days post injection there was no difference in numbers of T-cells between the carrier-only and uninjected mice suggesting a full recovery. Interestingly there was a statistically significant increase in both the $CD4^+$SP (uninjected $0.4x10^7 \pm 0.02x10^7$; carrier $0.6x10^7 \pm 0.3x10^7$ $p \leq 0.005$) and $CD8^+$SP (uninjected $0.2x10^7 \pm 0.03x10^7$; carrier $0.36x10^7 \pm 0.002x10^7$ $p \leq 0.005$) populations in carrier only injected mice when compared to uninjected controls. The DN compartment was the only compartment that displayed low cell numbers compared to the uninjected control, this is possibly due to the exhaustion of this population in order to replenish the DP, and other T-cell populations (Figure 4.2 C). Consistent with data displayed in Figure 4.1 A, the tamoxifen-injected mice displayed a prolonged negative effect on T-cell numbers. Although the $CD8^+$SP ($0.3x10^7 \pm 0.09x10^7$ $p > 0.05$) and $CD4^+$ SP cells ($0.15x10^7 \pm 0.04x10^7$) displayed no significant difference from the uninjected controls, the DP (uninjected $3.5x10^7 \pm 0.3x10^7$; tamoxifen$1.6x10^7 \pm 0.49x10^7$ $p \leq 0.05$) and DN populations (uninjected $1.5x10^7 \pm 0.1x10^7$; tamoxifen $0.17x10^7 \pm 0.07$ $x10^7$ $p \leq 0.0005$) still displayed a significant reduction in cell number.

When analysed 14 days post injection there was no difference in cell number of T-cells between uninjected, carrier only and tamoxifen injected mice, suggesting a full recovery of T-cell numbers after tamoxifen injections.

4.1.2 Effect of tamoxifen on TEC

Preliminary analysis of the TEC compartment showed little or no difference in overall number of TEC between the untreated, and carrier- and tamoxifen-injected groups. However these experiments did not utilize additional markers of the cortical and medullary TEC compartments, so although there was no difference detected in gross numbers of TEC, more subtle effects on TEC remained to be established (Figure 4.3).

The experiments outlined above showed that there was an acute effect of both tamoxifen and carrier injection on thymus total cellularity by as early as 24 hours after injection, with the lymphoid cells showing the greatest reduction in numbers. This pointed to an effect of carrier solution on the thymus, rather than the tamoxifen. However, analysis at later time-points post injection revealed that although the initial acute effect was comparable in tamoxifen and carrier-only injected mice, the latter showed only a transient loss of thymic cellularity with complete restoration of total cell numbers to untreated levels by day 3 post injection, and a recovery of normal thymocyte numbers observed 7 days post injection, while the tamoxifen-injected mice showed a more prolonged negative effect on total thymic cell number and thymocyte number. Furthermore this negative effect was dose-dependent, with 1.5mg injected mice showing a restoration of cellularity by day 7, while cellularity was restored in the 2mg injected groups only at 14 days post injection.

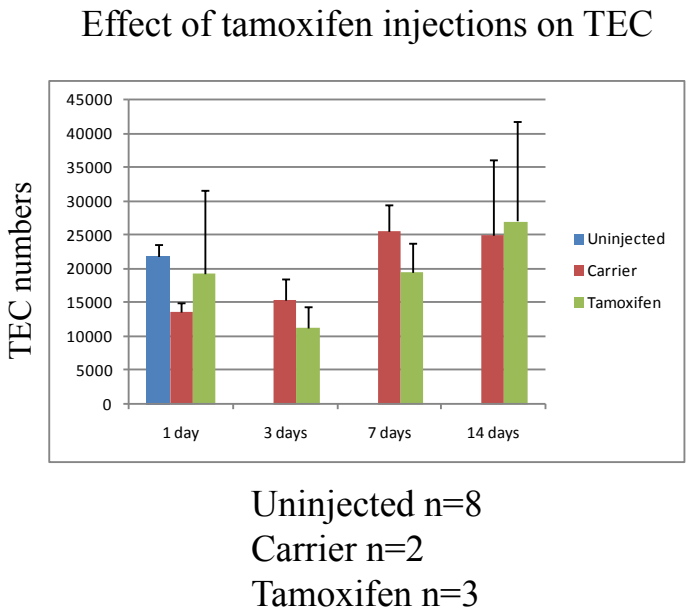


Figure 4.3 Effect of single 2mg tamoxifen data on TEC.
BL6 mice 5-7 weeks of age were injected with a single dose of 2mg tamoxifen and taken for analyses at 1-14 days post injection, these nice showed no statistically significant difference in TEC numbers.

4.2 Effect of tamoxifen on adult TEC

The data presented in Chapter 3 establish the optimum regime for tamoxifen-induction of Cre recombinase activity in adult *Foxn1*^{CreERt2}mice, namely four intraperitoneal injections of 3mg tamoxifen over the course of 4 days. Based on the data presented in section 4.1 above, it was therefore important to establish what effect this prolonged exposure had on thymus cellularity, and specifically on the major TEC subsets, prior to undertaking lineage tracing experiments. Therefore, I performed a more detailed analysis of the effect of tamoxifen on TEC, in mice injected with tamoxifen using this regime.

Thus, mice were injected with 4x3mg of tamoxifen over a 4 day interval, or were injected with carrier-only using the same injection regime. When analysed 48 hours after the last tamoxifen injection, a marked difference in size was observed between tamoxifen-injected and carrier-injected thymi (Figure 4.4A). As before, the tamoxifen-injected mice showed a dramatic decrease in total cell numbers – in this case, nine-fold ($9.3x10^7 \pm 0.7x10^7$ to $2x10^7 \pm 1.5\ x10^7$) (Figure 4.4 B; p=0.0086). This analysis revealed no significant difference in total TEC numbers between the untreated, carrier- and tamoxifen-injected mice ($p > 0.05$) (Figure 4.4. C).

I next investigated whether the tamoxifen treatment specifically affected individual TEC subsets, by flow cytometric analysis using EpCam to identify the total TEC population, then Ly51 staining to identify the cortical TEC; $EpCam^+Ly51^-$ cells were taken as medullary TEC. MHC Class II was used to further subdivide each TEC compartment into MHC $ClassII^{hi}$ and MHC $ClassII^{lo}$ cells. This analysis indicated no statistically significant difference in the MHC Class II^{hi} mTEC compartment, with untreated mice having $10.6x10^3 \pm 4.0x10^3$ MHC Class II^{hi} mTEC in comparison to $4.9x10^3 \pm 2.7x10^3$ MHC Class II^{hi} mTEC in the tamoxifen injected mice (n=3, p=0.14). Tamoxifen injection seemed to have little to no effect on the other TEC compartments, with cell numbers of untreated and tamoxifen-injected mice displaying no significant differences (Figure 4.4C). Unfortunately there were no carrier only injected controls available for analyses at this timepoint.

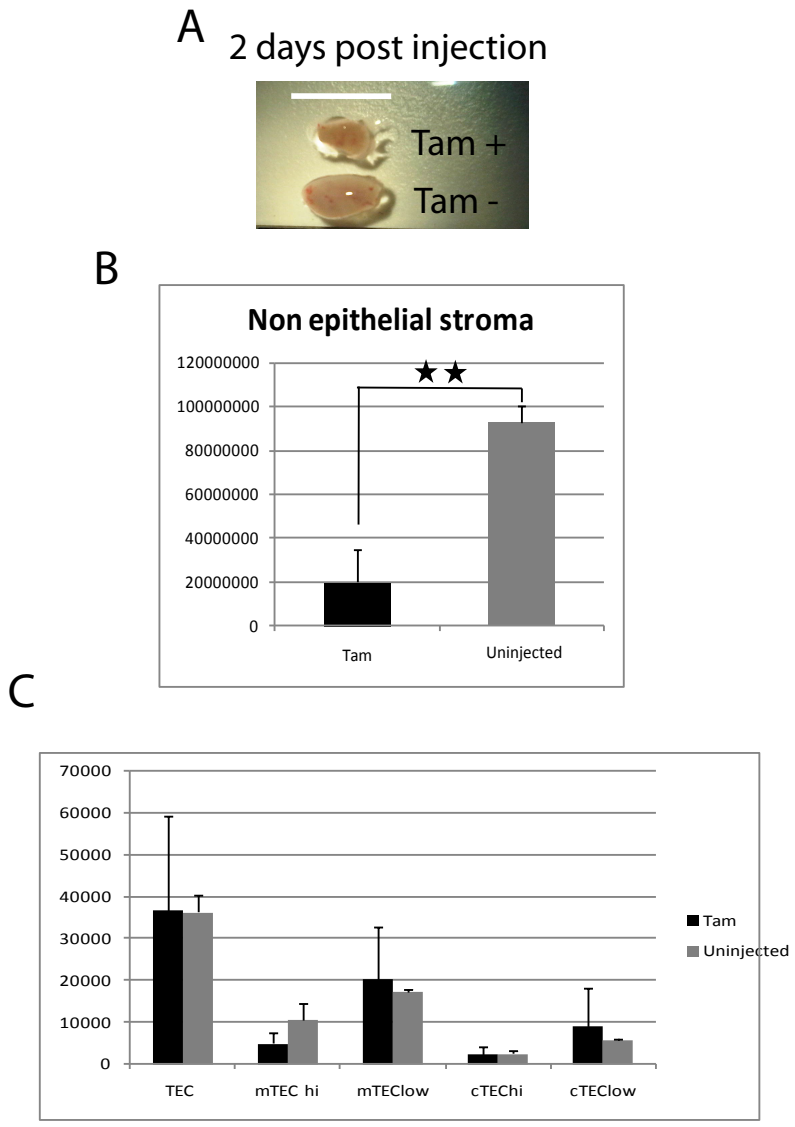


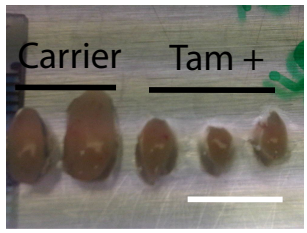
Figure 4.4. Tamoxifen injection lead to a decrease in size of tamoxifen injected thymi compared to uninjected control (A) and a decrease in thymic cellularity (B) 2 days post injection. There was no statistically significant difference in numbers of TEC (C).

The thymi of mice that had received 4x3mg injections of tamoxifen remained small even 7 days post injection compared to carrier-injected mice, and in fact showed a greater decrease in size then the thymi recovered 2 days post injection (Figure 4.5 A). In addition these tamoxifen-injected mice showed a significant decrease in total cell numbers compared to carrier-only controls. This effect was primarily on the lymphoid compartment (Figure 4.5 B; tamoxifen injected, $0.7x10^7 \pm 0.67x10^7$ cells per lobe; carrier injected, $4.23x10^7 \pm 1.35x10^7$ cells per lobe, p=0.028).

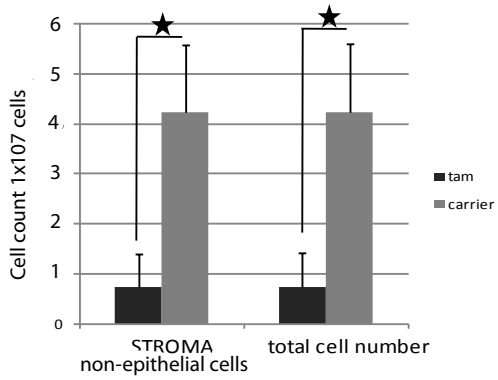
There was no significant difference in total TEC numbers between the carrier-only and tamoxifen injected mice at 7 days post injection (Figure 4.5 C; tamoxifen-injected, $24.4x10^3 \pm 6.505x10^3$; carrier-only injected $32.9x10^3 \pm 15.9x10^3$, p=0.442). Strikingly, there was an approximately four-fold decrease in the numbers of MHC ClassII^{hi} TEC in the tamoxifen-injected mice ($1.48x10^3 \pm 0.59x10^3$) versus the carrier injected mice ($5.6x10^3 \pm 1.64\ x10^3$)(p=0.02). No difference in the number of MHC ClassII^{lo} cells was detected between these groups (Figure 4.5 C).

When subdivided into cortical and medullary TEC using Ly51 and UEA1 respectively in addition to MHC Class II expression, the tamoxifen-injected mice displayed a 4.5 fold decrease in MHC ClassII^{hi} mTEC compared to carrier controls (tamoxifen injected, $1.3x10^3 \pm 0.335\ x10^3$, carrier only controls $5.1x10^3 \pm 2.1\ x10^3$, p=0.04). There was also a 1.8 fold decrease in MHC ClassII^{lo} mTEC in the tamoxifen-injected mice compared to carrier-only injected controls (tamoxifen injected, $10.1x10^3 \pm 3.15x10^3$, carrier-only control $18.5x10^3 \pm 8.7x10^3$, p=0.2), as well as a 1.4 fold increase in Ly51$^+$ cells in tamoxifen-injected mice ($4.1x10^3 \pm 2.6x10^3$) versus carrier injected controls ($2.9x10^3 \pm 1.92x10^3$, p=0.62) (Figure 4.5 C), however these results were not statistically significant.

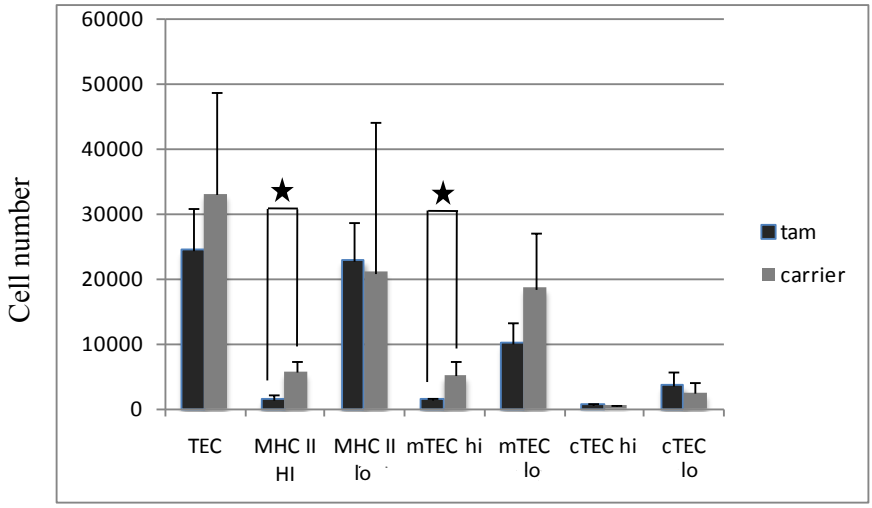
A 1 week after injection



B Effect of tamoxifen injections on non-epithelial cells
1 week post injection



C Effect of tamoxifen injections on TEC subsets



7 days post injection

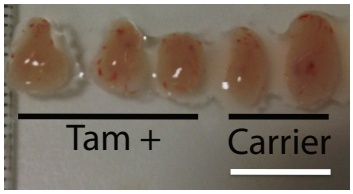
Figure 4.5. Effect of tamoxifen injection on thymus 7 days post injections. Mice were given 4 injections of 3mg tamoxifen (n=3) , or carrier (n=2) 4 months postnatally and analysed. 1 week after the last injection. Thymi if mice injected with tamoxifen show a significant reduction in size (A) (white scale bar represent 1cm) and total and non-epithelial cell numbers when compared to carrier only controls. Although there was no statistically significant reduction in total TEC numbers, there was a significant decrease in numbers of MHC IIhi cells, and the mTEChi in particular. The mTEClo also showed a decrease in cell number, while the cTEClo displayed a slight increase in cell numbers (C).
★ - $p<0.05$

When mice were analysed 3 weeks post injection, the thymi of the tamoxifen injected animals were of comparable size to the carrier-only injected controls (Figure 4.6 A).

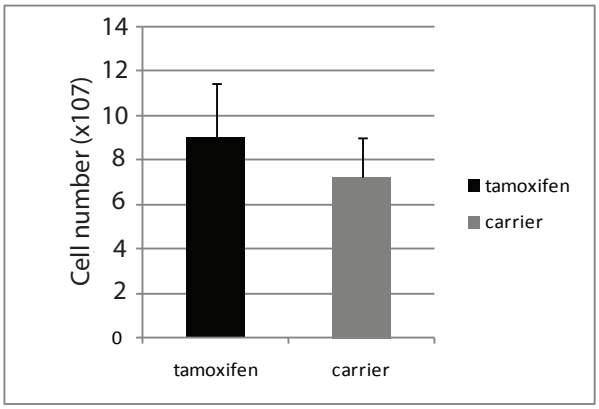
When comparing total cell numbers I found that there was little difference between tamoxifen- and carrier-injected mice, with no significant difference between total TEC numbers in carrier and tamoxifen-injected mice at this time-point (Figure 4.6 B,C).

However analysis of TEC subsets 3 weeks post injection revealed a marked increase in cell number of several TEC subsets compared to the 1 week time-point . Tamoxifen-injected mice showed an overall increase in MHC ClassII^{hi} cells, in Ly51^{+} MHC ClassII^{hi} cells in particular ($4.7x10^3$±$0.41x10^3$, and 857±412 respectively),compared to carrier only injected controls ($3.0x10^3$±$0.764x10^3$, p=0.046 versus tamoxifen-treated, and 396±133, p=0.23 versus tamoxifen-treated, respectively). The mTEC MHC ClassII^{lo} population showed an almost 2 fold decrease in cell numbers (tamoxifen-injected, $3.7x10^3$±$0.495x10^3$ n=3; carrier-injected $6.570x10^3$±$1.601x10^3$ cells, p=0.05 n=2)(Figure 4.6 C). Analyses of total TEC numbers showed a 3 fold decrease in TEC numbers from when compared to the 1 week and 2 day timepoint. However the uninjected control for this timepoint was not available, and so does not allow to control for variation in TEC isolation efficiency.

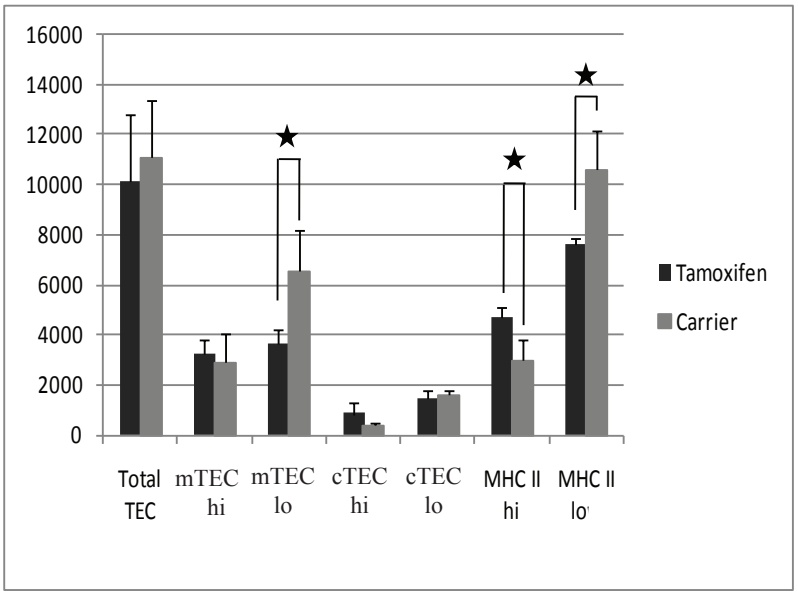
A 3 weeks post injection



B Effect of tamoxifen injections on non-epithelial cells
3 week post injection



C Effect of tamoxifen injections on main TEC subsets



3 weeks post injection

Figure 4.6 Effect of tamoxifen on the thymus 3 weeks post injection.
Mice were given 4 injections of 3mg tamoxifen (n=3), or carrier (n=2) at 4 months postnatally and analysed 3 weeks after the last injection. There was little to no difference in size between thymi of the tamoxifen and carrier injected mice (scale bar represents 1cm) (A), as well as no difference in cell number of the non-epithelial cells (B). There was no difference in total TEC numbers between the tamoxifen and carrier injected mice, however tamoxifen injected mice displayed a significant decrease in the MHC IIlo compartment, specifically in the mTEClo cells, and a significant increase in cells numbers of the MHC IIhi compartment (C). ★ - $p < 0.05$

The above data indicate that tamoxifen injection results in a transient decrease in thymus size, and that recovery from these effects is dose dependent, with higher doses of tamoxifen requiring a progressively prolonged period for regeneration. The damage to the organ is not limited to the effect of tamoxifen on thymocytes, but also affects the TEC compartment.

Furthermore these experiments showed that certain populations of TEC are more susceptible to tamoxifen-induced damage, with the MHC ClassII^{hi} mTEC showing a more pronounced decrease in numbers 1 week after injection, with cell numbers returning to the levels of carrier injected mice at 3 weeks post injection. Also a decrease in the mTEC MHC II^{lo} was detected at 3 weeks post injection, and possibly 1 week post injection. While other TEC populations seemed to show little effect at day 2 and 7 post injection, an increase in the Ly51^{+} MHC ClassII^{hi} population was observed 3 weeks post injection. However the disruption to thymus cellular composition was restored between 1-3 weeks post injection. Taking these data into consideration it is important to point out that any studies performed using this mouse model with the current injection regime might not show steady state regeneration of the organ but rather may show the cellular mechanisms that are used in thymus regeneration after injury, however this is currently unclear.

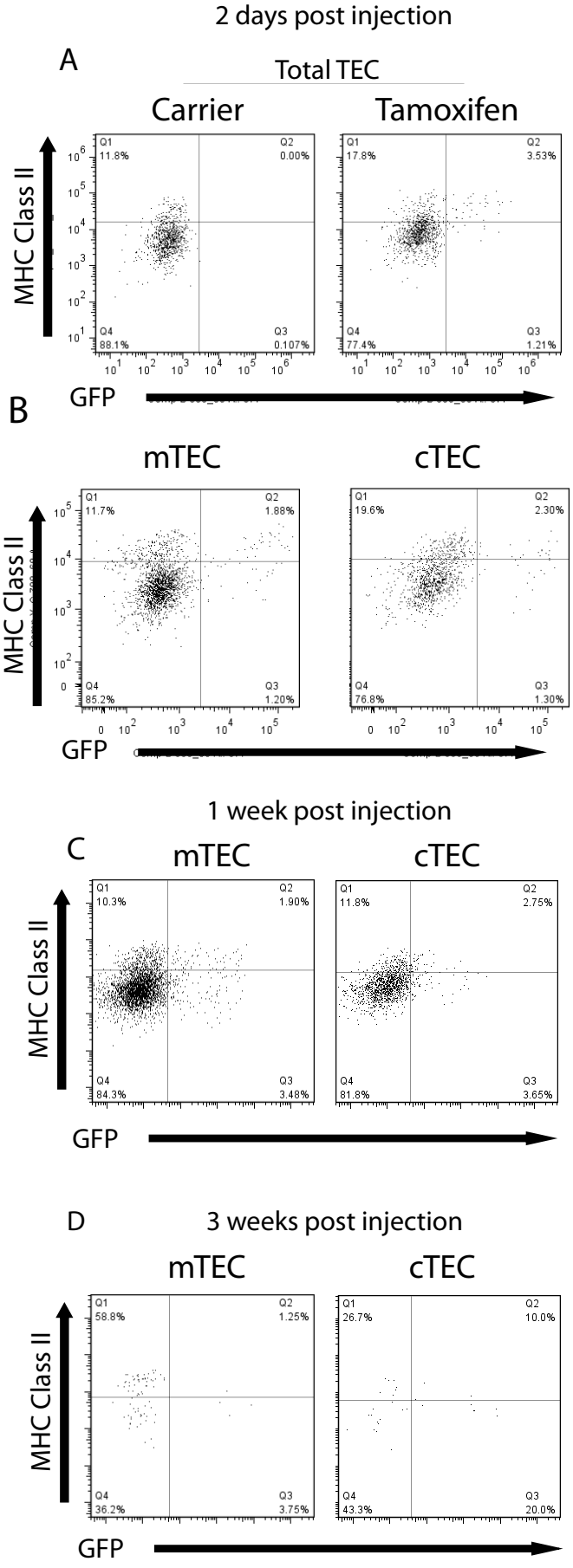
4.3 Lineage tracing

Having established the effect of tamoxifen on overall thymus size and on specific TEC subsets, I next set out to extend the studies performed in Chapter 3, to determine the *in vivo* fate of cells that could be heritably genetically labeled using *Foxn1*^{CreERt2}. In these experiments, I analysed the same Foxn1$^{CreERT2/CreERT2}$;Red/Green mice described in 4.2. I first determined the recombination efficiency two days after the final tamoxifen injection. This revealed an average recombination rate of 2.72±1.97% in the MHC Class II^{hi} TEC compartment, and of 1.8±1.2% in the MHC Class II^{lo} TEC compartment. Thus, consistent with the data shown in Chapter 3, a higher recombination rate was observed in the MHC Class II^{hi} than in the MHC Class II^{lo} TEC compartment (Figure 4.7 A, 4.8 A; n=3; p=0.052).

To further analyze the cell-type in which recombination occurred, I used Ly51 to identify the cTEC with Ly51^{-} cells being taken as mTEC, and also used MHC Class II to further subdivide the populations into MHC Class II^{hi} and MHC Class II^{lo} mTEC and cTEC. When analyzing the mTEC population the MHC Class II^{lo} population showed an average of 0.9±0.73% recombined cells among total mTEC, while the MHC Class II^{hi} showed a 1.53±1.31% recombined cells among total mTEC. These data likely reflected preferential recombination in the mTEC MHC Class II^{hi} compartment (p=0.054). The same pattern was discerned in the cTEC compartment with MHC Class II^{lo} GFP^{+} cells showing an average of 1.39±1.31% recombined cells and the MHC Class II^{hi} GFP^{+} population 2.2±2% recombined cells. However the recombination rates in these populations were not statistically significant (Figure 4.7 A,B; n=3; p=0.5).

The data presented in Figure 4.7 A and B are consistent with those presented in Chapter 3 for mice injected with 4x3mg tamoxifen. Collectively they demonstrate that this tamoxifen administration regime results in low level recombination in all four of the major TEC subsets, with apparently preferential activation in the MHC Class II^{hi} cells. As discussed in Chapter 3, this is consistent with our unpublished data showing higher levels of *Foxn1* mRNA expression in MHC Class II^{hi} cells, with the highest levels of expression postnatally being detected in the MHC Class II^{hi}

Figure 4.7 Proportional increase of GFP+ cells is observed 3 week pot injection.
Foxn1CreERT2/CreERT2;R/G mice were injected with 3mg tamoxifen for 4 days at 4 months of age. Analyses at two days post injections revealed GFP+ cells in the cTEC and mTEC, with more GFP+ cells detected in the MHC IIhi compartment of TEC (A,B). Proportion of GFP+ cells displayed no significant difference from the 2 day timepoint when analysed 7 days post injection (C). However there was a dramatic increase in the proportion of GFP+ cell in the MHC IIlo compartment, specifically in the cTEClo, 3 weeks post injection (D).


2 days post injection
A
Total TEC
Carrier
Tamoxifen
MHC Class II
GFP
Q1 11.8%
Q2 0.00%
Q4 88.1%
Q3 0.107%
Q1 17.8%
Q2 3.53%
Q4 77.4%
Q3 1.21%
B
mTEC
cTEC
Q1 11.7%
Q2 1.88%
Q4 85.2%
Q3 1.20%
Q1 19.6%
Q2 2.30%
Q4 76.8%
Q3 1.30%
1 week post injection
C
mTEC
cTEC
Q1 10.3%
Q2 1.90%
Q4 84.3%
Q3 3.48%
Q1 11.8%
Q2 2.75%
Q4 81.8%
Q3 3.65%
D
3 weeks post injection
mTEC
cTEC
Q1 58.8%
Q2 1.25%
Q4 36.2%
Q3 3.75%
Q1 26.7%
Q2 10.0%
Q4 43.3%
Q3 20.0%

cTEC and the lowest in the MHC Class II^{lo} mTEC (N. Bredenkamp unpublished). However, the difference in recombination rate between the mTEC^{lo} and cTEC^{hi} was not statistically significant (n=3; p=0.37).

In mice analysed at 1 week after the final tamoxifen injection, the proportion of GFP^{+} cells remained the same as at 2 days post injection. This could be due to the natural proliferation rate in the thymus (Gray et al, 2006) or the fact that the thymus has not yet begun to regenerate following tamoxifen treatment, as described in section 4.2 (Figure 4.7 C, 4.8 A, B, C).

However in mice analysed 3 weeks after the last tamoxifen injection, a dramatic increase in GFP-labeled cells was observed (n=3) (Figure 4.7C, 4.8 A). This pattern was observed in two independent experiments. Interestingly, although at this point the numbers of MHC Class II^{hi} mTEC are restored to pre-treatment levels, as shown in section 4.2, only a moderate increase in the proportion or number of labeled cells is observed in the mTEC (Figure 4.8 B, C). Since this population displays no loss of proportion or number of GFP^{+} cells overtime this might suggest that this population might be able to replenish itself to a certain extent, or that cells that were labeled in the mTEC are slow cycling and have not divided during the course of this analysis. To distinguish between the two, data on proliferation of these cells needs to be obtained.

Strikingly in both the MHC Class II^{Io} and MHC Class II^{hi} cTEC subpopulations, cells labeled with GFP had increased considerably in both proportion and number by 3 weeks post-injection, with the MHC Class II^{Io} cTEC showing an almost twenty-fold increase (Figure 4.8B); 1.58±0.64% at one week post injection; 20.06±9.03% at 3 weeks post injection, n=3,p=0.02).There was an increase in the amount of cTEC^{lo} GFP^{+} cells at 3 weeks, however this difference was not statistically significant, this might be due to high levels of variation in total TEC numbers in between individual mice (4.8 C). These results were consistent with IHC analysis (Figure 4.9, 4.10, 4.11), which showed small islets of GFP positive cells both in the cortex and medulla in sections acquired from mice 2 days after the final tamoxifen injection (Figure 4.9 A).

When analysed 1 week after injection GFP areas were present in both the cortex and medulla, with larger areas visible in the cortex than in the medulla (Figure 4.10 A,B). Consistent with the flow cytometric data, a dramatic increase in GFP^+ cells as a proportion of all TEC was observed in the cortex at 3 weeks following the final tamoxifen injection (Figure 4.11 A,B). No green cells were observed in the carrier only controls at any time-point analysed (Figure 4.9B, 4.10C).

Collectively, these data suggest that the population of cells initially labeled by CreERt2 activity contain thymic epithelial stem or progenitor cells that actively replenish cTEC and possibly mTEC. The progenitor cTEC appear to be preferentially contained within the labeled population, as the proportion of cTEC carrying the heritable label appears to increase over time.

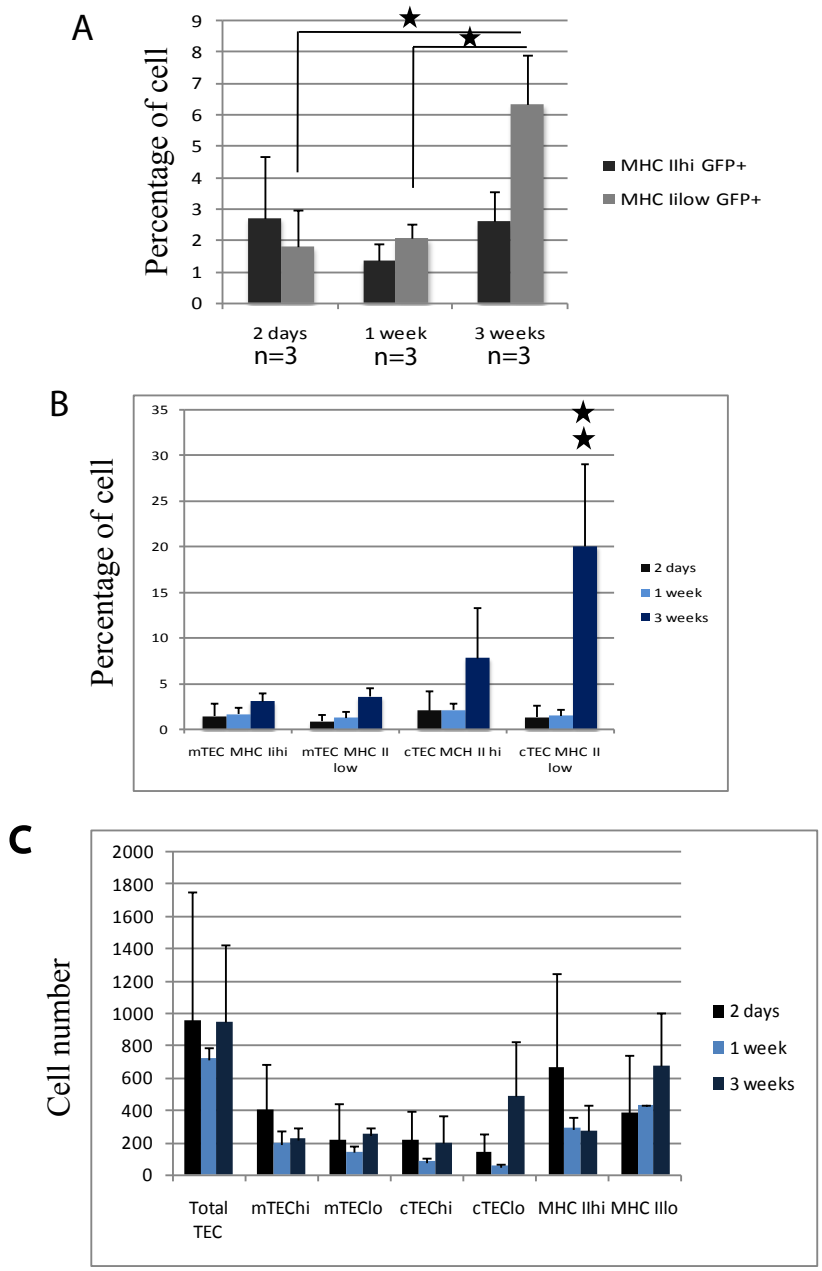


Figure 4.8 Distribution and number of GFP labelled cells in a pulse chase experiment in Foxn1CreERT2/CreERT2;RG mice.
4 month old mice Foxn1CreERT2/CreERT2;R/G mice were given 4 injections with 3mg at 4 months tamoxifen and analysed 2, 7, 21 days post injection. These mice displayed little difference in proportion and number of labelled cellls between two days and one week timepoints (n=3) (A,B,C), while mice analysed 3 weeks after injections displayed a significant increase in labelled cells in the MHC IIlo compartment (A), and increase in proportion in the cTEChi (B) and number and proportion of labelled cells in the cTEClo compartment (,B,C). ★- $p<0.05$,★★- $p<0.005$

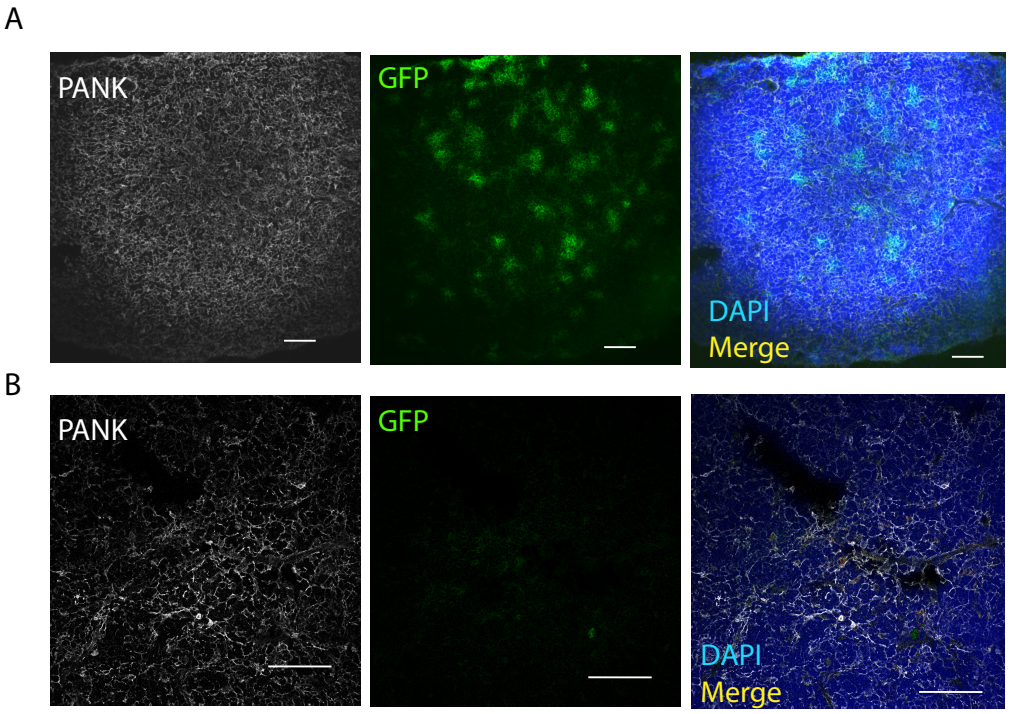
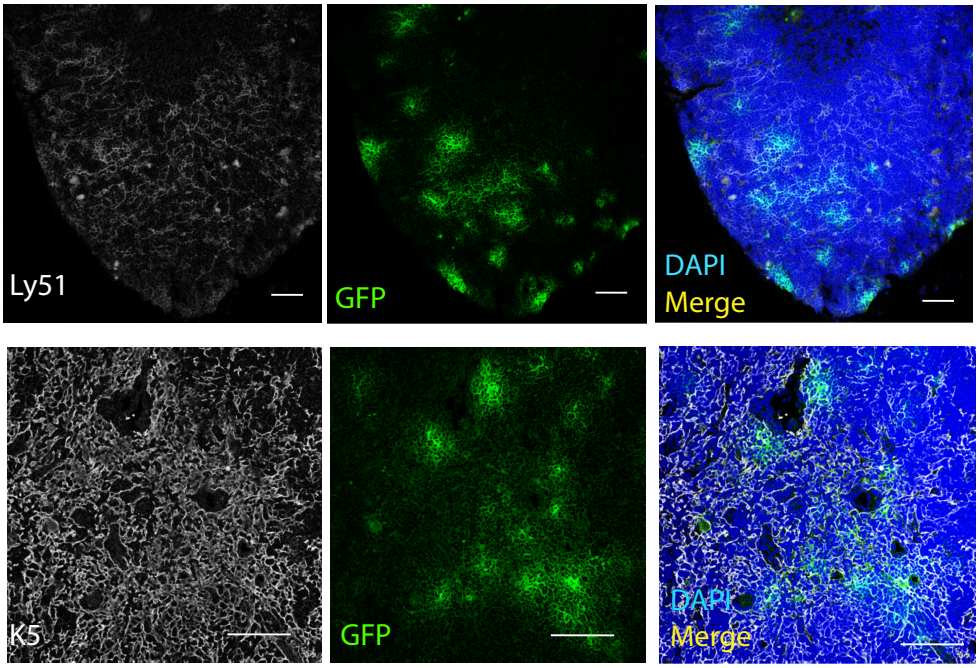


Figure 4.9. GFP+ cells were detected in the cortex and medulla 2 days post injection. Foxn1CreERT2/CreERT2;R/G mice were injected with 3mg tamoxifen for 4 days at 4 months of age. Two days post injection GFP+ cells were detected in cortex and medulla (A), carrier only injected mice did not show any GFP+ cells (B).
Scale bar represents 150µm

Tamoxifen injected



Carrier injected

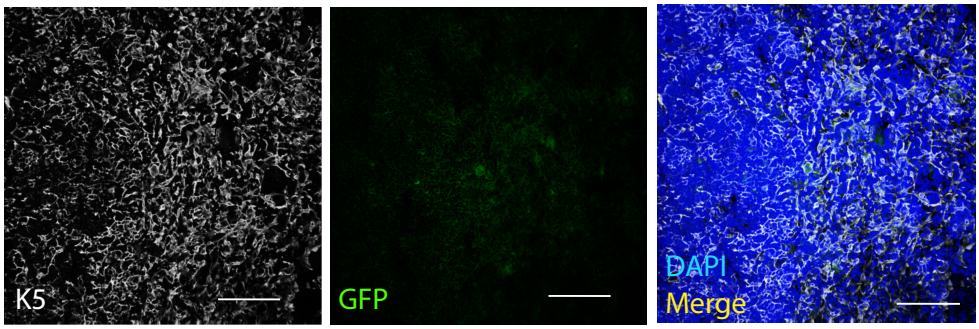


Figure 4.10. IHC analyses of localization of GFP+ cells in the thymus 1 week after tamoxifen injection.
Foxn1CreERT2/CreERT2;R/G mice were given 4 injection of 3mg tamoxifen over the course of 4 days and analysed 1 week later. GFP+ TEC were found in the cortex and the medulla (A, B), and no GFP+ cells were present in the carrier only controls.
Scale bar represent 150 μm.

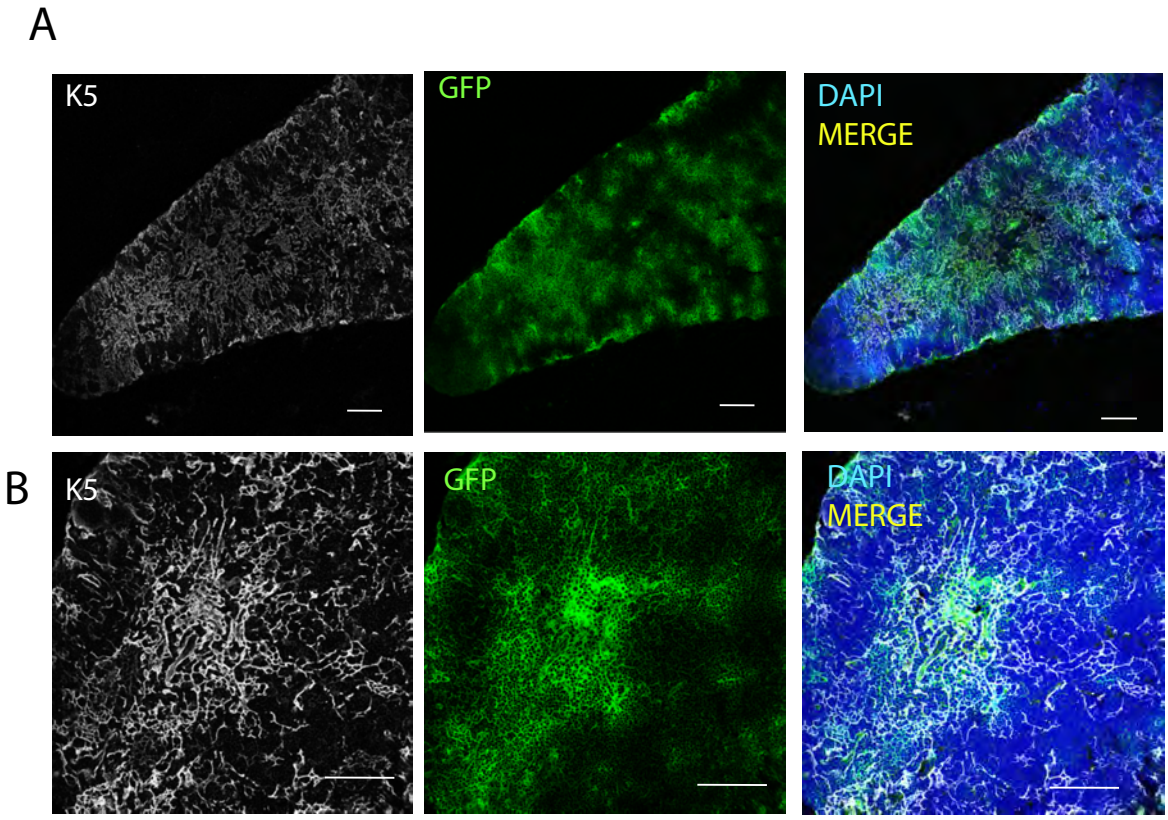


Figure 4.11. Expansion of GFP+ cells in the cortex.
Foxn1CreERT2/CreERT2;R/G mice were given 4 injection of 3mg tamoxifen over the course of 4 days and analysed 3 week later. GFP+ TEC were found in the cortex and the medulla (A, B), with a significant expansion of GFP+ cells in the cortex.
Scale bar represent 150 μm.

4.4 Discussion

The data presented in this Chapter first describe the effect of tamoxifen on the adult thymus and then contribute to understanding the relationship between the different postnatal TEC subsets in a model of thymus regeneration. These data establish that tamoxifen administration can cause a severe decrease in total thymic cell numbers, with the most pronounced loss indicated in the thymocyte compartment. Though the number of TEC was not decreased, there was evidence suggesting an effect on some of the TEC compartments. A severe reduction in cell number and proportion was evident in the MHC Class II^{hi} mTEC, with restoration of the compartment taking place only by 3 weeks after the last injection.

Interestingly, although unaffected by the initial injections, mTEC MHC $ClassII^{lo}$ displayed a reduction in cell number 1 week post injection, and a further decrease at 3 weeks, this could be due to apoptosis of these cells following tamoxifen damage. However this cell loss coincides with the restoration of the MHC $Class^{hi}$ mTEC compartment, which would be consistent with their proposed role as the progenitors of MHC $Class^{hi}$ mTEC (Grey et al, 2007, Gabler et al, 2007, Rossi et al, 2007). Further data must be acquired on apoptosis and proliferation rates in this compartment before any conclusions must be made.

Interestingly the same pattern was observed when treating mice with cyclosporine or dexamethazone (Fletcher et al, 2009), suggesting a uniform response of the thymus to different cytotoxic drugs. Since TEC exist in equilibrium with T-cells, a state referred to as cross-talk, damage to the T-cell compartment elicits a response in the TEC compartment, this is also true if the roles are reversed (Anderson et al, 2001; van Ewijk, 2000). A uniform response may indicate a lack of direct damage to TEC but rather a response to decreased number of T-cells, as there was no difference in TEC subsets at 2 days post injection.

In contrast to the MHC $Class^{hi}$ mTEC, cTEC show no adverse effect post tamoxifen injections and in fact show a slight increase in number, although the difference is not statistically relevant.

A substantial caveat of this analysis, however, is the absence of untreated control mice at 1 week and 3weeks after injection, as well as the absence of carrier-only injected controls for the 2 day time-points analysed. This was partly due to the lack of availability of mice of the proper age for the controls, due to an elevated lethality when administering tamoxifen and carrier injections to mice over the course of 4 days. Since an affect of carrier on the thymus was established in section 4.1, it is reasonable to assume that with a prolonged treatment the recovery rate of these mice would be longer. If this is correct, the absence of uninjected controls lead to inability to control for effects of prolonged exposure to carrier solution on the TEC, and as a result the effect of tamoxifen on the TEC could have been severely underestimated in this analyses. This will be rectified in future analyses performed on this mouse line.

This Chapter also provides data on tamoxifen-induced *in vivo* cell labeling in Foxn1$^{CreERT2/CreERT2}$;Red/Green mice at 4 months of age. As described in Chapter 3, with the established injection regime, a low-level of recombination level was observed, specific to the TEC compartment, after tamoxifen injection. The recombination rate appeared higher in the MHC Class II^{hi} compartment, that expresses higher levels of *Foxn1*, and GFP^{+} cells were observed in both mTEC and cTEC. However since the injection regime is 4 days long, the possibility that these cells could have arisen from MHC Class II^{lo} cells that differentiated into the MHC Class II^{hi} cells, or by division of the MHC Class II^{hi} cells, cannot be excluded. Interestingly the level of GFP^{+} cells remained relatively stable when analysed seven days post injection, consistent with data showing a prolonged negative effect of tamoxifen on the system, and a persistent decrease in thymus size and total cell number, as well as a 5 fold reduction in number of MHC Class Ii^{hi} mTEC at this time point.

There was no statistical difference between the levels of GFP^{+} cells between the 2days, 1 week, 3 week time-points for the MHC Class II^{hi} compartment of TEC. However there was a significant increase in GFP^{+} cell proportion in MHC Class II^{lo} TEC 3 weeks after injection when compared to the 1 week and 2 day groups ($p=0.03$). Interestingly a substantial increase in both proportion and number was observed in the cTEC^{lo} compartment of cells. Since there is no numerical loss of

cTEC after tamoxifen treatment, the proportional increase in GFP^+ cells could indicate several possible mechanisms of maintenance of the cTEC populations. It could be possible that a cortical progenitor residing in the MHC Class II^{lo} cTEC compartment was labeled during the initial pulse, and has proceeded to expand later in development, possibly also giving rise to MHC Class II^{hi} cTEC- which would explain their lagging increase. However it is equally possible that the MHC Class II^{hi} cTEC are contributing to the MHC Class II^{lo} cTEC compartment, that in turn undergoes expansion. The data provided does not allow these possible models of regeneration to be distinguished. In order to address this issue in future experiments tamoxifen titration will be performed in order to attempt labeling only in the MHC Ii^{hi}. The use of the confetti reporter mice might also be used in an attempt to gain more information on the relationship between TEC subsets (Snippert et al. 2010). Surprisingly there seems to be a discrepancy between IHC and flow cytometric analyses, with IHC giving the impression of a more numerous GFP+ population than is identified by Flow cytometry. This inconsistency was reporter in another cell type, where it appeared that 10% more GFP+ splenocytes could be identified by IHC than by flow cytometric analyses (Muzumdar et al. 2007). It remains to be seen if a similar discrepancy occurs when analyzing TEC and how this might influence the interpretation of the data presented.

Chapter 5: Identification of a multipotent epithelial progenitor in the postnatal thymus.

Introduction:

The thymus is broadly divided into cortical and medullary compartments, both of which contain an array of diverse, phenotypically distinct epithelial cells (Gutierrez, et al 1991), raising the question of how these different cell types are related and how they are maintained in the postnatal thymus. Earlier studies revealed that some classes of human thymic epithelial tumours contained cells that expressed both cortical and medullary markers (Schluep, Willcox et al., 1988), while *in vitro* studies indicated that cells within the tumour were able to generate cTEC and mTEC, suggesting the presence of a common thymic epithelial progenitor or stem cell (Lampert, 1988). These assumptions were further strengthened when analyses of human and mouse embryonic thymi identified epithelial cells that co-expressed markers that become restricted to the separate mTEC and cTEC populations later in adult development (Haynes, Scearce et al. 1984; Lampert 1988; Schluep, Willcox et al. 1988). In recent studies, thymic epithelial cells isolated using the mAbs MTS24 and MTS20 were demonstrated to be sufficient to generate a correctly organized thymus upon ectopic transplantation (Bennett 2002, Gill, Malin et al. 2002). These cells were able to give rise to both cortical and medullary epithelium even at low cell numbers, providing a functional indication for the existence of a common thymic epithelial progenitor cell-type.

Recently, studies using a sophisticated genetic model provided strong evidence for a bipotent progenitor. These studies showed that reactivation of *Foxn1* in a single epithelial cell in a reversible *Foxn1* null mouse model, was sufficient to generate a functional thymic lobule containing both medullary and cortical compartments (Bleul et al, 2006). In a separate study a microinjection technique was used, where a single YFP tagged TEPC isolated from E12.5 thymic lobes when injected into WT thymic lobes were able to give rise to both mTEC and cTEC, indicating the existence of a bipotent progenitor (Rossi et al. 2006). Interestingly though it is well established that

the earliest thymic progenitors in the thymus express Plet1 (Depreter et al. 2008)and that from E12.5 to E15.5 these cells when purified are able to generate all thymic epithelial cell types and initiate thymus organogenesis (Bennet et al, 2002; Gill, Malin et al., 2002). However this capacity of $Plet1^{+}$ cells was lost, when cells were isolated at E18.5 (Rossi, Chidgey et al., 2007).

The mechanisms of cellular regeneration by which the postnatal thymus is maintained during homeostasis and involution are currently unclear. It has been shown by reaggregation or injection of cells into embryonic thymi that MHC Class II^{lo} mTEC ($mTEC^{lo}$) can give rise to $mTEC^{hi}$, including $Aire^{+}$ cells (Rossi, Kim, et al. 2007; Gray et al. 2006) suggesting that this population of cells contains progenitor cells able to give rise to other mTEC lineages. In a recently published paper some evidence was shown to support the existence of a postnatal multipotent progenitor in the thymus (Park et al, 2013). In this study a transgenic mouse model was used to preferentially label the cTEC or mTEC and hypothesized that a transient TEC population expressing markers of both cTEC and mTEC contained multipotent progenitor cells. However the identity of these cells remains unknown, nor has the relationship between the mature and immature postnatal TEC compartments been established.

Previous work in our lab, which involved characterization and isolation of $Plet1^{+}$and $Plet1^{-}$ TEC from adult mice, established that the postnatal $Plet1^{+}$ TEC population has the potential to give rise to both cortical and medullary TEC when reaggregated with E12.5 thymic lobes and grafted under the kidney capsule. Postnatal $Plet1^{-}$ TEC, when isolated under the same conditions and grafted, could also contribute to both compartments. However, unlike $Plet1^{+}$ TEC the input $Plet1^{-}$ TEC fraction contained both cortical and medullary TEC before grafting and therefore, only the $Plet1^{+}$ TEC showed clear evidence of differentiation. I therefore set out to refine this work, by determining whether the $Plet1^{+}$ population contained a postnatal common thymic epitheial stem or progenitor cell.

The work described in chapter 5 aimed to identify the potential of phenotypically defined subsets of TEC in the adult mouse thymus, using a reaggregation assay. The work presented demonstrates the potency of different postnatal medullary and

cortical epithelial subsets and provides the evidence of a progenitor cell type that is able to give rise to both mTEC and cTEC compartments.

5.1 Characterization of postnatal TEC populations

I first performed a series of flow cytometric analyses to further characterize the Plet1^{+} and Plet1^{-} postnatal populations. At the time of analyses the heterogeneity of the Plet1^{-} subsets had been well established. By IHC, majority of mTEC express K5 while some express K14 or UEA1, and subset of mTEC expresses Aire (Klug et al, 1998; Anderson et al, 2002; Gray et al, 2006), while cTEC express K8, CD205, Ly51 and β5t (Klug et al. 1998; Gray et al. 2006). By flow cytometric analyses, all mTEC express UEA1 and can be further subdivided into MHC II^{lo} and MHC II^{hi}, with the MHC II^{hi} containing the Aire positive cells. cTEC can be readily identified by the expression of Ly51 and like the mTEC also have a MHC II^{hi} and MHC II^{lo} population (Gray et al, 2006). The postnatal Plet1^{+} population however, remained largely uncharacterized. Thus, I initially set out to define the Plet1^{+} and Plet1^{-} TEC subsets that would be tested functionally using the assay of TEC potency described above. All experiments described in this chapter were performed using TEC isolated from four to eight week old C57BL/6 mice.

TEC were identified by first gating on forward and side scatter (Figure 5.1 A) and excluding the lineage positive cells from the analyses (lineage contained CD45, CD11c, TER119, CD31) and then gating on EpCam^{+} cells (Figure 5.1 B). TEC are an extremely heterogenous population that stain with a variety of markers, as mentioned above, that allow differentiation between the different subsets, as shown in Figure 5.1. Ly51, a marker of cTEC, marked 6-30% of total TEC on average. The majority of this population was MHC II^{hi}, with only a small minority of MHCII^{lo} cells (Figure 5.1 C). These cells did not express UEA1 (Figure 5.1 D).

UEA-1 marks a subset of mTEC by IHC but by flow cytometric analysis marks all mTEC (Gray et al, 2006). These cells did not co-stain with Ly51, but contained distinct MHC Class II^{hi} and MHC Class II^{lo} subpopulations (Figure 5.1D,E).

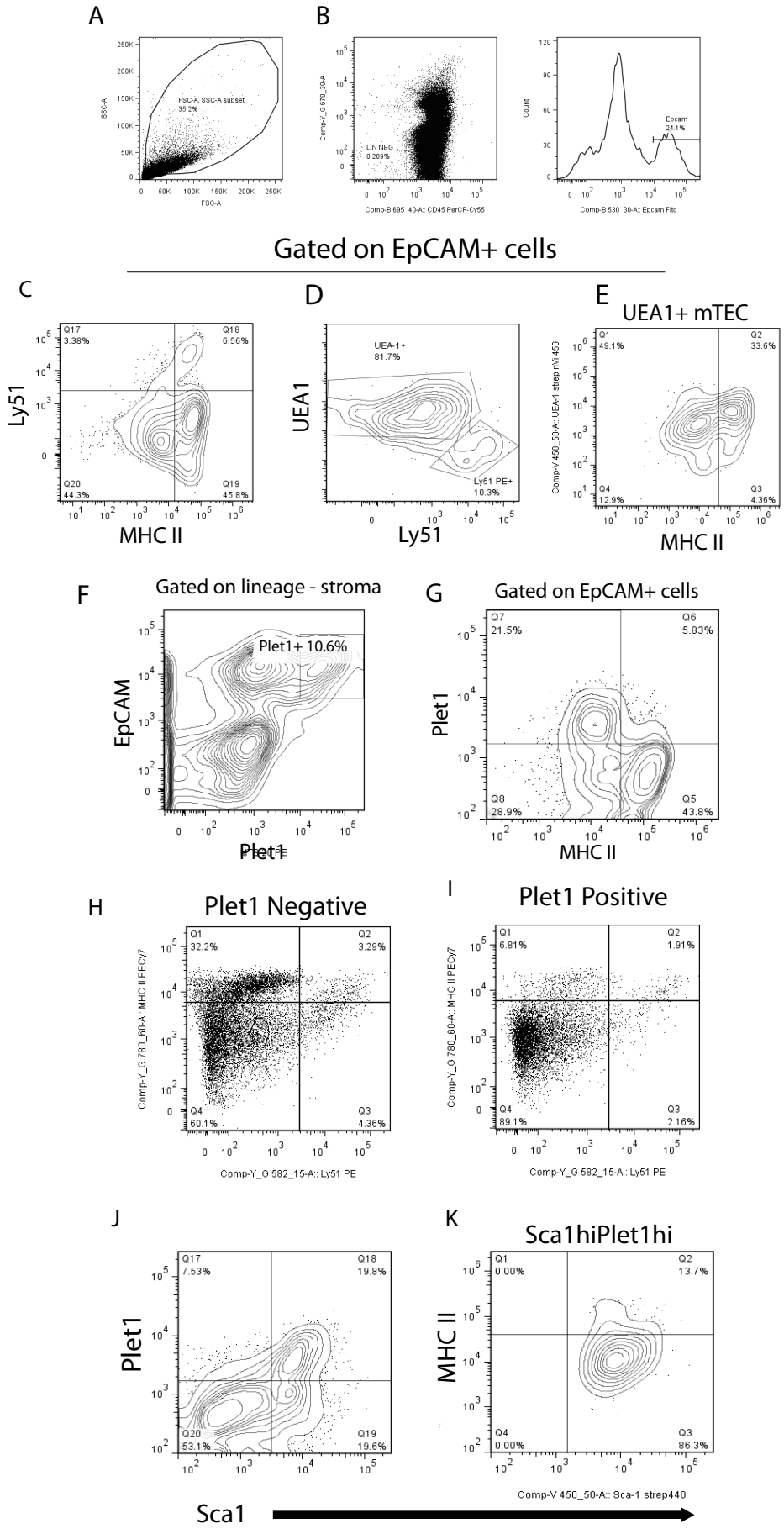
At four to eight weeks postnatally, Plet1^{+} cells comprised 7.09±2.52% of thymic stromal cells (Figure 5.1 F) and 33.17±6.05% (Figure 5.1 G) of the EpCam^{+} cells

(TEC). Most Plet1^{+} TEC were MHC II^{lo}, making up 28.2±6.4% of total TEC, with the Plet1^{+} MHC II^{hi} typically comprising 4.93±0.94% of total TEC (Figure 5.1 G). When TEC are subdivided into Plet1^{+} and Plet1^{-} fractions, both contained mTEC and cTEC as defined by UEA1 and Ly51 staining. However the distribution of these subpopulations was strikingly different, with the Plet1^{-} fraction containing most of the mTEC^{hi} and cTEC^{hi} and cTEC^{lo} populations, while the Plet1^{-} population consisted mostly of mTEC^{lo}, with only a few percent expressing mTEC^{hi}, or cTEC markers (Figure 5.1 H,I).

Approximately two thirds of Plet1^{+}TEC co-expressed Sca-1, a marker associated with stem cells in other lineages including haematopoietic stem cells (Spranrude et al, 1988). These Plet-1^{+}Sca-1^{+} TEC constituted a subpopulation of Sca-1^{+} TEC; Sca1 marks up to 40% of EpCam^{+} cells (Figure 5.1 J). The Sca1^{+}Plet1^{+} TEC did not stain for Ly51, suggesting that these cells were located within the thymic medulla. Approximately 50% of Sca1^{+} TEC co-stained with Plet1 (Figure 5.1 J). The Plet1^{+}Sca1^{+} TEC population was comprised mostly of MHC II^{lo} cells (Figure 5.1 K).

CD49F and CD24, markers which are associated with stem cells in other tissues, stained almost all TEC in flow cytometric analyses, indicating that these markers were not suitable for TEC subset analyses.

Figure 5.1 Characterization of Plet1+ TEC population by flow cytometry
Representative plot for the procedure of TEC gating shown in A-B.
TEC can be subdivided into Ly51+ cTEC and UEA1+ mTEC, and can be further subdivided into MHCIIhi and MHCIIlo compartments (C-E). Plet1+ cells tipically comprise up to 10% of the thymic stroma (F), and up to 30% of TEC (G). Plet1+ compartment consists mostly of mTEClo cells, with only a small percent expressing Ly51, as apose to the Plet1- TEC (H,I). Most Plet1 positive cells coexpress Sca-1, and these double positive cells are MHC IIlo (J,K).


A
B
FSC-A, SSC-A subset
35.2%
LIN NEG
0.209%
Epcam
24.1%
Gated on EpCAM+ cells
C
D
E
UEA1+ mTEC
Q17
3.38%
Q18
6.56%
Q20
44.3%
Q19
45.8%
Ly51
MHC II
UEA-1+
81.7%
Ly51 PE+
10.3%
UEA1
Ly51
Q1
49.1%
Q2
33.6%
Q4
12.9%
Q3
4.36%
F
Gated on lineage - stroma
Plet1+ 10.6%
EpCAM
Plet1
G
Gated on EpCAM+ cells
Q7
21.5%
Q6
5.83%
Q8
28.9%
Q5
43.8%
Plet1
MHC II
H
Plet1 Negative
I
Plet1 Positive
Q1
32.2%
Q2
3.29%
Q4
60.1%
Q3
4.36%
Q1
6.81%
Q2
1.91%
Q4
89.1%
Q3
2.16%
Comp-Y_G 780_60-A:: MHC II PECy7
Comp-Y_G 582_15-A:: Ly51 PE
J
K
Sca1hiPlet1hi
Q17
7.53%
Q18
19.8%
Q20
53.1%
Q19
19.6%
Q1
0.00%
Q2
13.7%
Q4
0.00%
Q3
86.3%
Plet1
MHC II
Comp-V 450_50-A:: Sca-1 strep440
Sca1

5.2 TEC potency assay: experimental strategy

I next set out to determine which of the postnatal TEC subpopulations defined above contained progenitor or stem cell activity, using an assay of TEC potency recently developed in this laboratory. Thus, TEC populations were sorted from thymi of four to eight week old aGFP mice, that constitutively and ubiquitously express a membrane tethered GFP (see Materials and Methods). At this age the thymus is fully structured but has yet to display any signs of involution, in terms of loss of architecture (Manley et al., 2010; Sempowski et al., 2002).

Thymi were obtained by dissection and were then enzymatically digested using a collagenase/dispase mix (see Materials and Methods). In order to enrich this single cell suspension for TEC, the cells were resuspended with magnetically labeled anti-CD45 antibodies, and run through a magnetic column to remove the majority of T-cells. The remaining cells were then resuspended, stained with a panel of antibodies, and specific subpopulations were purified by flow cytometric cell sorting as described in Materials and Methods. After gating on FSC and SSC, dead cells were excluded using DAPI. The remaining T-cells and other non-epithelial components were gated out using a lineage cocktail containing anti-CD4, anti-CD8, anti-TCRB, anti-CD3e, TER-119, and anti-CD19 antibodies. The gates were then set on the $Epcam^{+}GFP^{+}$ population of cells (Figure 5.2 A,B). This $Epcam^{+}$ population was then split into $UEA1^{+}$ mTEC, which make up the majority of the $EPCAM^{+}$ cells, and $Ly51^{+}$ cTEC, which typically comprised 6-30% of $Epcam^{+}$ cells(Figure 5.2C) depending on the efficiency of the enzymatic digestion. The majority of $Plet1^{+}$ cells were detected in the mTEC, with only a minor population of $Plet1^{+}$ cells in the $Ly51^{+}$ population, comprising 0.5-1% of total TEC (Figure 5.2 D,E).

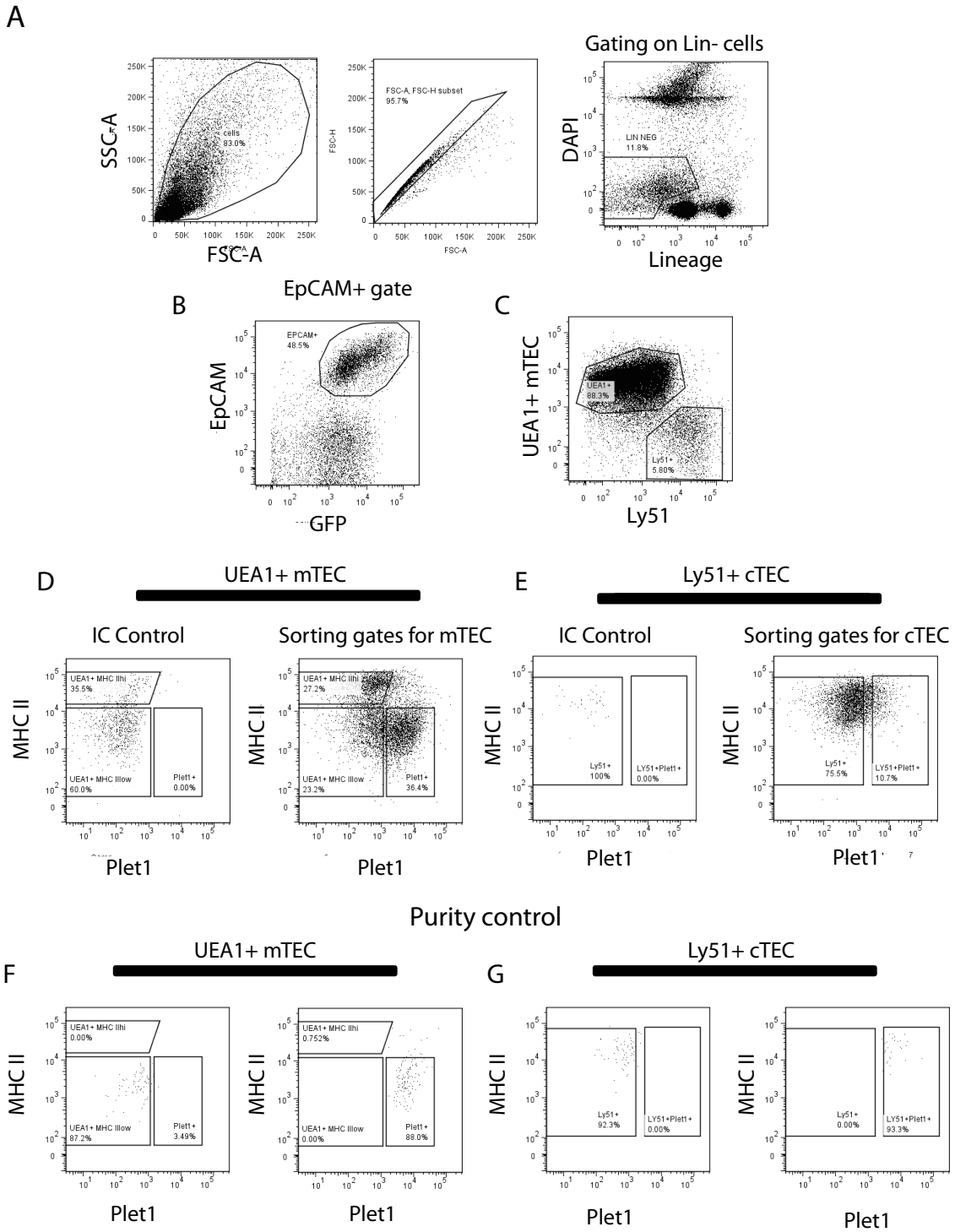


Figure 5.2 Sorting strategy for TEC potency essay, setting of forward and side scatter, excluding dead cells and lineage negative cells and gating on the EpCAM+(A,B), Epcam positive cells were divided into cortincal and medullary TEC using Ly51 and UEA1 respectively (C). UEA1+ mTEC were then subdivided into three main populations UEA1+MHCIIhiPlet1-, UEA1+Plet1-MHCIIlo, UEA1+Plet1+MHCIIlo (D). Ly51+ cortical cells were split into two populations with one coexpressing Ly51 and Plet1 (E). Representative sorting purity checks are illustrated in F,G.

In these studies, I chose to analyse five TEC populations for the existence of a multipotent or unipotent progenitors:

UEA1^{+}MHCII^{hi}Plet1^{-}TEC

UEA1^{+}MHCII^{lo}Plet1^{-}TEC

UEA1^{+}MHCII^{lo}Plet1^{+}TEC

Ly51^{+} Plet1^{-} TEC

Ly51^{+}Plet1^{+} TEC

Representative purity checks for these sorted populations are presented in Figure 5.2 F,G.

In my initial analyses, 10,000 cells of each population were isolated. These cells were then reaggregated with E12.5 or E13.5 dissociated embryonic thymi and MEFs and the reaggregates grafted under the kidney capsule of immunologically compatible mice (Figure 5.3). The exception was Ly51^{+}Plet1^{+} TEC, where due to the rarity of the population only 1500 cells were isolated per graft. I chose to aggregate the test populations with dissociated embryonic thymi, as reaggregates based on fetal thymic cells are well established to be able to form a new thymic organoid upon transplantation (Bennett et al, 2002), and I wished to test the potency of the test cells within an environment known to be able to provide inductive signals for TEC differentiation and organization. MEFs were used to increase cell numbers in the reaggregate, for ease of handling. In the experiments described below, the grafts were left for four weeks before analysis. During this time, the grafts increased substantially in size and developed properly structured cortical and medullary areas. Any grafts that displayed large cystic areas or failed to grow over the course of the 4 weeks were discarded, only fully formed organoids were incorporated in the analyses. At this time they were removed and analyzed for the presence of GFP cells by IHC.

In order to distinguish between cortex and medulla, a numbers of markers were used - with UEA1 and K14 used to identify mTEC subsets and Ly51, CD205 and β5t used

to identify cTEC. DAPI density was also used in addition to markers described above, with DAPI dense areas being characteristic of cortex and DAPI sparse areas, of medulla.

All grafts were analysed for the presence of GFP^+ cells. If these were located, they were stained with a panel of antibodies to determine their lineage, and the percentage of contribution to different TEC subsets scored. In addition, all grafts were tested for the presence of $CD45^+$ cells which signifies that these grafts are functionally competent and able to attract T-cell precursors.

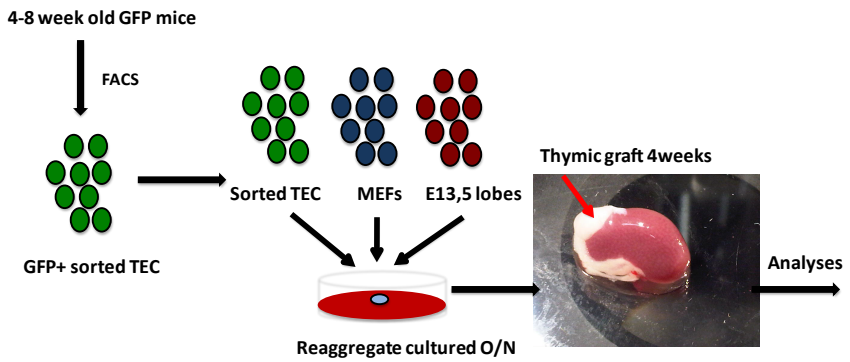


Figure 5.3 Schematic representaion of reaggregation and grafting assay.

5.2 Differentiative potential of UEA1$^+$ mTEC.

Three UEA1$^+$ TEC populations were tested in the grafted RFTOC assay described above. Of these, two populations - UEA1$^+$MHCII^{hi}Plet1$^-$and UEA1$^+$MHCII^{lo}Plet1$^-$ TEC - gave a low incidence of medullary contribution, with no cortical contribution detected.

For the UEA1$^+$MHCII^{hi}Plet1$^-$ TEC (n=5), a single GFP area was detected in one out of five grafts (Figure 5.4 A,B). The GFP positive cells stained positive for K14 and were negative for Ly51 and β5t, Plet1 and CD205, and displayed a dispersed DAPI stain, indicating that they were medullary TEC.

The UEA1$^+$MHCII^{lo}Plet1$^-$ TEC cells (n=2) produced one small medullary area in 1 out of 2 grafts analysed, determined by DAPI density.

No contribution of the UEA1$^+$MHCII^{lo}Plet1$^+$ TEC (n=5) was detected in three of three grafts.

These data indicated that among the three mTEC populations analysed, two were able to give limited contribution to the grafts while the third made no contribution. In addition these cells only contributed to mTEC, indicating that these cells were restricted to the mTEC lineage. It was not possible to determine in these analyses whether the input cells had differentiated, but the small size of the GFP$^+$ foci suggested strongly that these populations did not contain progenitor TEC.

5.3 Differentiative potential of Ly51$^+$ cTEC

5.3.1 Potency of the Ly51$^+$ Plet1$^-$ population.

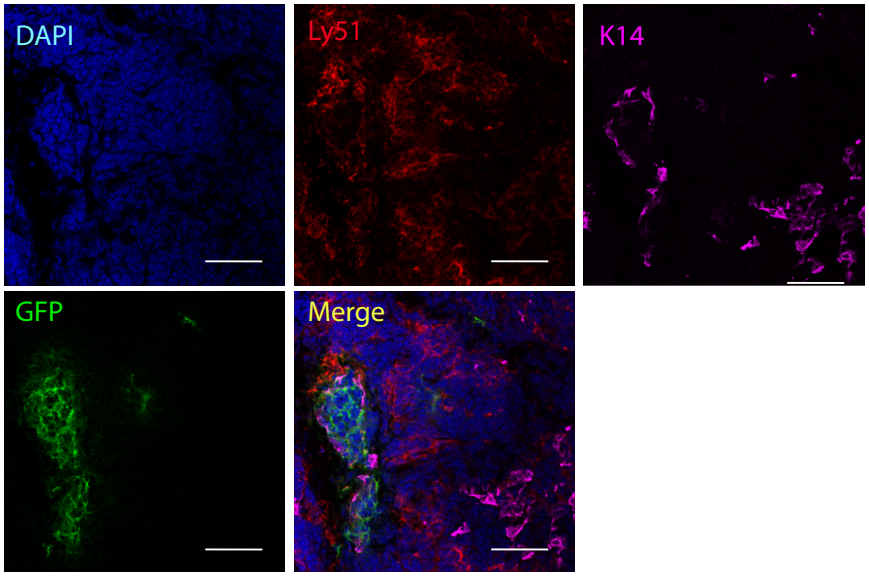
In grafts seeded with Ly51$^+$MHCII$^+$Plet1$^-$ test TEC (Figure 5.4 B), extensive areas of GFP$^+$ TEC were detected in all grafts analysed, with 0 to 49 GFP$^+$areas per section (average, 14.76±11.84, n = 3). These GFP$^+$ cells displayed characteristic markers of cTEC – including Ly51 (Figure 5.4 B,D), β5t (Figure 5.4C),and were found exclusively in DAPI-dense cortical areas. In all grafts analysed, multiple islets of GFP$^+$TEC were observed, many of which were situated in the periphery of the thymic lobe. These GFP$^+$ clusters were negative for K14 and Plet1. Out of the 389 GFP$^+$ cluster analysed, a few that consisted of single cells or a cluster of three cells stained positive for K14, however these cells were not situated in the medulla, and did not look like properly formed mTEC regions.

These data thus indicated that the Ly51$^+$MHCII$^+$Plet1$^-$ TEC population contained cells that were able to contribute to cTEC networks for at least four weeks after grafting. Although this subpopulation was not subdivided into MHC II^{hi} and MHC II^{lo} cells, it is likely that the Ly51$^+$MHC II^{lo} cells are responsible for the extensive contribution to the TEC network, since Ly51$^+$MHC II^{hi} cells are known to be largely post mitotic (Nick Bredenkamp, unpublished).

Figure 5.4 UEA1+MHCIIhi Plet1- cells are only able to contribute poorly to mTEC, while Ly51+Plet1- TEC are able to contribute extensively to cTEC only. UEA1+MHCIIhi Plet1- were only able to contribute to 1/5 grafts analysed. These cells contributed to mTEC only as demonstrated by K14 staining (A). While the Ly51+Plet1- cells were able to robustly contribute to cTEC, and stained for typical cTEC markers Ly51, β5t (B,C,D). Scale bar represents 150μm.

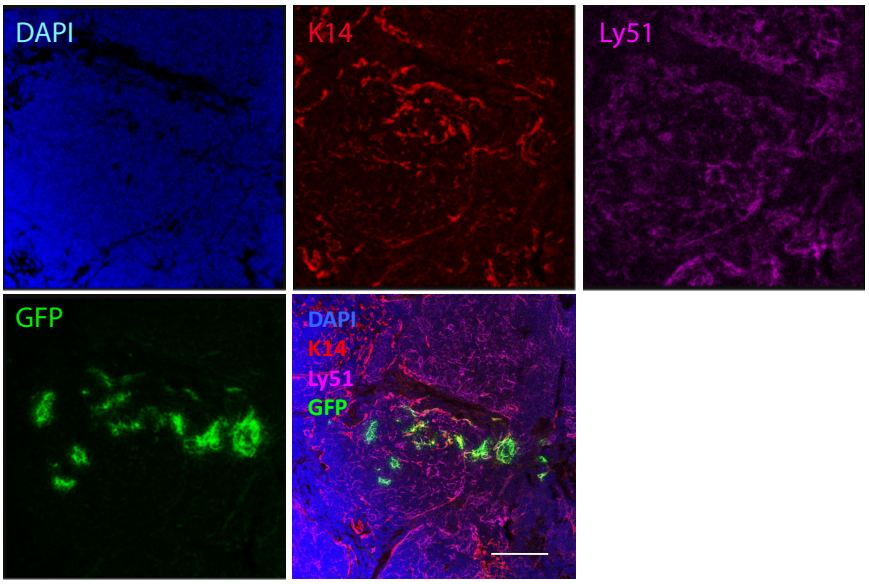
UEA1+ MHCIIhi Plet1- cells contribute to medulla

A

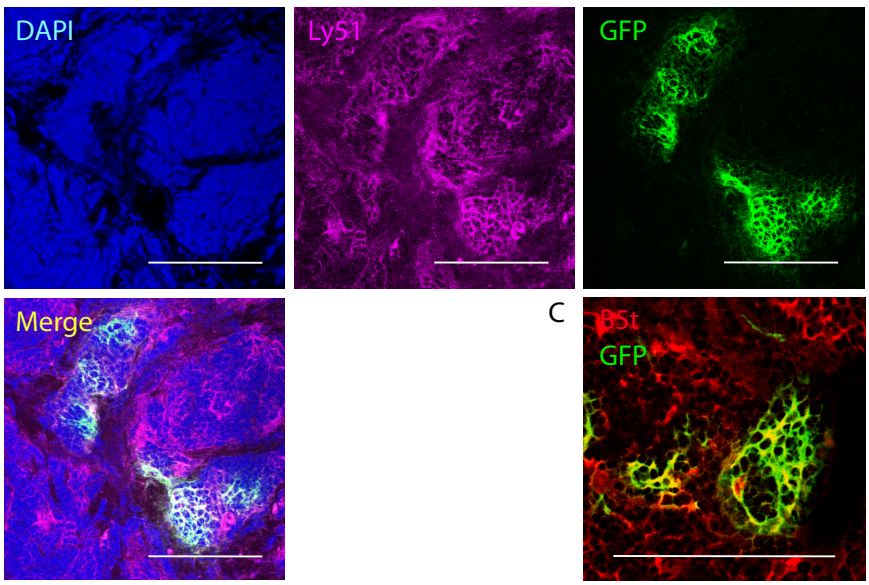


Ly51+ MHCII+ Plet1- cells contribute to cortex

B



D



C

5.3.2 Potency of Ly51$^+$Plet1$^+$ TEC.

I next tested the potency of the minor Ly51$^+$Plet1$^+$MHCII$^+$ TEC subpopulation. The grafts for this population were established using only 1500 test TEC, due to the technical difficulty in obtaining higher numbers. In three out of three grafts analysed, 1500 Ly51$^+$Plet1$^+$MHC Class II$^+$ cells gave rise to a few extensive GFP$^+$ clusters (Figure 5.5 A). These clusters were found in both medullary and cortical areas, with GFP$^+$ TEC in the cortical areas expressing Ly51 and CD205 (Figure 5.5B), and medullary areas being negative for Ly51 and positive for K14 and UEA1 (Figure 5.6 A).

The Ly51$^+$Plet1$^+$ cells were also the only cells that gave rise to cells that stained for Plet1, making these cells the only cells that gave rise to all the main TEC subsets. These GFP$^+$Plet1$^+$ cells were located on the outskirts of the medulla, possibly in the CMJ region (Figure 5.6 B).

Out of 46 GFP$^+$ areas analysed in the Ly51$^+$Plet1$^+$ cell grafts, 14 were medullary regions (30.96±5.71%; standard deviation used) and 32 were cortical areas (69±5.7%, n=2).

These data demonstrate that the Ly51$^+$Plet1$^+$ population is the only TEC subset analysed that can give rise to both cTEC and mTEC, making this the only subset exhibiting possible multipotent progenitor activity. In addition the contribution to cTEC in these grafts is more extensive than to mTEC, suggesting that this subset contains cells already primed towards the cTEC lineage.

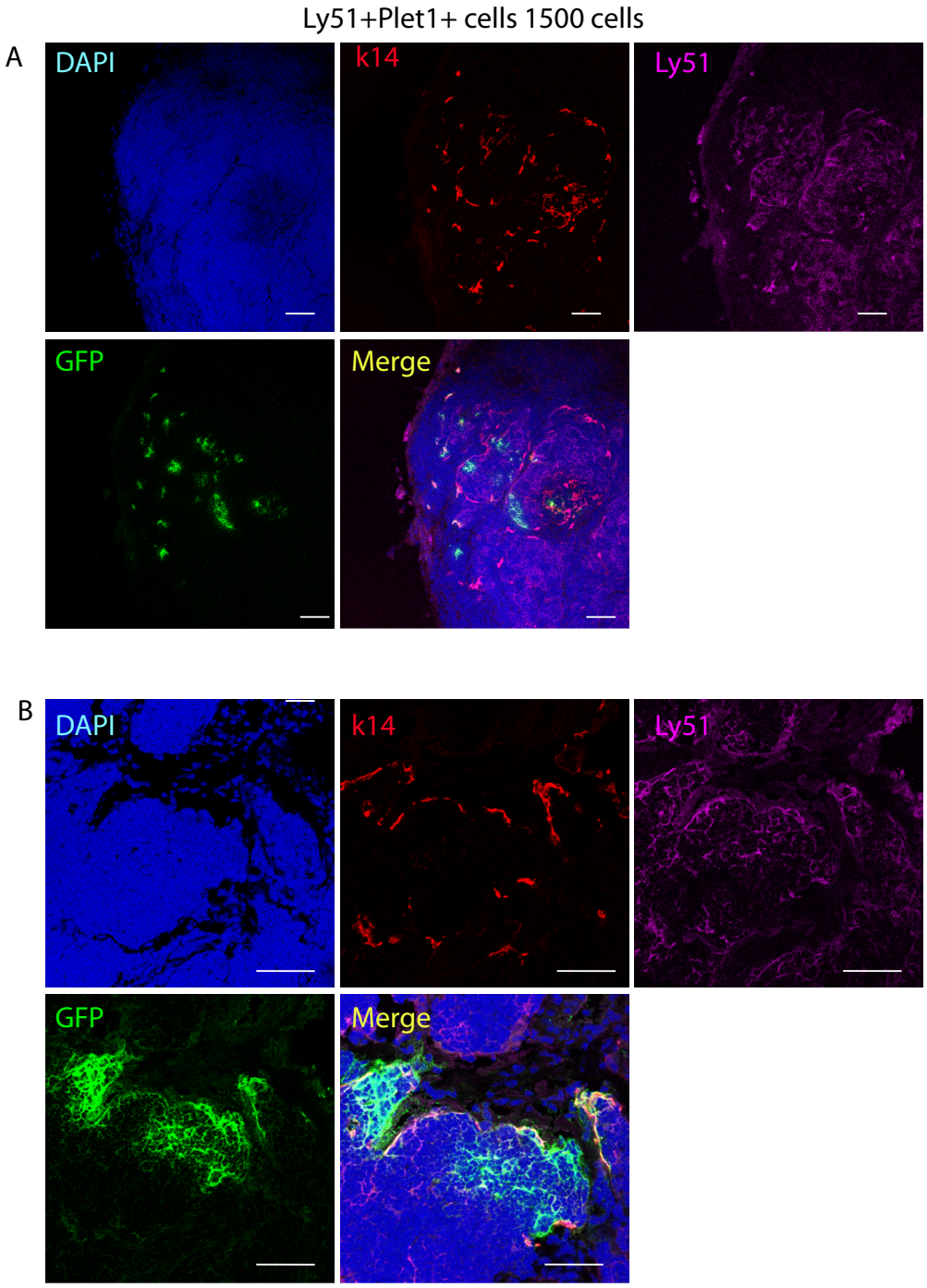


Figure 5.5 1500 Ly51+Plet1+ test cells can contribute to both mTEC and cTEC. IHC analyses of grafts showed contribution to both mTEC (stained with K14) and cTEC (identified by Ly51 staining) (A,B). Scale bar represents 150µm

5.4 Frequency of TEPC within the Ly51$^+$Plet1$^+$ TEC.

In order to determine whether the Ly51$^+$Plet1$^+$ TEC population of the postnatal thymus contained a common TEPC, able to generate both cortical and medullary TEC subtypes, or separate cTEC and mTEC progenitors, I used a limiting dilution approach to establish the frequency at which these cells were able to give rise to cortical and medullary TEC.

For this I generated grafts containing a dilution series of test cells, such that the grafted RFTOC were initially, seeded with 500, 250, 125 or 60 Ly51$^+$Plet1$^+$GFP$^+$ TEC. Recovered grafts were sectioned and sections containing GFP$^+$ cells were identified by eye using a fluorescence microscope, and further confirmed with GFP staining. The GFP$^+$ cells were then stained for a variety of markers.

5.4.2 Analyses of contribution of 500 inputLy51$^+$Plet1$^+$GFP$^+$test cells

Grafts seeded with 500 Ly51$^+$Plet1$^+$ cells all contained extensive contribution of GFP$^+$ cells in both medullary and cortical areas (n = 3). The clusters of GFP$^+$ cells in grafts initially seeded with 500 test cells contained one to two hundred TEC, with over 20 GFP$^+$ areas identified in each graft. GFP$^+$ TEC within cortical areas expressed Ly51 and CD205, and within medullary areas expressed K14, UEA1 (Figure 5.7 A,B,C). GFP$^+$ cells expressing Plet1 were also detected.

Out of 59 areas analysed in 3 grafts, 32 were located in the cortex and 26 in the medulla. On average in the 3 grafts analysed, contribution to mTEC was observed in 37±23.6% of GFP$^+$ clusters, with 62.6±24.02% contributing to cTEC.

Taking this data into account, it is clear that 500 cells were sufficient to contribute to the graft architecture, producing cells of cTEC and mTEC lineages. There were no differences observed in number of GFP areas per graft or the rate of contribution to mTEC and cTEC in these grafts from the grafts seeded with 1500 Ly51$^+$Plet1$^+$ test cells.

5.4.2 Analyses of contribution of 250 input Ly51$^+$Plet1$^+$GFP$^+$ test cells

All grafts seeded with 250 Ly51$^+$Plet1$^+$ TEC also showed contribution to both cortex and medulla (n=3).As above, GFP$^+$ TEC in cortical areas stained positive for Ly51 and CD205, and in medullary areas were positive for K14 (Figure 5.8 A,B,C). There was a lower incidence of GFP$^+$ areas compared to the grafts seeded with 500 Ly51$^+$Plet1$^+$ cells, however the rate of contribution to cTEC and mTEC remained almost the same as in the grafts seeded with 500 Ly51$^+$Plet1$^+$ test cells, with 76±1.41% of GFP$^+$ cells detected in the cortex, and 24±1.41% in medullary regions.

5.4.3 Analyses of contribution of 125 input Ly51$^+$Plet1$^+$GFP$^+$ test cells

Analysis of grafts generated with 125 Ly51$^+$Plet1$^+$GFP$^+$ test TEC also revealed the presence of test cell-derived TEC in both the cortex and medulla. Of note is that even at this low cell number of input test cells, islets containing Plet1$^+$GFP$^+$ TEC were detected in the grafts in addition to islets containing either Ly51$^+$Plet1$^-$ TEC or K14$^+$Plet1$^-$UEA1$^+$ TEC (n=3) (Figure 5.9 A,B,C). In these grafts only 3-8 areas were detected per graft. With an average of 41.5%±12% of GFP$^+$ cells located in the cortex, and 58%±11.3% located in the medulla.

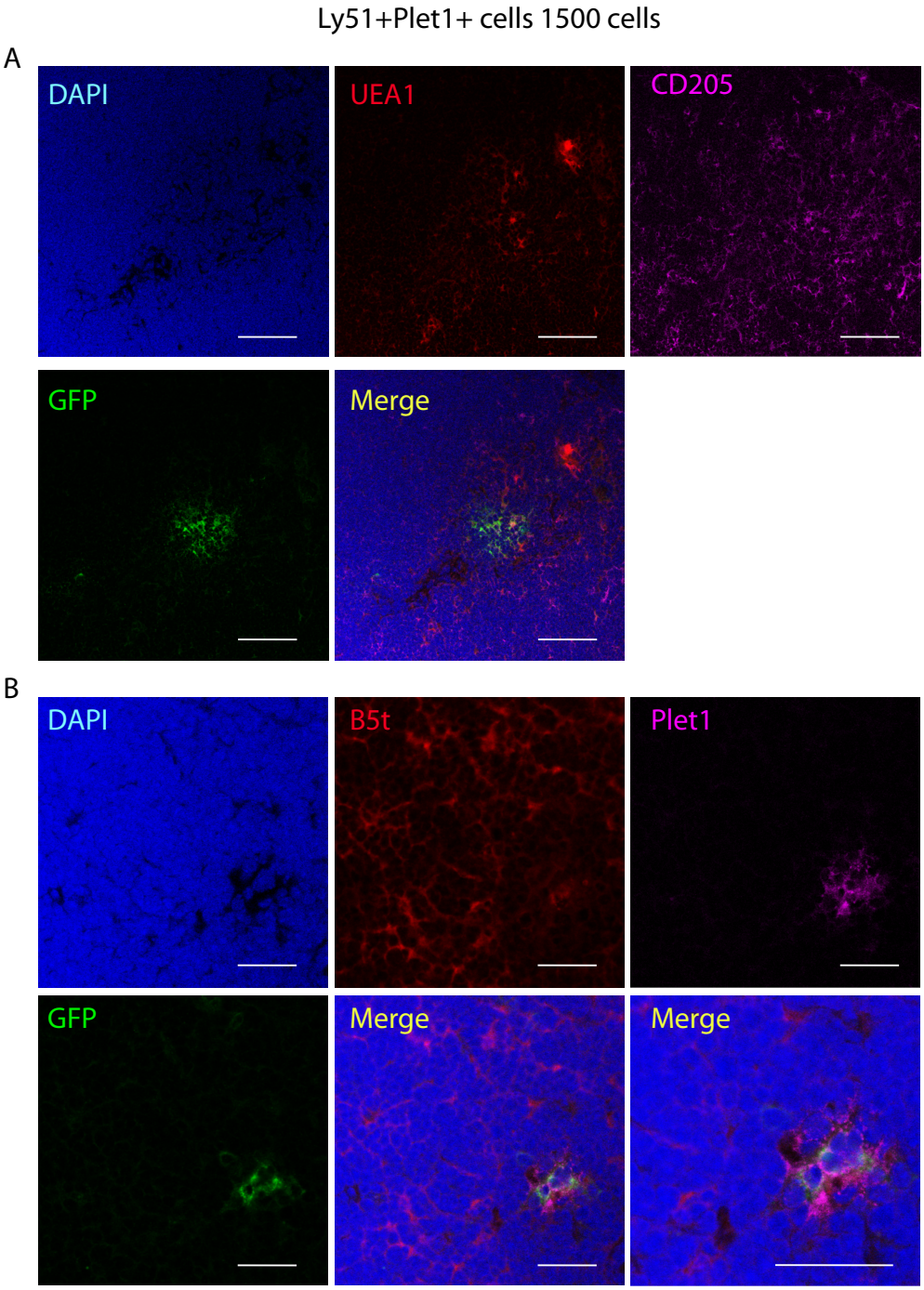


Figure 5.6 Ly51+Plet1+ cells are able to contribute to cTEC and mTEC including UEA1+ mTEC (A), and Plet1+ cells (B).
Scale bar represents 150μm.

Figure 5.7 500 Ly51+Plet1+ test cells contribute to cTEC and mTEC.
500 Ly51+Plet1+ cells test cells were able to contribute to both mTEC (K14, UEA1) (A,B), and cTEC (CD205) (C).

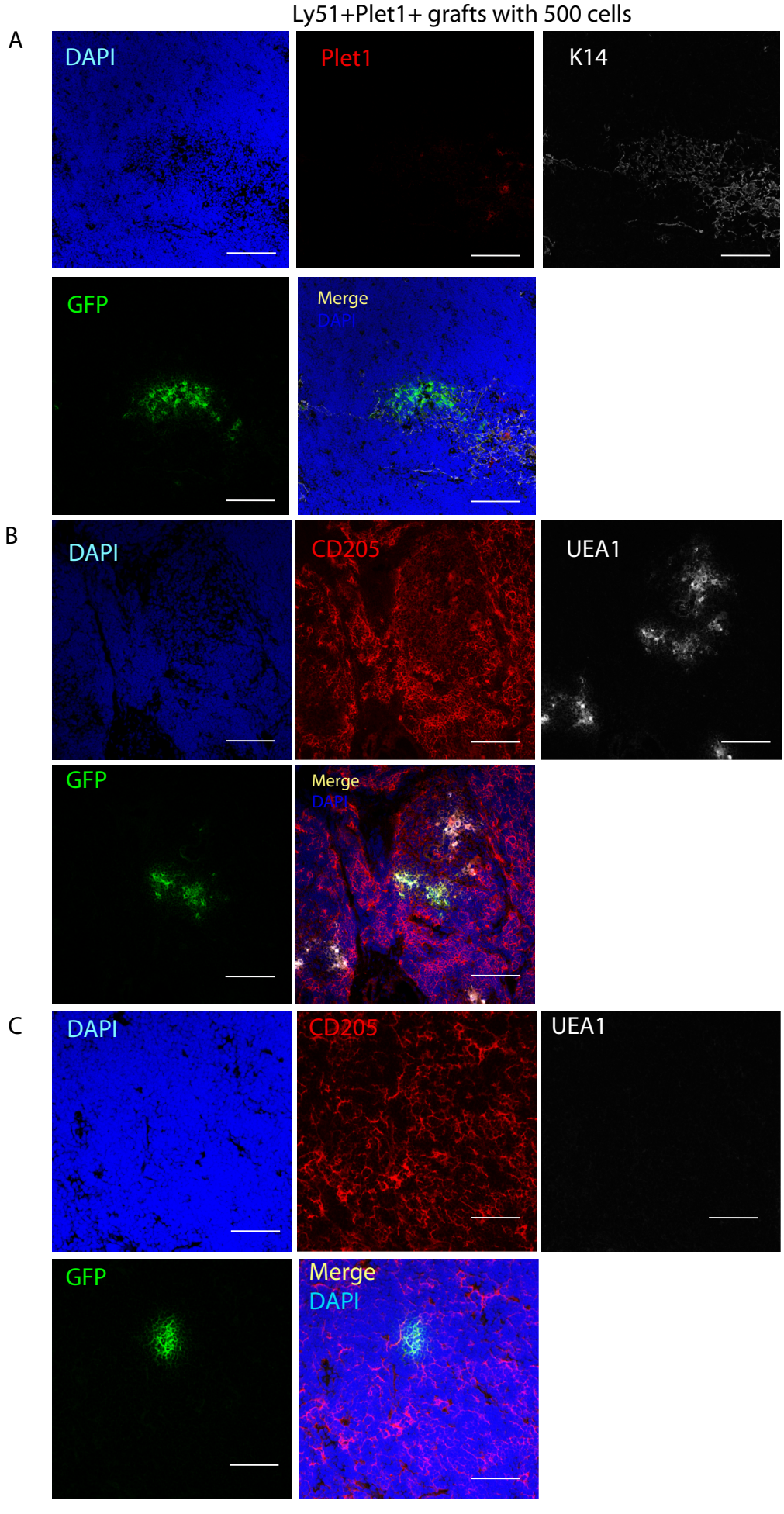

Ly51+Plet1+ grafts with 500 cells
A
DAPI
Plet1
K14
GFP
Merge
DAPI
B
DAPI
CD205
UEA1
GFP
Merge
DAPI
C
DAPI
CD205
UEA1
GFP
Merge
DAPI

Figure 5.8 250 Ly51+Plet1+ test cells are able to contribute to both cTEC and mTEC
Grafts formed with Ly51+Plet1+ test cells were able to contribute to cTEC, as shown by Ly51 and CD205 staining (A,C), and mTEC illustrated by K14 staining (B)
Scale bar represents 150μm

Ly51+Plet1+ cells 250 cells

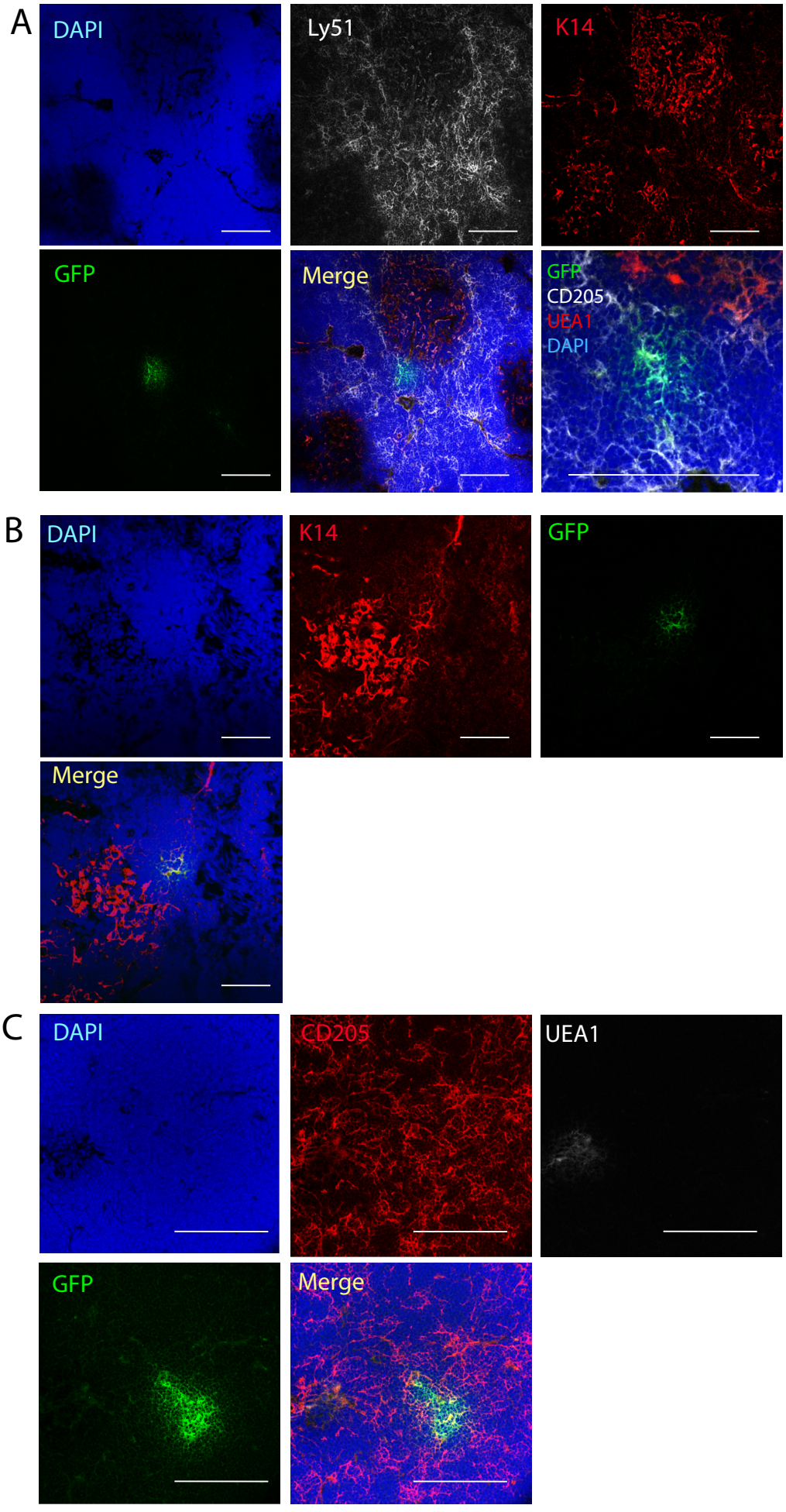
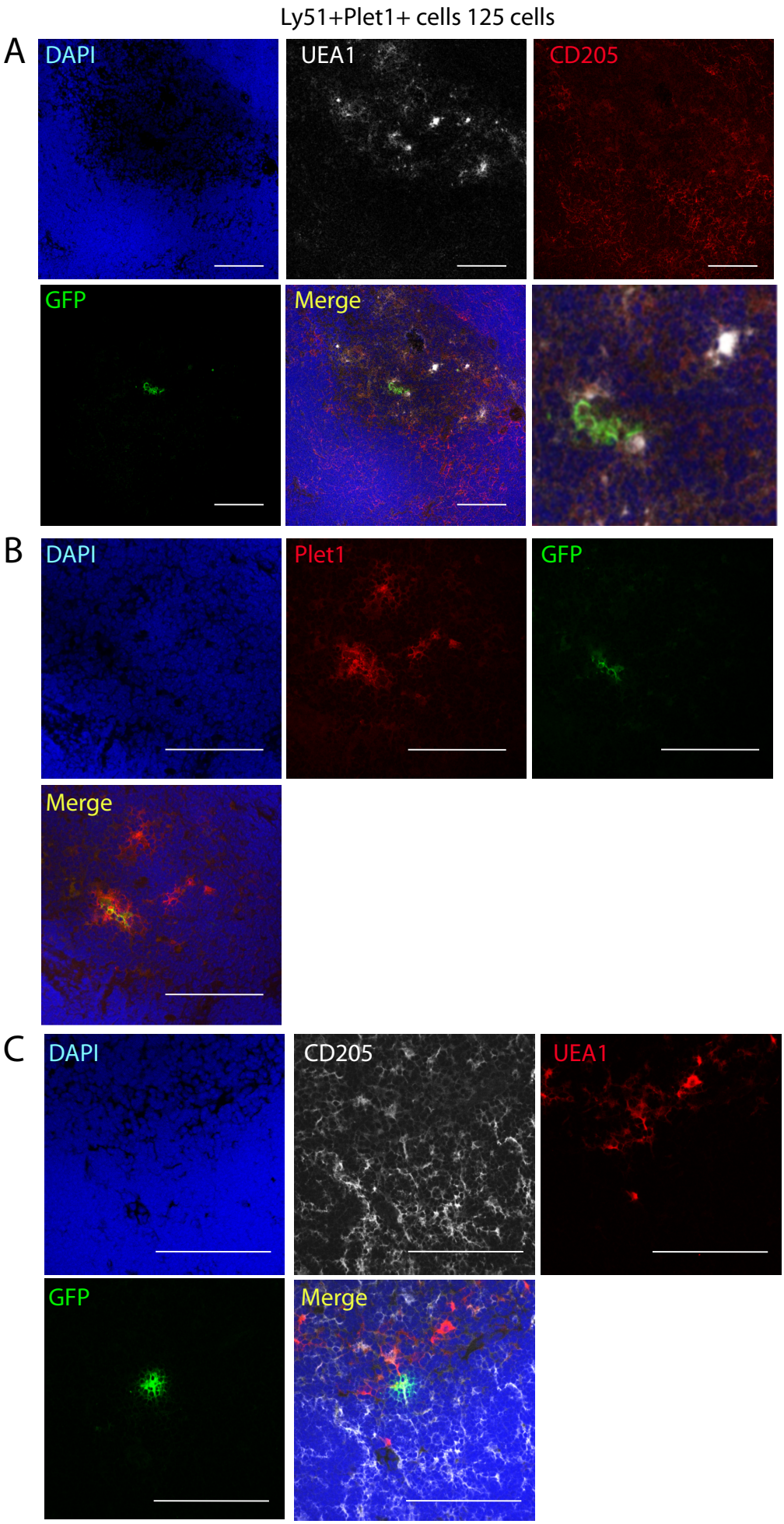


Figure 5.9 125 Ly51+Plet1+ cells are able to contribute to cTEC and mTEC
Grafts with 125 Ly51+Plet1+ cells showed contribution to both mTEC (stained with UEA1+, Plet1+) (A,B), and cTEC (positive for CD205) (C).
Scale bar respresents 150μm.


Ly51+Plet1+ cells 125 cells
A
DAPI
UEA1
CD205
GFP
Merge
B
DAPI
Plet1
GFP
Merge
C
DAPI
CD205
UEA1
GFP
Merge

5.4.4 Analyses of contribution of 60 Ly51$^+$Plet1$^+$GFP$^+$ test cells

No GFP$^+$ TEC were detected in the cortical or medullary compartments of any of three grafts generated with an input of 60 Ly51$^+$Plet1$^+$ test cells.

Collectively, these data establish that Ly51$^+$Plet1$^+$ TEC can give rise to both cTEC and mTEC in grafts with as few as 125 input test cells, identifying these cells as potential stem/progenitor cells. Even at these low input cell numbers, contribution to both cortex and medulla observed, making it extremely likely that there is a common multipotent progenitor in this population, rather than two distinct progenitors primed for the mTEC or cTEC lineages. The Ly51$^+$Plet1$^+$ population is also the only population that yielded Plet1$^+$GFP$^+$ cells. Whether these cells were generated by proliferation of the input Ly51$^+$Plet1$^+$, or whether they represent Ly51$^+$Plet1$^+$ cells that have not undergone proliferation and/or differentiation is as yet unclear. Taking into consideration the data discussed above and the rate of contribution to the grafts, the frequency of progenitor cells in the Ly51$^+$Plet1$^+$ cells can be estimated to be from 1/87.5 – 1/92.5, with an average of 1/90 cells, as determined by limiting dilution analysis (Hu & Smyth 2009).

5.5 Localization of Ly51$^+$Plet1$^+$ cells in the postnatal thymus

Previously in our laboratory work on characterization of Plet1$^+$ cells by IHC was carried out. This analyses established that in contrast to the flow cytometric data presented in Figure 5.1, by IHC Plet1$^+$ TEC seemed to be restricted to the medulla, and did not display a broad staining pattern. Rather, Plet1 stained small islets in the medulla (Figure 5.10 A). However after identifying the Ly51$^+$Plet1$^+$ population as possible progenitors it was important to identify their localization *in vivo*. In order to do this, I analysed every third section of 4 week old mouse thymi by IHC. As expected, most Plet1$^+$ TEC were situated in the medulla and did not co-stain with Ly51 (Figure 5.10 B). Interestingly a rare population of Ly51$^+$Plet1$^+$ cells was detected as single cells at the cortical medullary junction or cortex (Figure 5.10 B).

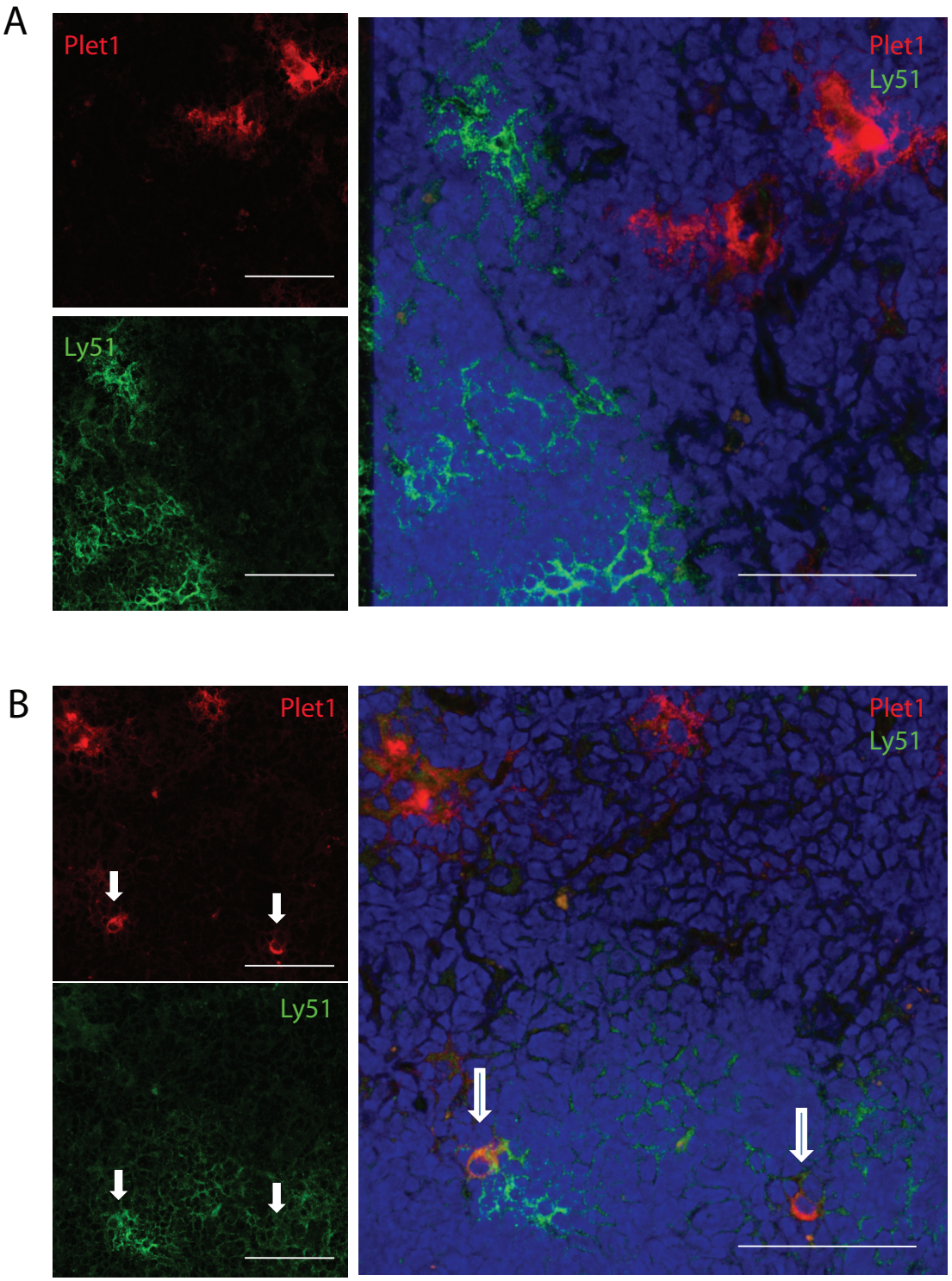


Figure 5.10 Ly51+Plet1+ cells are located at the CMJ.
4-8 week old C57/BL6 thymic were sectioned and stained for Ly51 and Plet1. Most Plet1 positive cells were situated in the medulla (A), however rare single cells double positive for Ly51 and Plet1 were located at the CMJ

5.6 Capacity of Ly51^{+}Plet1^{+} TEC to initiate *de novo* thymus formation.

In all previous experiments the E13.5 dissociated thymic cells supplied as part of the reaggregate were responsible for the formation of the thymus organoid under the kidney capsule, and provided an inductive environment to support differentiation of the test cells. I therefore next tested whether the Ly51^{+}Plet1^{+} TEC could form a thymus without the support of *ex vivo* E13.5 dissociated thymi. It is well established that interaction with thymocytes is required for generation of a patterned thymus containing established cortical and medullary compartments. Thus, for this purpose I sorted TN thymocytes from 4 week old wild type C57BL/6 mice (Figure 5.11A-D) and reaggregated them with 1600 C57BL/6 Ly51^{+}Plet1^{+}TEC, and MEFs isolated from CBAxC57BL/6 F1 mice.

These grafts were cultured overnight on a membrane and then grafted under the kidney capsule as above. Two of two grafts were recovered three weeks later, and processed for analysis as described above. In these analyses, every 9th section was stained to determine the presence of thymic tissue.

In both grafts, small areas of thymic tissue were readily identified by their dense DAPI staining. Further staining showed that these areas contained cells expressing K5 and K8 (Figure 5.12 A), as well as CD205^{+} cells. They also displayed isolated areas of K14^{+} cells (Figure 5.12 B), this could suggest the presence of cortical and medullary compartments.

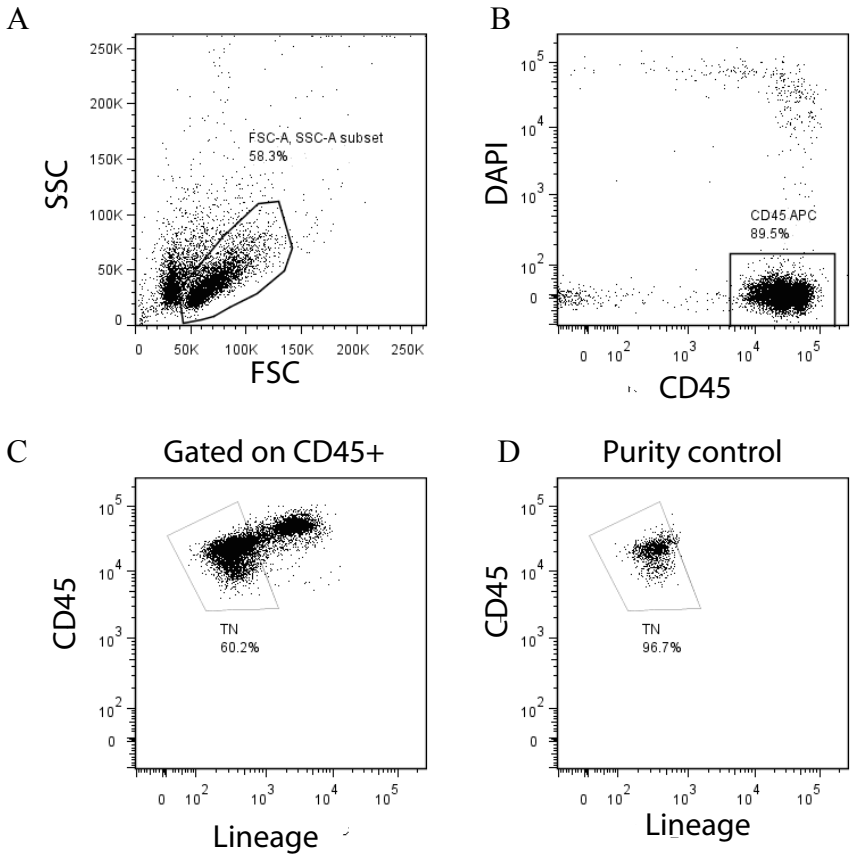
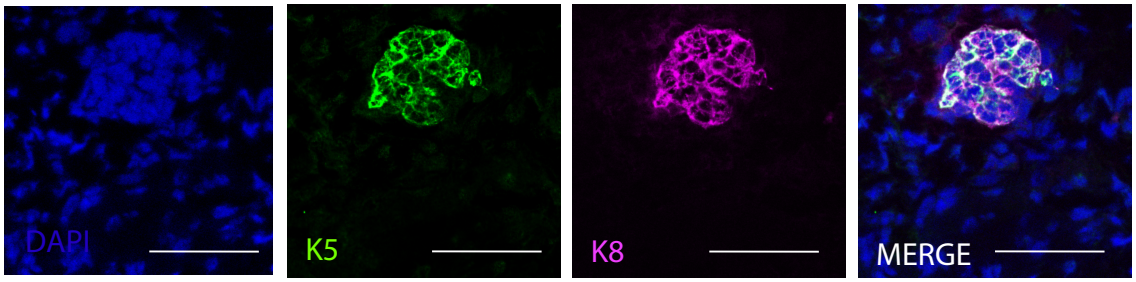


Figure 5.11 Strategy for TN cell sorting.
Representative plots of sorting strategy for TN cells (A-C), and purity check for sorted population (D).

A



B

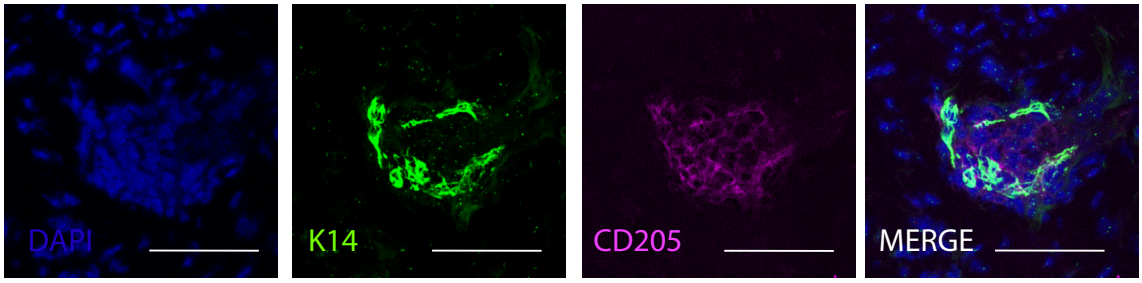


Figure 5.12. IHC analyses of Ly51+Plet1+ grafts reaggregated with MEFs only. Grafts display a number of small DAPI dense areas that stain positive for K5 and K8 (A), and K14 and CD205 (B)

These preliminary data suggest that the Ly51^{+}Plet1^{+} cells are not only capable of contributing to an established TEC enviroment, but are also able to form a thymic organoid when grafted without the support of the E13.5 dissociated thymi.

In the future similar experiments will be performed, however the grafts will be left for longer to allow for further development to occur. These will then be analysed in order to see if these cells can form a functional organoid with distinct medullary and cortical compartment and capable of attracting T-cells.

5.7 Summary

In this Chapter, I set out to determine which of the postnatal TEC sub-populations contained thymic epithelial progenitor or stem cell activity, and further to determine whether that activity represented a common TEP/SC, or distinct sub-lineage specific TEP/SC. I initially used five TEC subpopulations defined by flow cytometry, and then tested the differentiative potential of these sub-populations systematically using an assay of TEC potency. The main findings of this work are as follows (Figure 5.13 A):

Out of the five populations analysed only two gave a robust contribution to TEC networks in all grafts analysed. The major cortical TEC population, comprising Ly51^{+}Plet1^{-}TEC, could contribute extensively to cTEC networks for at least 4 weeks post-grafting. Cells in this population could give rise to multiple GFP^{+} islets, all of which were positive for markers commonly used to define cortical TEC (β5t, Ly51, CD205). Out of over three hundred areas analysed, only two possible medullary areas were detected in grafts seeded with Ly51^{+}Plet1^{-} test cells. These clusters were small and contained single or only a few GFP^{+}cells. From these data, I conclude that at least some cells in the Ly51^{+}Plet1^{-} population are capable of contributing to cTEC lineages, but that these cells do not display lineage plasticity and are restricted to the cortical lineage. It is not yet clear whether the cells detected represent persisting input cells, or the progeny of a cTEC-restricted progenitor or stem cell.

Interestingly the presumptive medullary TEC subpopulations analysed (defined by strong staining with the lectin UEA1) could contribute to TEC networks only poorly or not at all in this assay. Indeed, of these UEA1^{+} TEC populations, the UEA1^{+}Plet1^{-}

MHC Class II^{hi} population was the only one that generated GFP^{+} TEC that remained in the grafts for at least 4 weeks post grafting. These cells were situated in the medulla and displayed medullary markers, but constituted single cells or small clusters and showed no evidence of large foci of cells similar to those generated in the cortex from Ly51^{+}Plet1^{-} test cells. At four weeks of age, the mTEC MHC II^{hi} and MHC II^{lo} are actively cycling with up to 15% of cells expressing Ki67 in the MHC II^{hi} compartment (Fletcher et al. 2009) (Nick Bredenkamp unpublished). Taking this into account, I conclude that the UEA1^{+} subpopulations of the postnatal thymus do not contain TEP/SC that can be detected in this assay. This may point to the inability of these mTEC subpopulations to self-replenish.

In contrast, the Ly51^{+}Plet1^{+} TEC sub-population was able to give rise to both cortex and medulla in 100% of grafts analysed, when the grafts were seeded with 125 or more test cells. Interestingly, even at 125 test cells per graft contribution to both cTEC and mTEC was detected, while 60 test cells per graft did not yield any GFP^{+} areas. The ability to generate cTEC and mTEC is thus lost at the same threshold of input test cells, suggesting the presence of a multipotent progenitor, rather than unipotent progenitors for both compartments.

By analysing the above presented data, the frequency of the multipotent progenitor cells in the Ly51^{+}Plet1^{+} population can be calculated at 1/87.5 – 1/92.5, with an average of 1/90 cells.

In this analysis both the MHC II^{hi} and MHC II^{lo} Ly51^{+}Plet1^{+} cells were tested together, most Ly51^{+}Plet1^{+} cells are MHC II^{hi}, with a minor subpopulation of MHC II^{lo} cells. Future work will include establishing the potential of these two subpopulations, to determine which of the two contains the progenitor cells.

Thus, this study identifies Ly51^{+}Plet1^{+} cells as the first phenotypically defined common epithelial progenitor/stem cells in the postnatal thymus, that are able to give rise to all TEC sublineages. This was also the only population that gave rise to Plet1^{+} cells, which could be an indication of self renewal and thus may indicate that these cells are not only multipotent progenitors, but stem cells.

In order to differentiate between the two, grafts were left for a longer period under the kidney capsule, to assess if the $Ly51^{+}Plet1^{+}$ population is capable of long term continuous contribution to the thymic organoid, a property that would be indicative of a stem cell population. These experiments are currently ongoing.

The data presented above, taken with the data presented in chapter 4, allows for a better understanding of the relationship between different subsets of postnatal TEC, and the cellular mechanisms by which the thymus is maintained. A representation of the possible mechanisms is presented in Figure 5.13 B.

A

		No. cells	
Immature mTEC	UEA1+Plet1+MHC Class II lo	10,000	No green cells detected
	UEA1+Plet1- MHC Class II lo	10,000	No extensive contribution
Mature mTEC	UEA1+ MHC Class II hi	10,000	1/5 grafts showed small medullary area after a month
Immature and mature cTEC	Ly51+ Plet1-, MHC Class II hi and int	10,000	3/3 show extensive contribution to cortex. 1-2/300 areas analyzed possibly medullary but very small
Unassigned TEC Located at the CMJ	UEA1-Ly51+ Plet1+, MHC Class II hi and lo	1500	3/3 - contribution to cortex and medulla. Up to 30% of GFP+ cells are found in medullary areas.
		500	3/3 -contribution to cortex and medulla.
		250	3/3 -contribution to cortex and medulla.
		125	3/3-contribution to both cortex and medulla
		60	3/3 No contribution to cortex or medulla, a few green cells found in cysts.

B

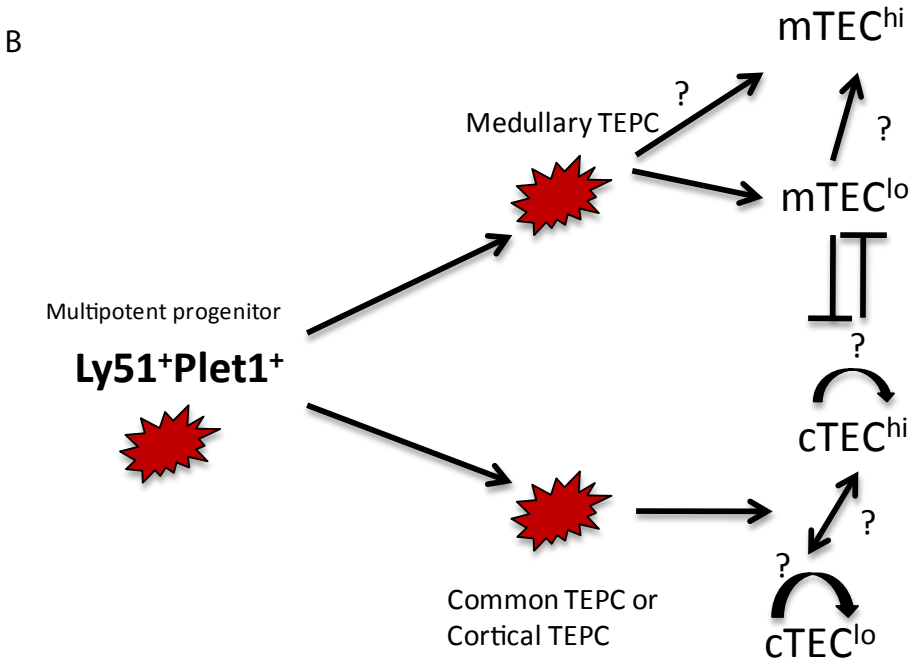


Figure 5.13 Summary table of all grafting experiments analysed (A), Posible mechanism for thymus regeneration.

Chapter 6: Summary and concluding remarks

Data presented in this thesis examined the possibility of the existence of a multipotent TEC progenitor, and the lineage relationship between distinct TEC subsets in the postnatal thymus. In order to achieve these goals I used two approaches: genetically heritable lineage tracing, using the *Foxn1*^{CreERT2} mouse strain, and a TEC potency assay. This has allowed to produce the first evidence of a phenotypically defined multipotent progenitor TEC type in the postnatal thymus, and gain further insight into the lineage relationship between different TEC subsets.

Data presented in this thesis describe the characterization of a novel mouse line – the *Foxn1*^{CreERt2} strain. The data presented establish that, in the E12.5 fetal thymus, the *Foxn1*^{CreERt2} mouse line drives recombination specifically in *Foxn1*-positive cells, with high efficiency, with no non-specific labeling detected in any other tissues, and no spontaneous recombination detected in carrier-only controls. However there was a substantial difference in recombination efficiency when using different reporter strains, with only the Red/Green and sGFP-7 mice producing high levels of recombination.

In postnatal mice significant levels of recombination were observed only in the Foxn1$^{CreERT2/CreERT2}$;Red/Green mice. However recombination level was low, with no more than 10% of total TEC labeled with GFP, with 3 fold more GFP+ cells detected in the MHC II^{hi} compartment, than the MHC II^{lo}.

From these data I concluded that this mouse model was not suitable for addressing my initial goal of determining whether the *Foxn1*$^{+}$ or negative cells are responsible for thymus maintenance, as most *Foxn1* positive cells are not labeled using this delete strain.

I have also shown that tamoxifen administration has an impact on the thymus. Administration of tamoxifen lead to a decrease in size and total cellularity, with the lymphocytes showing a severe decrease in number. Though the number of TEC was not decreased, there was evidence suggesting an effect on some of the TEC compartments. A severe reduction in cell number and proportion was evident in the

MHC Class II^{hi} mTEC, with restoration of the compartment taking place only by 3 weeks after the last injection. mTEC MHC ClassII^{lo} displayed a reduction in cell number 1 week post injection, and a further decrease at 3 weeks.

A substantial caveat of this analysis, however, is the absence of untreated control mice at 1 week and 3weeks after injection, as well as the absence of carrier-only injected controls for the 2 day time-points analysed. This could lead to an underestimation of the effect of tamoxifen on the TEC subsets.

This thesis also provides data on tamoxifen-induced *in vivo* cell labeling in Foxn1$^{CreERT2/CreERT2}$;Red/Green mice at 4 months of age. I observed a significant increase in GFP^{+} cell proportion in MHC II^{lo} TEC 3 weeks after injection when compared to the 1 week and 2day groups specifically in the cTEC^{lo} compartment of cells. Since cTEC compartments were largely unaffected by tamoxifen treatment, the proportional increase in GFP^{+} cells could indicate several possible mechanisms of maintenance of the cTEC populations. It could be possible that a cortical progenitor residing in the MHC ClassII^{lo} cTEC compartment was labeled during the initial pulse, and has proceeded to expand and, possibly is capable of giving rise to MHC ClassII^{hi} cTEC- which would explain their lagging increase. However it is equally possible that the MHC ClassII^{hi} cTEC are contributing to the MHC ClassII^{lo} cTEC compartment, that in turn undergoes expansion. The data provided does not allow these possible models of regeneration to be distinguished. In order to address this issue in future experiments tamoxifen titration will be performed in order to attempt labeling only in the MHC II^{hi}. The use of the confetti reporter mice might also be used in an attempt to gain more information on the relationship between TEC subsets (Snippert et al. 2010).

Furthermore using a TEC potency assay I showed the first evidence of a phenotypically defined multipotent postnatal TEC progenitor capable of giving rise to all TEC subsets, including the Plet1+ subset.

I tested 5 distinct populations of TEC in the postnatal thymus. Out of the five populations analysed only two gave a robust contribution to TEC networks in all grafts analysed. The major cortical TEC population, could contribute extensively to

cTEC networks for at least 4 weeks post-grafting and give rise to multiple GFP+ cell clusters throughout the thymic organoid. This data suggests that at least some cells in this population are able to contribute to cTEC lineages, and display no linage plasticity.

The mTEC subpopulations analysed (defined by strong staining with the lectin UEA1) could contribute to TEC networks only poorly or not at all in this assay, with only the UEA1^{+}Plet1^{-}MHC Class II^{hi} population capable of generating GFP^{+} TEC that remained in the grafts for at least 4 weeks post grafting. These cells were situated in the medulla and displayed medullary markers, but constituted single cells or small clusters. Taking into account that at this age, the mTEC MHC II^{hi} and MHC II^{lo} are actively cycling with up to 15% of cells expressing Ki67 in the MHC II^{hi} compartment (Fletcher et al. 2009) (Nick Bredenkamp unpublished), it would seem that the UEA1^{+} subpopulations of the postnatal thymus do not contain TEP/SC that can be detected in this assay.

Strikingly the Ly51^{+}Plet1^{+} TEC sub-population was able to give rise to both cortex and medulla in 100% of grafts analysed. The ability to give rise to both mTEC and cTEC persisted even when grafts were seeded with low test cells numbers and the ability to contribute to TEC was lost at the same threshold of input test cells, suggesting the presence of a multipotent progenitor, rather than unipotent progenitors for both compartments. These cells were also able to form small thymic organoids when transplanted without the support of E12.5 WT thymic stroma, though it remains to be seen if these organoids are functional and capable of attracting T-cells.

The frequency of the multipotent progenitor cells in the Ly51^{+}Plet1^{+} was determined between 1/87.5 – 1/92.5, with an average of 1/90 cells.

Future work will include analyses of long term grafts to determine if the Ly51+Plet1+ population is able to contribute to TEC lineages long term, which would indicate stem cell activity. I would also like to determine the transcriptional profile of these cells, in hopes of finding a transcription factor that is highly expressed specifically in the Ly51+Plet1+ compartment. Provided that a suitable candidate is found, in vivo lineage tracing can be performed using the appropriate

CreERT2 mouse strain. This would shed light on the function of these cells in a homeostatic environment.

Bibliography:

Abdul-Hai, A. et al., 1996. Stimulation of immune reconstitution by interleukin-7 after syngeneic bone marrow transplantation in mice. *Experimental Hematology*, 24, pp.1416–1422.

Alpdogan, O. et al., 2006. Keratinocyte growth factor (KGF) is required for postnatal thymic regeneration. *Blood*, 107(6), pp.2453–60.

Alpdogan, Ö. et al., 2003. IL-7 enhances peripheral T cell reconstitution after allogeneic hematopoietic stem cell transplantation. *Journal of Clinical Investigation*, 112, pp.1095–1107.

Anderson, M.S. et al., 2002. Projection of an immunological self shadow within the thymus by the aire protein. *Science (New York, N.Y.)*, 298(5597), pp.1395–401.

Andrew, D. & Aspinall, R., 2001. Il-7 and not stem cell factor reverses both the increase in apoptosis and the decline in thymopoiesis seen in aged mice. *The Journal of Immunology*, 166, pp.1524–1530.

Ardavín, C., 1997. Thymic dendritic cells. *Immunology today*, 18(7), pp.350–61. Available at: http://www.ncbi.nlm.nih.gov/pubmed/21374246.

Bajoghli, B. et al., 2011. A thymus candidate in lampreys. *Nature*, 470(7332), pp.90–4.

Bajoghli, B. et al., 2009. Evolution of genetic networks underlying the emergence of thymopoiesis in vertebrates. *Cell*, 138(1), pp.186–97.

Balciunaite, G. et al., 2002. Wnt glycoproteins regulate the expression of FoxN1, the gene defective in nude mice. *Nature immunology*, 3(11), pp.1102–8.

Bennett, A.R. et al., 2002. Identification and characterization of thymic epithelial progenitor cells. *Immunity*, 16(6), pp.803–14.

Blackburn, C.C. et al., 1996. The nu gene acts cell-autonomously and is required for differentiation of thymic epithelial progenitors. *Proceedings of the National Academy of Sciences of the United States of America*, 93(12), pp.5742–6.

Blackburn, C.C. & Manley, N.R., 2004. Developing a new paradigm for thymus organogenesis. *Nature reviews. Immunology*, 4(4), pp.278–89.

Bleul, C.C. et al., 2006. Formation of a functional thymus initiated by a postnatal epithelial progenitor cell. *Nature*, 441, pp.992–996.

Bolotin, E. et al., 1996. Enhancement of thymopoiesis after bone marrow transplant by in vivo interleukin-7. *Blood*, 88, pp.1887–1894.

Boyd, R.L. et al., 1993. Inside the thymus The thvmic microenvironment. *Immunology today*, 14, pp.445–59.

Chen, L., Xiao, S. & Manley, N.R., 2009. Foxn1 is required to maintain the postnatal thymic microenvironment in a dosage-sensitive manner. *Blood*, 113(3), pp.567–74.

Cheng, L. et al., 2010. Postnatal tissue-specific disruption of transcription factor FoxN1 triggers acute thymic atrophy. *The Journal of biological chemistry*, 285(8), pp.5836–47.

Corbeaux, T. et al., 2010. Thymopoiesis in mice depends on a Foxn1-positive thymic epithelial cell lineage. *Proceedings of the National Academy of Sciences of the United States of America*, 107(38), pp.16613–8.

Cordier, A.C. (1974) Ultrastructure of the thymus in “Nude” mice. J. Ultrastruct. Res. 47, 26-40.

Cordier, A.C. and J.F. Heremans (1975). “Nude mouse embryo:ectodermal nature of primordial thymic defect.” Scand J Immunol 4(6): 707-10.

Cordier, a C. & Haumont, S.M., 1980. Development of thymus, parathyroids, and ultimo-branchial bodies in NMRI and nude mice. *The American journal of anatomy*, 157(3), pp.227–63.

Depreter, M.G.L. et al., 2008. Identification of Plet-1 as a specific marker of early thymic epithelial progenitor cells. *Proceedings of the National Academy of Sciences of the United States of America*, 105(3), pp.961–6.

Dor, Y. et al., 2004. Adult pancreatic beta-cells are formed by self-duplication rather than stem-cell differentiation. *Nature*, 429(6987), pp.41–6.

Dowling, M.R. & Hodgkin, P.D., 2009. Why does the thymus involute? A selection-based hypothesis. *Trends in Immunology*, 30, pp.295–300.

Duijvestijn, a. M. & Hoefsmit, E.C.M., 1981. Ultrastructure of the rat thymus: The micro-environment of T-lymphocyte maturation. *Cell and Tissue Research*, 218(2), pp.279–292.

Van Ewijk, W. et al., 1999. Thymic microenvironments, 3-D versus 2-D? *Seminars in immunology*, 11(1), pp.57–64.

Flanagan, S.P., 1966. “Nude”, a new hairless gene with pleiotropic effects in the mouse. *Genetical Research*, 8, pp.295–309.

Fletcher, A.L. et al., 2009. Ablation and regeneration of tolerance-inducing medullary thymic epithelial cells after cyclosporine, cyclophosphamide, and dexamethasone treatment. *Journal of immunology (Baltimore, Md. : 1950)*, 183(2), pp.823–31.

Foster, K. et al., 2008. Contribution of neural crest-derived cells in the embryonic and adult thymus. *Journal of immunology (Baltimore, Md. : 1950)*, 180(5), pp.3183–9.

Frank, J. et al., 1999. Exposing the human nude phenotype. *Nature*, 398(6727), pp.473–4.

George, A.J.T. & Ritter, M.A., 1996. Thymic involution with ageing: obsolescence or good housekeeping? *Immunology Today*, 17, pp.267–272.

Gilchrist, D.S. et al., 2003. Labeling of hematopoietic stem and progenitor cells in novel activatable EGFP reporter mice. *Genesis (New York, N.Y. : 2000)*, 36(3), pp.168–76.

Gill, J. et al., 2002. Generation of a complete thymic microenvironment by MTS24(+) thymic epithelial cells. *Nature immunology*, 3(7), pp.635–42.

Godfrey, D.I. et al., 1990. The phenotypic heterogeneity of mouse thymic stromal cells. *Immunology*, 70(1), pp.66–74.

Gordon, J. et al., 2004. Functional evidence for a single endodermal origin for the thymic epithelium. *Nature immunology*, 5(5), pp.546–53.

Gordon, J. et al., 2001. Gcm2 and Foxn1 mark early parathyroid- and thymus-specific domains in the developing third pharyngeal pouch. *Mechanisms of development*, 103(1-2), pp.141–3.

Gordon, J. et al., 2007. Specific expression of lacZ and cre recombinase in fetal thymic epithelial cells by multiplex gene targeting at the Foxn1 locus. *BMC developmental biology*, 7, p.69.

Gray, D. et al., 2007. Proliferative arrest and rapid turnover of thymic epithelial cells expressing Aire. *The Journal of experimental medicine*, 204(11), pp.2521–8.

Gray, D.H.D. et al., 2006. Developmental kinetics, turnover, and stimulatory capacity of thymic epithelial cells. *Blood*, 108(12), pp.3777–85.

Gray, D.H.D., Chidgey, a P. & Boyd, R.L., 2002. Analysis of thymic stromal cell populations using flow cytometry. *Journal of immunological methods*, 260(1-2), pp.15–28.

Gu, G., Brown, J.R. & Melton, D. a, 2003. Direct lineage tracing reveals the ontogeny of pancreatic cell fates during mouse embryogenesis. *Mechanisms of development*, 120(1), pp.35–43.

Hale, L.P., 2004. Histologic and molecular assessment of human thymus. *Annals of Diagnostic Pathology*, 8, pp.50–60.

Hamazaki, Y. et al., 2007. Medullary thymic epithelial cells expressing Aire represent a unique lineage derived from cells expressing claudin. *Nature immunology*, 8(3), pp.304–11.

Hameyer, D. et al., 2007. Toxicity of ligand-dependent Cre recombinases and generation of a conditional Cre deleter mouse allowing mosaic recombination in peripheral tissues. *Physiological genomics*, 31(1), pp.32–41.

Haynes, B.F. et al., 1984. Phenotypic characterization and ontogeny of mesodermal-derived and endocrine epithelial components of the human thymic microenvironment. *The Journal of Experimental Medicine*, 159, pp.1149–1168.

Heng, T.S.P. et al., 2005. Different Models of Thymic Involution 1. *Journal of Immunology*, 175, pp.2982–2993.

Hinterberger, M. et al., 2010. Autonomous role of medullary thymic epithelial cells in central CD4(+) T cell tolerance. *Nature immunology*, 11(6), pp.512–9.

Hu, Y. & Smyth, G.K., 2009. ELDA: extreme limiting dilution analysis for comparing depleted and enriched populations in stem cell and other assays. *Journal of immunological methods*, 347(1-2), pp.70–8.

Ito, M. et al., 2005. Stem cells in the hair follicle bulge contribute to wound repair but not to homeostasis of the epidermis. *Nature Medicine*, 11, pp.1351–4.

Itoi, M. et al., 2001. Two distinct steps of immigration of hematopoietic progenitors into the early thymus anlage. *International immunology*, 13(9), pp.1203–11.

Itoi, M., Tsukamoto, N. & Amagai, T., 2007. Expression of Dll4 and CCL25 in Foxn1-negative epithelial cells in the post-natal thymus. *International immunology*, 19(2), pp.127–32.

Jaks, V. et al., 2008. Lgr5 marks cycling, yet long-lived, hair follicle stem cells. *Nat Genet*, 40, pp.1291–1299.

Jensen, K.B. et al., 2009. Lrig1 expression defines a distinct multipotent stem cell population in mammalian epidermis. *Cell stem cell*, 4(5), pp.427–39.

Jiang, X. et al., 2000. Fate of the mammalian cardiac neural crest. *Development (Cambridge, England)*, 127(8), pp.1607–16.

Kalu, D.N. et al., 1991. A comparative study of the actions of tamoxifen, estrogen and progesterone in the ovariectomized rat. *Bone and mineral*, 15(2), pp.109–23.

Kato, S. & Schoefl, G.I., 1989. Microvasculature of normal and involuted mouse thymus. Light- and electron-microscopic study. *Acta Anatomica*, 135, pp.1–11.

Klug, D.B. et al., 2002. Cutting edge: thymocyte-independent and thymocyte-dependent phases of epithelial patterning in the fetal thymus. *Journal of immunology (Baltimore, Md. : 1950)*, 169(6), pp.2842–5.

Klug, D.B. et al., 1998. Interdependence of cortical thymic epithelial cell differentiation and T-lineage commitment. *Proceedings of the National Academy of Sciences of the United States of America*, 95(20), pp.11822–7.

Kretzschmar, K. & Watt, F.M., 2012. Lineage tracing. *Cell*, 148, pp.33–45.

Lampert, I.A. and Ritter (1988). The origin of the diverse epithelial cells of the thymus: is there a common stem cell? Thymus Update. M.D. Kendall and M.A. Ritter, Hardwood Academic:5-25.

Lee, D., Prowse, D.M. & Brissette, J.L., 1999. Association between mouse nude gene expression and the initiation of epithelial terminal differentiation. *Developmental biology*, 208(2), pp.362–74.

Levy, V. et al., 2007. Epidermal stem cells arise from the hair follicle after wounding. *FASEB journal : official publication of the Federation of American Societies for Experimental Biology*, 21(7), pp.1358–66.

Lind, E.F. et al., 2001. Mapping precursor movement through the postnatal thymus reveals specific microenvironments supporting defined stages of early lymphoid development. *The Journal of experimental medicine*, 194(2), pp.127–34.

Linton, P.J. & Dorshkind, K., 2004. Age-related changes in lymphocyte development and function. *Nature Immunology*, 5, pp.133–139.

Luche, H. et al., 2007. Faithful activation of an extra-bright red fluorescent protein in "knock-in" Cre-reporter mice ideally suited for lineage tracing studies. *European journal of immunology*, 37(1), pp.43–53.

Lynch, H.E. et al., 2009. Thymic involution and immune reconstitution. *Trends in immunology*, 30(7), pp.366–73.

Mackall, C.L. et al., 2001. IL-7 increases both thymic-dependent and thymic-independent T-cell regeneration after bone marrow transplantation. *Blood*, 97, pp.1491–1497.

Mackall, C.L. et al., 1998. Thymic function in young/old chimeras: substantial thymic T cell regenerative capacity despite irreversible age-associated thymic involution. *European journal of immunology*, 28(6), pp.1886–93.

Manley, N.R. et al., 2011. Structure and function of the thymic microenvironment. *Frontiers in bioscience a journal and virtual library*, 17, pp.2461–2477.

Michael Nehls, Dietmar Pfeifer, Michael Schorpp, Hans Hedrich, T.B., 1994. New member of the winged-helix protein family disrupted in mouse and rat nude mutations. *Nature*, 372, pp.103–7.

Min, D. et al., 2007. Sustained thymopoiesis and improvement in functional immunity induced by exogenous KGF administration in murine models of aging. *Blood*, 109, pp.2529–2537.

Min, H., Montecino-Rodriguez, E. & Dorshkind, K., 2004. Reduction in the developmental potential of intrathymic T cell progenitors with age. *The Journal of Immunology*, 173, pp.245–250.

Morris, R.J. et al., 2004. Capturing and profiling adult hair follicle stem cells. *Nature Biotechnology*, 22, pp.411–417.

Muzumdar, M.D. et al., 2007. ARTICLE A Global Double-Fluorescent Cre Reporter Mouse. , 605(September), pp.593–605.

Nantes, U. De, 1975. TRACING OF CELLS OF THE AVIAN THYMUS THROUGH EMBRYONIC LIFE IN INTERSPECIFIC CHIMERAS * Various types of immunological deficiency diseases are related to develop- mental anomalies of primary lymphoid organs (1 , 2) . Since the thymus is directly concern. , 142, pp.17–40.

Nobori, S. et al., 2006. Thymic rejuvenation and the induction of tolerance by adult thymic grafts. *Proceedings of the National Academy of Sciences of the United States of America*, 103, pp.19081–19086.

Nowell, C.S. et al., 2011. Foxn1 regulates lineage progression in cortical and medullary thymic epithelial cells but is dispensable for medullary sublineage divergence. *PLoS genetics*, 7(11), p.e1002348.

Ortman, C.L. et al., 2002. Molecular characterization of the mouse involuted thymus: aberrations in expression of transcription regulators in thymocyte and epithelial compartments. *International Immunology*, 14, pp.813–822.

Oshima, H. et al., 2001. Morphogenesis and renewal of hair follicles from adult multipotent stem cells. *Cell*, 104, pp.233–245.

P.P. Sfikakis, N. Kostomitsopolos, C. Kittas, J. Stathopolous, P. Karayannacos, A. Dellia-Sfikakis, D.M., 1998. Tamoxifen exerts testosterone dependent and independent e}ects on thymic involution. *International Journal of Immunopharmacology*, 20(1998), pp.305–312.

Petrie, H.T., 2002. Role of thymic organ structure and stromal composition in steady-state postnatal T-cell production. *Immunological reviews*, 189(1), pp.8–19.

Pido-Lopez, J. et al., 2002. Molecular quantitation of thymic output in mice and the effect of IL-7. *European Journal of Immunology*, 32, pp.2827–2836.

Radtke, M.L. & Kolesar, J.M., 2005. Palifermin (Kepivance) for the treatment of oral mucositis in patients with hematologic malignancies requiring hematopoietic stem cell support. *Journal of oncology pharmacy practice : official publication of the International Society of Oncology Pharmacy Practitioners*, 11(3), pp.121–5.

Revest, J.M. et al., 2001. Development of the thymus requires signaling through the fibroblast growth factor receptor R2-IIIb. *Journal of immunology (Baltimore, Md. : 1950)*, 167(4), pp.1954–61.

Rochat, a, Kobayashi, K. & Barrandon, Y., 1994. Location of stem cells of human hair follicles by clonal analysis. *Cell*, 76(6), pp.1063–73.

Rodewald, H., A second chance for the thymus.

Rodewald, H.R. et al., 2001. Thymus medulla consisting of epithelial islets each derived from a single progenitor. *Nature*, 414, pp.763–768.

Rodewald, H.-R., 2008. Thymus organogenesis. *Annual review of immunology*, 26, pp.355–88.

Rossi, S.W. et al., 2006. Clonal analysis reveals a common progenitor for thymic cortical and medullary epithelium. *Nature*, 441(7096), pp.988–91.

Rossi, S.W., Jeker, L.T., et al., 2007. Immunobiology: Keratinocyte growth factor (KGF) enhances postnatal T-cell development via enhancements in proliferation and function of thymic epithelial cells. *Blood*, 109, pp.3803–3811.

Rossi, S.W., Kim, M.-Y., et al., 2007. RANK signals from CD4(+)3(-) inducer cells regulate development of Aire-expressing epithelial cells in the thymic medulla. *The Journal of experimental medicine*, 204(6), pp.1267–72.

Rossi, S.W., Chidgey, A.P., et al., 2007. Redefining epithelial progenitor potential in the developing thymus. *European Journal of Immunology*, 37, pp.2411–8.

Rothenberg, E. V & Dionne, C.J., 2002. Lineage plasticity and commitment in T-cell development. *Immunological reviews*, 187, pp.96–115.

Savino, W., Villa-verde, D.M.S. & Lannes-vieira, J., 1993. viewpoint Extracellular matrix proteins in intrathymic T-cell migration and differentiation ? *Immunity*, (4), pp.2–5.

Schlake, T. et al., 1997. The nude gene encodes a sequence-specific DNA binding protein with homologs in organisms that lack an anticipatory immune system. *Proceedings of the National Academy of Sciences of the United States of America*, 94(8), pp.3842–7.

Schluep, M. et al., 1988. Myasthenia gravis thymus: clinical, histological and culture correlations. *Journal of autoimmunity*, 1(5), pp.445–67.

Sheridan, J.M. et al., 2009. A novel method for the generation of reaggregated organotypic cultures that permits juxtaposition of defined cell populations. *Genesis (New York, N.Y. : 2000)*, 47, pp.346–351.

Sempowski, G.D. et al., 2002. T cell receptor excision circle assessment of thymopoiesis in aging mice. *Molecular immunology*, 38, pp.841–8.

Snippert, H.J. et al., 2010. Intestinal crypt homeostasis results from neutral competition between symmetrically dividing Lgr5 stem cells. *Cell*, 143(1), pp.134–44.

Srinivas, S. et al., 2001. Cre reporter strains produced by targeted insertion of EYFP and ECFP into the ROSA26 locus. *BMC developmental biology*, 1, p.4.

Steinmann, G.G., Klaus, B. & Müller-Hermelink, H.K., 1985. The involution of the ageing human thymic epithelium is independent of puberty. A morphometric study. *Scandinavian journal of immunology*, 22, pp.563–75.

Sutherland, J.S. et al., 2005. Activation of thymic regeneration in mice and humans following androgen blockade. *The Journal of Immunology*, 175, pp.2741–2753.

Takahama, Y., 2006. Journey through the thymus: stromal guides for T-cell development and selection. *Nature reviews. Immunology*, 6(2), pp.127–35.

Tibbetts, T.A. et al., 1999. Progesterone receptors in the thymus are required for thymic involution during pregnancy and for normal fertility. *Proceedings of the National Academy of Sciences of the United States of America*, 96, pp.12021–12026.

Tumbar, T. et al., 2004. Defining the epithelial stem cell niche in skin. *Science*, 20, pp.359–363.

Wijngaert, F.P. Van De et al., 1984. and“ l [” tssue Resealv . h Heterogeneity of epithelial cells in the human thymus. , pp.227–237.

Zhang, Y. et al., 1996. Inducible site-directed recombination in mouse embryonic stem cells. *Nucleic acids research*, 24(4), pp.543–8.

Zook, E.C. et al., 2011. Overexpression of Foxn1 attenuates age-associated thymic involution and prevents the expansion of peripheral CD4 memory T cells. *Blood*, 118(22), pp.5723–31.